Coherent structures—reality and myth[a)]

A. K. M. F. Hussain
University of Houston, Houston, Texas 77004

(Received 18 August 1981; accepted 10 May 1983)

The nature and significance of large-scale coherent structures in turblent shear flows are addressed. A definition for the coherent structure is proposed and its implications discussed. The characteristic coherent structure properties are identified and the analytical and experimental constraints in the eduction of coherent structures are examined. Following a few comments on coherent motions in wall layers, the accumulated knowledge from a number of recent and ongoing coherent structure investigations in excited and unexcited free shear flows in the author's laboratory is reviewed. Also briefly addressed are effects of initial conditions, the role of coherent structures in jet noise production and broadband noise amplification, the feedback effect of coherent structures, the use of the Taylor hypothesis in coherent structure description, negative production, turbulence suppression via excitation, validity of the Reynolds number similarity hypothesis, etc. From the detailed quantitative results, a picture of the state of the art in coherent structure studies emerges. While coherent structures are highly interesting characteristic features of (perhaps all) turbulent shear flows, it is argued that their dynamical significance has been overemphasized. These are predominant only in their early stages of formation following instability, or in resonant situations and excited flows, or in regions adjacent to a wall of a turbulent boundary layer. The coherent Reynolds stress, vorticity, and production are comparable to (and not an order of magnitude larger than) the time-average Reynolds stress, vorticity, and production, respectively, in fully developed states of turbulent shear flows, where incoherent turbulence is also important and cannot be ignored. The concept and importance of coherent structures are here to stay; understanding and modeling of turbulent shear flows will be incomplete without them; but they are not all that matter in turbulent shear flows.

I. INTRODUCTION

The significance of turbulence in most natural and technological flows as well as its inherent complexity cannot be overemphasized. Despite dedicated efforts of many able scientists over the decades, turbulence continues to persist as one of the least understood arenas of the natural sciences. New ideas and interpretations are highly desirable, but also must be carefully examined. Such a scrutiny risks the possibility of discouraging progress, but has the potential of saving unfruitful digressions and wasted efforts. While the "rise and fall of ideas" is not new to turbulence, there is continuing, albeit slow and sporadic, progress in our understanding of turbulent shear flows.[1,2]

Turbulence research has experienced two revolutions in the past decade. The first, rather profound, is the discovery of large-scale coherent structures. The second is the integration of the digital computer as an active (even interactive) component of the turbulence research arsenal.

A. Computer as a research tool

Today computer-controlled experimental research in turbulence is more the rule than the exception. Apart from the obvious advantage of being able to rapidly process high-frequency signals and large volumes of data, computers have facilitated automated and accurate sensor calibration and traverse, experiment control, and data acquisition; measurement of phase-average properties; precise use of event-dependent criteria like conditional sampling to capture random events and their spatial features; simultaneous recording of multivariable data and use of multiple criteria for signal enhancement, pattern recognition, structure eduction, and classification; etc. The computer has not only improved signal processing and data accuracy but also has reduced operator interference. [In free shear flow experiments (for example, jets), data acquisition under remote computer control has eliminated errors introduced by the physical presence of the operator.] In many sophisticated experiments, the computer has enabled the researcher to relegate to it reliable executions of tedious or complex chores. The computer thus has encouraged the experimentalist to explore subtle but important features of turbulence which would otherwise have been prohibitive or even impossible.

In parallel with its on-line usage as a versatile laboratory instrument, the computer has also been used extensively in numerical solutions of the partial differential equations governing turbulent flows. The solution of the time-dependent Navier–Stokes equation in three dimensions is thus an aspect of the second revolution. The computation of the time-dependent solutions and their graphic presentations have advanced to such a level of sophistication and perfection that the computer-generated "flow-visualization" movies amazingly mimic laboratory flow-visualization movies and even provoke many researchers to fantasize that laboratory experiments would no longer be necessary. In many ways, the computed realizations appear attractive: the computed results can be "visualized" in any arbitrary plane with-

[a)] This paper was presented 22 November 1981 at a special session of the annual meeting of the Division of Fluid Dynamics of the American Physical Society in Monterey, California honoring the memory of L. S. G. Kovasznay.

 0031-9171/83/102816-35$01.90

out repeating the experiment; the crispness of fluid markers can be retained even in highly turbulent situations; any statistics can be "measured" from computed solutions; etc. This way, the researcher can be relieved of many of the innumerable constraints of laboratory research.

The requirements regarding the size and speed of the computer in numerical experimentation far exceed those (typically minicomputers) used in laboratory experimentation. It is not likely that computers will be large and fast enough in the foreseeable future to allow computation of high-Reynolds-number flow details with a resolution equal to the Kolmogoroff scale. Consequently, some form of subgrid modeling is unavoidable, and empirical input will continue to be important. Carefully controlled experimental data will continue to be needed for both directing the development of and validating numerical simulations.

B. Coherent structures

The discovery of large-scale coherent structures has engendered new excitement in turbulence research. The predominant notion of turbulent flow until recently was that of a (mostly) fine-grained vortical fluid in a state of total chaos. The first revolution has fostered the expectation that turbulent shear flows consist of quasideterministic structures—obviously randomly distributed in space and time—which are all that matter (in turbulent transport and noise production), and that transport and entrainment are mostly induction-driven rather than due to gradient diffusion. Of course, true entrainment (i.e., acquisition of random, three-dimensional vorticity by ambient nonvortical fluid in constant density flows) must be via molecular diffusion.

The discovery of large-scale quasideterministic structures, in flows which were hitherto considered much more chaotic,[3–5] is quite exciting because the time evolution of a realization of deterministic structures might be mathematically tractable. In this sense, it is tempting to represent turbulence as traveling vorticity waves because there is some evidence that most turbulent shear flows act as waveguides.[6–9] In spite of the attractiveness of this approach from the viewpoint of simplicity of mathematical representation, limited efforts in this direction[10–12] did not generate any significant enthusiasm. On a statistical basis, a turbulent shear flow can of course be viewed as a superposition of traveling waves.[6,9] However, the propagation distance and the characteristic time scales (of the decaying wave modes) are too small for this representation to be useful. The phenomenon being inherently nonlinear, the mathematics becomes quite intimidating when nonlinear wave interactions are considered (see Ref. 13 for a recent review). There have been some efforts to predict growth of disturbances in fully developed turbulent shear flows via linear or quasilinear theories. However, while predictions showing agreement with experimental data (say, some lower-order quantities like intensity) are impressive, it is difficult to understand how a linear theory can be expected to predict highly nonlinear behavior, especially in free turbulent shear flows.[14–17] A linear instability of the time-mean profile[16,17] should have little to do with the evolution of a disturbance in the flow. Such a study might be relevant if the turbulence could be viewed as truly fine-grained, with time scales considerably smaller than that of the instability wave. However, such an instability study is questionable especially when the turbulent shear flow itself consists of highly organized spatially discrete strong coherent structures whose time scale is comparable to that of the instability wave.

C. Flow visualization

In parallel with the two revolutions mentioned earlier, a laboratory experimental technique that has found widespread use is flow visualization, which has significantly enhanced the understanding of turbulent shear flows. Even though flow visualization was in fashion in the early developments of viscous fluid mechanics, the advent of economic and simple (constant-temperature) hot-wire anemomenters saw diminished use of flow visualization owing to economy of effort and increased emphasis on quantitative data. However, it was indeed flow visualization which brought about the first revolution[3–5] as well as contributed greatly to the second revolution. Flow visualization, which appears to have found a rebirth, is beginning to become an integral part of coherent structure investigation. It can be extremely helpful in not only obtaining a clear perception of the nature of the flow[3–5,18–28] but also in planning sophisticated experiments[29–36] and directing as well as calibrating numerical experiments on the computer.[37–46] Still another facet of flow visualization, namely image processing,[33,47–49] is an integral part of both the revolutions.

Flow visualization typically provides more information than one can instantaneously interpret. Unfortunately, the description of coherent structures is too qualitative when based on flow visualization but is extremely restrictive when based on quantitative (say, hot-wire or LDA) data. The inherent constraints of the two approaches can be summarized as: "flow visualization presents excessive information but very little hard data, and anemometer data give some hard data but very limited flow physics." Consequently, efforts should be made to pursue in parallel both flow-visualization and quantitative data in coherent structure investigations.[50] (Note that image processing is a happy blending of both of these approaches and promises to be a highly powerful research tool of the future.) The success of both approaches, however, depends on some kind of conditional sampling directed by the imagination (hence the prejudice) of the experimenter. Here lies the dilemma: prejudices, which are essential for the success of a coherent structure study, can also become liabilities as these can easily mislead one; one can usually see in flow visualization what one wants to see just as one can find different structures in the same signal. To quote Lumley:[51] "one can find in statistical data irrelevant structures with high probability,... they are formed by chance juxtaposition of other, relevant structures and have no significance."

A caution is in order regarding flow visualization. Smoke or dye boundaries in regions sufficiently far from the points of introduction cannot be trusted as reliable boundaries of coherent structures, because marked fluid may not be the coherent vorticity-bearing fluid. For example, the periodic smoke lumps in the far wake of a cylinder due to smoke

introduced at the cylinder may have little to do with vortical structures. (As an aside, note that streaklines more closely resemble constant vorticity lines with increasing values of the Reynolds number, the two lines being identical for inviscid flow.[52])

The profound impact of the coherent structure approach should be evident from the fact that it is being pursued by essentially every turbulence researcher in one form or another. However, whether this newfound excitement is a passing fad fueled by overzealous researchers (perhaps with vested investments in this topic) needs a careful scrutiny. This paper is a limited effort to provoke such an inquiry.

II. WHAT ARE COHERENT STRUCTURES?

In spite of widespread contemporary interest in these structures, there is very little agreement on what is meant by "coherent structures." Furthermore, it appears unlikely that different researchers would agree upon a particular definition. However, this author feels that it is necessary to state what is meant by coherent structures before these structures or their dynamic significance can be discussed.

A. Definition

A coherent structure is a connected, large-scale turbulent fluid mass with a phase-correlated vorticity over its spatial extent. That is, underlying the three-dimensional random vorticity fluctuations characterizing turbulence, there is an organized component of the vorticity which is phase correlated (i.e., coherent) over the extent of the structure. (Let us call this spatially phase-correlated vorticity the *coherent vorticity*.) The largest spatial extent over which there is coherent vorticity denotes the extent of the coherent structure. Thus, turbulence consists of coherent and phase-random (i.e., incoherent) motions; the latter is superimposed on the former and typically extends beyond the boundary of a coherent structure.

Since a coherent structure can be embedded in a turbulent ambient, turbulence intermittency (defined on the basis of instantaneous vorticity fluctuations), in general, cannot be used to identify the boundary of a coherent structure. Intermittency will be useless in educing coherent structures in a turbulent pipe or channel flow. The best way to characterize the boundary of the structure is by the boundary of coherent vorticity. A number of other properties can be associated with the coherent structure (this will be discussed later). But none can identify the structure as precisely as the coherent vorticity.

Many researchers have attempted to infer coherent structure on the basis of correlation of linear momenta or pressure. This is not a rigorous or even acceptable approach. Imagine an irrotational fluid blob somehow "inserted" in a turbulent medium. The pressure or velocity fluctuations over the extent of the blob will be fairly well correlated even though the flow within the blob is neither turbulent nor even vortical. Correlation of velocity or pressure fluctuations extends beyond the boundary of a structure. The limitation of the correlation of linear momenta should be apparent in situations when there are net displacements of the flow region. For example, the flapping of a jet or a wake, which can be caused by ambient disturbances external to the flow, can produce large velocity or pressure correlations across the flow width even though no coherent structure is necessarily involved.

Implicit in the definition of the coherent structure is that its size is comparable to the transverse extent of the shear flow (identified by the presence of random vorticity). The motion at the Kolmogoroff scale is highly correlated as the Reynolds number at this scale is always unity, and significant variations in vorticity or velocity cannot occur within this scale. By coherent structure we do not mean structures at this scale but those which are *large scale*, even when this qualifier is not used. Thus, vortex rings, rolls, spirals, etc., are coherent structures. However, coherent motions at scales considerably smaller than the local characteristic flow length scale can occur. Examples include hairpin vortices, typical eddies, pockets, streaks, etc; these should perhaps be called *coherent substructures*. Coherent structures can consist of substructures. For example: the prototype turbulent spot is a packet of Λ vortices; the Brown–Thomas structure is quite likely to be the envelope of a large number of hairpin vortices; puffs, slugs, and patches appear to consist of a complex set of constituent substructures, etc.

B. Brief history of coherent structures

The presence of large-scale organized motions in turbulent shear flows, though apparent for a long time and implied by the mixing length hypothesis,[53] was suggested first by Townsend[54] and investigated in detail by Grant[55] and others.[56,57] The presence of organized motions in fully turbulent shear flows was apparent in the correlation data in jets by Corrsin[58] and turbulent wake data of Roshko.[59] It is worth noting that some of the prototype coherent structures were observed a long time back. For example, puffs in the transitional pipe flow were observed and emphasized by Reynolds in 1883 and extensively investigated during the fifties by Lindgren[60] and Rotta.[61] [The production mechanism in an equilibrium puff has been recently explained by Bandyopadhyay and Hussain (private communication).] The boundary layer "spot" was discovered by Emmons[62] in 1951 and investigated soon thereafter by others[63–65]; the periodic ring vortices in turbulent Couette flow were discovered by Pai in 1938.[53] Near-field coherent structures in jets and wakes were obvious long ago in virtually every flow-visualization picture (see Refs. 66 and 67, for example). The flow-visualization study of Kline *et al.*[3] was perhaps the first to recognize the presence and significance of quasideterministic and quasiperiodic coherent structures in a fully developed turbulent shear flow. Quite independently, and perhaps some time earlier, Hama pioneered the hydrogen bubble technique of flow visualization of the sublayer and observed the streamwise streaky structure (see Refs. 68 and 69), which received widespread attention through the persistent campaigns of Kline over the following decade. Again, parallel analytical efforts of Bakewell and Lumely,[70] via a proper orthogonal decomposition of the space-time correlation data, suggested counterrotating vortices adjacent to the wall; quantitative data by Gupta *et al.*[71] with a rake of hot wires provided further details of the sublayer motion.

The presence of coherent structures in jets were implicit in the studies of Bradshaw *et al.*[72] and Mollo-Christensen[73] and strongly suggested by Crow and Champagne[4]; however, it was not until the dramatic pictures of Brown and Roshko[5] in the mixing layer that the predominant presence of the coherent structures was recognized. It is not difficult now to discover coherent structures in many flow-visualization pictures in a variety of turbulent shear flows taken decades ago. Many researchers feel that "responsible workers have always described turbulence as having short and long-range order and structure" (Lumley, private communication), and that the large-scale coherent structures were discovered experimentally and emphasized long before the 1970's of Brown–Roshko–Winant–Browand.[53] However, there should be no question about the significance of studies reported in Refs. 3–5 in bringing out the ubiquitous presence and role of coherent structures in turbulent shear flows.

C. Further characteristics

A coherent structure is responsible for (large-scale) transports of significant mass, heat, and momentum without necessarily being highly energetic itself. That is, a coherent structure is characterized by high levels of coherent vorticity, coherent Reynolds stress, coherent production, and coherent heat and mass transports, but not necessarily a high level of kinetic energy (most of the turbulent kinetic energy will then be associated with incoherent turbulence). This does not necessarily mean that the total time-mean Reynolds stress and production are always primarily due to coherent structures. As we shall see, incoherent turbulence can also become comparably significant, especially in fully developed flows.

Coherent structures are spatially mutually exclusive, i.e., they cannot spatially overlap; each structure has its independent domain and boundary. Perhaps because of this nonsuperposition character, all coherent structure interactions are inherently nonlinear. Their interactions involve tearing and pairing (complete, partial, and fractional);[50,74,75] interactions result in new structures.

Two coherent structures can be under the influence of each other through induction in the sense of the Biot–Savart effect, but until the direct interaction (pairing or tearing) commences, this has no significant effect on the structure details.

A coherent structure may occur solo (say, the helical vortex) or adjacent to other similar structures (say, rolls, rings, etc.). In the latter case, the adjacent structures may be connected via "braids" which are regions of low vorticity and contain "saddles" (more discussion later). In all cases, the location of peak coherent vorticity denotes the structure "center."

Michalke[52] suggests the alternative, classical definition in terms of the coherence function C of the random variable f. It is clear that a coherent volume can be identified for each selected threshold value of C. Use of the coherence function of a velocity component or pressure for identification of a structure boundary is unacceptable on the basis discussed earlier. (Of course, a lot of useful information has been derived via pressure measurements.[76–78]) Use of vorticity fluctuations to measure C also suffers from the constraint that a weak coherent component embedded in a large-amplitude incoherent field can hardly be detected. Michalke also contends that the structure defined by coherent vorticity is merely the skeleton, and the external pressure and velocity fields are "the body surrounding the skeleton." This author disagrees on the grounds indicated earlier.

Bradshaw[79] objects to the author's suggestion that coherent structures can have significant Reynolds stress without having significant kinetic energy on the basis that $\overline{uv} \leqslant (\overline{u^2}\,\overline{v^2})^{1/2}$ must be satisfied globally as well as spectrally. Consider $u = u_c + u_r$, $v = v_c + v_r$, where subscripts c and r denote coherent and random, respectively. The suggestion that $\overline{u_c v_c} \sim \overline{uv}$ while satisfying $\overline{u_c^2} + \overline{v_c^2} \ll \overline{u^2} + \overline{v^2}$ is possible because $\overline{u_r v_r}$ will be considerably smaller than $(\overline{u_r^2}\,\overline{v_r^2})^{1/2}$, so that $\overline{uv} \leqslant (\overline{u^2}\,\overline{v^2})^{1/2}$ is satisfied globally as well as spectrally. Needless to say, $\overline{u_c v_c} \leqslant (\overline{u_c^2}\,\overline{v_c^2})^{1/2}$.

If we view an eddy as an orthogonal eigenmode of the flow,[80,81] then a coherent structure is not an eddy. Eddies coexist in spatial superposition, a small eddy extracting energy from a larger one by being strained by the latter and the energy cascade occurring via vortex stretching. Eddies can coexist in a state of equilibrium of energy fluxes: energy being supplied by the mean flow mostly at the larger scales but removed via dissipation at the smallest scales. On the other hand, there is no corresponding equilibrium state of energy exchange between coherent structures. (There are, however, many scales in the incoherent turbulence, and cascade is perhaps still an acceptable concept for eddies within the incoherent turbulence.) Any interactions between coherent structures results in a merger into newer structures via complete, partial, and fractional pairings or division via tearing. These interactions are all short lived, rather than symbiotic.

Consistent with our definition of a coherent structure being associated with a turbulent fluid mass, a coherent structure is not a wave. Thus, advection of a coherent structure should not be confused with the propagation of a wave.

Lumley[51] is correct in pointing out that proper orthogonal decomposition of a turbulent flow field does not require spatial superposition. However, spatial superposition of eddies is essential to the cascade concept.

Yule[82] suggests that coherent structures (i) are repetitive, (ii) have survival distances much larger than the structure size, and (iii) contribute significantly to the kinetic energy. On the basis of extensive observations, this author feels that at least the last two conditions are both unnecessary and unrealistic in general. The frequency of occurrence depends, of course, on the type of flow and region of each flow.

It is not clear whether coherent structures could be formed periodically in the absence of periodic disturbances. Since it is virtually impossible to produce a disturbance-free flow, a rigorous test is not realistic. Periodic structures can form under feedback if the flow is obstructed with solid boundaries, as in the cases of edgetone, jet tone, ring tone, hole tone, or plate tone phenomena.[83–94] In the absence of an obstruction, it is not clear if new structures can be formed via upstream feedback of older structures (Sec. VIIF). While structures could occur periodically in isolated packets, these packets occur randomly.[95,96]

The structure mass obviously does not remain unchanged in time. (In special cases of coherent structures in bounded flows like equilibrium puffs, slugs, and patches in pipes and channels and also Taylor cells and spiral turbulence in circular Couette flows, the coherent structure size can be invariant with time; of course, there are continual strong entrainment and detrainment across boundaries.) In general, the structure typically increases in volume due to diffusion of vorticity, and its peak vorticity decreases; however, this kind of entrainment due to "nibbling" at the structure boundary is not likely to be the dominant mode of entrainment. It is now commonly believed that most entrainment first occurs via the "engulfment" or trapping of irrotational fluid. That is, irrotational fluid is "drawn in" by the Biot–Savart effect of a vortical structure and stretched into relatively thin sheets between turbulent fluid folds, before fine-scale vorticity is imparted (efficiently) via molecular diffusion.

III. FORMATION OF COHERENT STRUCTURES

A coherent structure originates from instability of some kind. While the most common kinds are the Kelvin–Helmholtz instability of free shear layers (mixing layers, jets, wakes) and Tollmien–Schlichting and Görtler instabilities of wall layers, essentially every kind of instability (of either laminar or turbulent basic states) is potentially capable of generating coherent structures. There are, of course, special cases of coherent structure formation like puffs, slugs, and patches[60,97–99] in pipe and channel flows and spiral turbulence in circular Couette flow.[100–103] Perhaps the simplest example of coherent structures is the Taylor vortices (a result of centrifugal instability) in the circular Couette flow. Because the structure size can be made to remain invariant with time and because unlike those in shear flows (like jets and wakes), these structures are stationary in the laboratory frame, the Taylor vortices are extremely attractive for coherent structure studies.[2,104] Note that even though hydrodynamic stability (for example, see Ref. 105) typically implies that of a laminar flow, turbulent shear flows can also undergo instability.[16,17,106,107] Vortex formation from a turbulent wake was demonstrated by Taneda.[108] The instability and rollup of an axisymmetric mixing layer originating from a fully turbulent boundary layer was first reported by Clark and Hussain.[75] For an initially fully turbulent *plane* mixing layer, the formation, evolution, and the equilibrium state of large-scale coherent structures have been documented by Hussain and Zaman[109] (see Sec. VIIK).

The initial formation of coherent structures in a free shear flow is a function of the initial condition, i.e., the state of the flow at its initiation point.[110,111] Since the instability and rollup of a shear layer into structures and the subsequent evolutions and interactions must in some way depend on the initial condition, careful documentation of the initial condition is very important, especially because the initial condition will vary from one apparatus to another. In most previous investigations, the initial condition was never documented or even explored, presumably because either its significance was not recognized or the flow was sufficiently downstream such that it was considered to be independent of the initial condition.

A. Initial condition of a free shear layer

While the importance of the initial condition is now well recognized, there is as yet no consensus on the measures necessary to adequately identify the initial condition.[110–120] These measures may include the mean velocity profile and its various characteristic thicknesses (like the boundary layer, displacement, and momentum thicknesses) and the shape factor, the probability density functions of velocity fluctuations and their moments, the spectra of velocity fluctuations, spectrum and moments of the Reynolds stress, etc. In view of the sensor resolution problem, one has to be mostly content with the measurement of the longitudinal velocity only. However, care needs to be taken in these measurements to eliminate the probe-induced shear-layer tone.[87] The initial condition appears to have received the maximum attention in free shear flows. The effect of the initial condition is quite likely to be important in the boundary layer also, especially for the outer-layer large-scale structures.

For the sake of simplicity, the initial condition can be divided into four groups: laminar, nominally laminar, highly disturbed, and fully turbulent. The first and the last are the two asymptotic limiting states desired but the second and third cases are typically achieved, unless extreme care is taken. In the first case, the profile is identical with the Blasius profile and the rms longitudinal velocity fluctuation u' decreases monotonically from the free-stream value to zero at the wall. In the nominally laminar case, the mean velocity profile agrees with the Blasius profile but the fluctuation level is comparatively high, typically reaching a peak value (at $y \simeq \delta^*$) significantly higher than the free-stream value (the spectrum typically has a few dominant peaks but no significant broadband pedestal). The origin of disturbances in the nominally laminar case is not always clear, but the associated temporal variations of the laminar boundary layer thickness δ is primarily due to facility and laboratory acoustic modes (discussed shortly). The highly disturbed case has a mean profile different from the Blasius profile and has broadband velocity spectra. Typically it denotes a transitional case in situations where transition could not be successfully eliminated because of high speeds or surface roughness or free-stream turbulence. It may also result from incomplete transition by a poorly designed trip arrangement or failure of the trip-separated boundary layer to reattach and reach the equilibrium boundary layer state (typically due to inadequate length downstream of the trip).

The last case represents a fully developed turbulent boundary layer and is characterized by (i) a mean profile of the proper shape and shape factor of about 1.4; logarithmic and wake regions in the (u^+, y^+) coordinates with (ii) an adequate extent of logarithmic region and (iii) a wake strength appropriate for the value of Re_θ[121]; (iv) a profile of u'/U_* with its peak value in the range $2.5 \pm 10\%$, (v) the peak being located at $y^+ \cong 15$[122] and (vi) u' monotonically decreasing to the free-stream value[123]; and (vii) a broadband continuous spectrum $\phi_u(f)$ of $u(t)$ with an inertial subrange.

(In all studies in our laboratory involving a fully developed turbulent initial condition, all these seven conditions have been satisfied.) The fully turbulent case is easily obtained with an appropriate trip placed sufficiently upstream of the lip.

It is important to document the spectral content of the velocity fluctuations in each case. In addition, the spectrum and intensity of the free-stream turbulence at the initial state must also be documented. The free-stream turbulence is not normally the decaying turbulence from the upstream screens but is typically caused by fan blade wake and rotating stall, tunnel settling chamber cavity resonance, laboratory standing acoustic waves, feedback from downstream obstructions, shear-layer tone within and outside of the tunnel, etc. Thus, most of the "free-stream turbulence" is acoustic disturbances manifesting into a peak in $u'(y)$ at $y/\delta^* \simeq 1$,[123] where δ^* is the displacement thickness. If any of these frequencies falls within the unstable (receptivity) band of the shear layer, the shear layer will be driven at this frequency. Unless extreme care is taken, these free-stream disturbances will be present and the flow can be "driven," depending on the frequencies and amplitudes of these modes. Thus, all free shear flows may be considered to be indeed driven to some extent. Clearly, controlled excitation is one way of introducing time-dependent variations of the initial condition. In case of excitations, whose effects are felt primarily at the separating point, both the frequencies and amplitudes of excitation, i.e., the excitation spectrum, must be documented. If the amplitudes are large, the initial mean and turbulence profiles must be documented in the presence of the excitation.

It should be emphasized that the initial condition data are measured at the end of a straight (zero pressure gradient) length of a few hundred θ_e following the contraction; θ_e is the exit boundary layer momentum thickness. If an adequate straight lip is not added following the contraction, the boundary layer profile can deviate from the Blasius profile even when laminar.

The choice of an appropriate trip is still in the state of the art. Our experinence suggests that the optimum trip is a strip with a linear array of teeth aligned spanwise (prepared by cutting a series of notches) and projecting into the flow. These teeth should have their width, spacing, height, length (along flow) of about $100\theta_e$ each and be placed at least $1000\theta_e$ upstream from the lip; θ_e is the momentum thickness of the exit boundary layer in the absence of the trip.

In a number of studies in our laboratory we addressed the effects of the initial condition. It was found that evolutions of all time-average measures, including the momentum flux, of a plane jet were strong functions of the initial condition.[123] Because of the universal belief in momentum flux invariance of a free jet, this result was initially extremely puzzling. Even though complete explanation has not yet been possible because of inherently large uncertainties in pressure and hot-wire measurements in jets, the excess momentum flux can be attributed primarily to the negative pressure in the jet supported by the transverse velocity fluctuations and also to the pressure field induced by the entrainment flow. The time-average measures of the axisymmetric mixing layer have been found to be a function of the initial condition,[118–120] but not directly of the exit momentum thickness Reynolds number Re_θ.[111] On the other hand, the plane mixing layer has been found to achieve a state independent of the initial condition.[124] Controlled excitation can alter the initial region of a plane mixing layer, but not the layer sufficiently far downstream.[125] The near-field coherent structure properties also show some dependence on the initial condition (discussed in Sec. VII).

B. Formation mechanism

To return to the formation mechanism, intial coherent structures can result from the instability of initially laminar or turbulent or intermediate states. A structure then undergoes rapid evolutionary changes either via nonlinear interactions with other structures or decay via turbulent diffusion by incoherent turbulence. The rapid changes of structures as well as their occurrence everywhere in x suggests some kind of successive regeneration mechanism. Two obvious mechanisms come to mind. After a structure has decayed, the turbulent shear flow becomes susceptible to an instability determined by the instantaneous flow state, resulting in a new coherent structure. This instability, presumably, on the average, scales with the local average scale of the flow. The second possibility is that the structures do not totally decay; the distorted or subdivided structures find ways via mutual interactions to recombine and reemerge (again, presumably, scaling, on the average, with the local mean flow scale). Either of these two would be consistent with the observation that coherent structures can vary from one region to another in the same flow (as in the near and far fields of jets and wakes) or can be different in different flows. It seems that both instabilities occur in a flow, the latter mechanism being more likely; otherwise, there will be large regions of low peak coherent vorticity in the flow.

Even though many researchers have suggested instability to be that of the local mean profile, this author feels that the instantaneous dynamics must control the instability. The instantaneous profile in a turbulent shear flow seldom resembles the time-mean profile, from which it departs wildly. That is, a disturbance never sees the mean profile. Since instability is sensitive to the details of the profile, it is hard to understand how an instability analysis based on the mean profile can explain coherent structure formation. The flow being highly time-dependent, instability analysis of a static mean profile[14–17] seems hardly relevant. Also, if instability of the mean profile were the controlling factor, then a variety of distinct modes (for example, $m = 0, \pm 1, \pm 2$ modes in the far field of a circular jet) could not form in the same flow In flows where there is no driving freestream (as in jet far fields), the regeneration mechanism is much harder to imagine than in flows with a free stream (as in a mixing layer, a wake, or a boundary layer).

IV. ANALYTICAL TREATMENT OF COHERENT STRUCTURES

Even if the coherent structures in a turbulent shear flow were identical, these would occur at random phases and

their description must involve phase-dependent information. Thus, similar to the time-average concept, an artifice such as the *phase average* [126] needs to be introduced. This is the ensemble average of any property at a particular age (i.e., phase) of the structure. That is,

$$\langle f(x, y, z, t)\rangle = \lim_{N\to\infty} \frac{1}{N} \sum_{i=1}^{N} f_i(x, y, z, t + t_i), \tag{1a}$$

where t is the time corresponding to the reference phase (or age) and t_i denotes the random instants of occurrence of successive structures of the selected phase. When these structures occur at regular intervals (a situation that essentially occurs in vortex shedding, in flow resonances like the shear-layer tone and edge tone or when structures are induced via controlled excitation), this definition reduces to the *periodic phase average*

$$\langle f(\mathbf{x}, t)\rangle = \lim_{N\to\infty} \frac{1}{N} \sum_{i=1}^{N} f_i(\mathbf{x}, t + iT), \tag{1b}$$

where T is the period of occurrence of the structure and t is the instant corresponding to the reference phase.

The phase average was first introduced[126,127] to analyze the behavior of a periodic traveling wave in a turbulent shear flow. Similar mathematical formulation can be developed to understand the dynamics of coherent structures and incoherent turbulence.

A. Triple decomposition

In the presence of coherent structures (considering one mode at a time when a variety of coherent structures are involved in the same flow), one may consider the instantaneous variable to consist of three components: the time-independent component, the coherent component, and the incoherent turbulence. That is, for any instantaneous variable $f(\mathbf{x}, t)$,

$$f(\mathbf{x}, t) = F(\mathbf{x}) + \tilde{f}_c(\mathbf{x}, t) + f_r(\mathbf{x}, t), \tag{2a}$$

where

$$\bar{f} = F, \quad \langle f\rangle = F + \tilde{f}_c \tag{2b}$$

and $\bar{f}$ is the time average of f and $\langle f\rangle$ is the phase average of f. Thus, at any given location, provided that the phase of the structure is also known, the three fields can be determined. The governing equations for the three components are discussed in the Appendix.

The energy fluxes between the three component fields are schematically depicted in Fig. 1; see the Appendix for the flux terms I, II, and III and the dissipation terms $\bar{\epsilon}$, $\tilde{\epsilon}_c$, and ϵ_r. Note that the relative widths of the paths are intended to qualitatively represent the relative energy fluxes; the relative widths will depend on the region of a flow and on the type of the flow. The dissipation by the time-average and coherent motion fields are expected to be much smaller than the incoherent turbulence dissipation ϵ_r; that is, $\bar{\epsilon} < \tilde{\epsilon}_c \ll \epsilon_r$. In the early stages of formation of the coherent structures, the term I is quite likely to be much larger than II, but in the fully developed regions, these two become comparable (Sec. VII).

Note that even though the coherent and incoherent turbulences are uncorrelated, i.e., $\overline{f_c g_r} = \langle \tilde{f}_c g_r\rangle = 0$, these two are not independent. Coherent structures both produce and

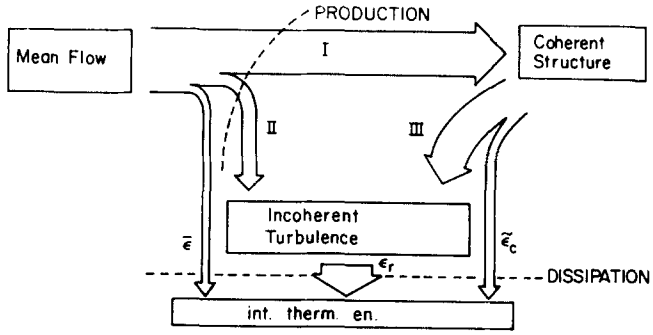

FIG. 1. Schematic of the energy fluxes between the mean, coherent, and incoherent fields.

spatially organize incoherent turbulence. That is, the coherent and incoherent turbulences are not totally uncoupled. However, neglect of these two terms can be justified on the basis of the differing time scales of the coherent and incoherent motions; the incoherent turbulence is typically of a time scale considerably smaller than that of the coherent structures.

The triple decomposition (2a) provides a formalism for discussing the physics of coherent structures vis-a-vis the time-mean flow and incoherent turbulence (see Refs. 29, 127, and 128). However, this artifice is not free from constraints. Implicit in this decomposition is the assumption that the coherent structure *is* a perturbation of the time-mean flow. But, the time-mean flow is the result of many such structures and their interactions. In a region occupied by a structure, the entire nonrandom motion is the coherent structure. In that sense, the coherent structure *is* the flow and not a mere perturbation.

B. Double decomposition

It is then tempting to use the double decomposition, introduced by Hussain,[129] so that the turbulent shear flow consists of coherent and incoherent motions only, i.e.,

$$f(\mathbf{x}, t) = f_c(\mathbf{x}, t) + f_r(\mathbf{x}, t). \tag{3}$$

The corresponding motions must be described in a coordinate moving with a particle in the coherent flow field. The governing equations with the double decomposition are discussed in the Appendix.

The double decomposition helps explain the interaction between coherent and incoherent motions. However, it also has the constraint that it cannot address the evolution of coherent structures or extraction of energy by coherent structures from the flow which drives the structures. Perhaps a quasi-Lagrangian description of the coherent structure in a frame moving with the convection velocity of the structure is a better approach. Here again, there are problems because the structure convection velocity has a large dispersion in any flow. Thus, either a totally Lagrangian formulation or a numerical solution of the Eulerian field seems desirable.

C. Characterization of coherent structures

What are the characteristic properties of coherent structures? The property identifying a coherent structure is

the coherent vorticity $\Omega_{ci} = \epsilon_{ijk}\partial u_{ck}/\partial x_j$. For a better perception of the properties, these will be discussed in one plane only (say, the x-y plane). Since coherent structures are two-dimensional or axisymmetric in many flows, properties in only one plane are required. The extension to three dimensions is straightforward. Depending on whether double decomposition or triple decomposition is used (see Appendix), the same property may have different representations. The properties that are relevant in coherent structure studies are shown in Table I. Note that $\bar{S}$ and $\langle S\rangle$ represent twice the strain rates. Note also that incoherent shear productions $-\overline{u_r v_r}\bar{S}/2$, and $-\langle u_r v_r\rangle\bar{S}/2$ as well as incoherent normal productions $-\overline{u_r^2}\partial U/\partial x$, $-\overline{v_r^2}\partial V/\partial y$, $-\langle u_r^2\rangle\partial U/\partial x$, and $-\langle v_r^2\rangle\partial V/\partial y$ are also of interest.

The function $\langle\psi\rangle$ takes the form $\langle\psi\rangle = \int_0^y (u_c - U_0)dy^*$ in plane flows and $\langle\psi\rangle = \int_0^r r^*(u_c - U_0)dr^*$ in axisymmetric flows, where U_0 is the structure convection velocity. This function would correspond to the streamfunction if the structures were steady and two dimensional; hence the name "pseudostream function." For further details see Ref. 29 which showed that contours of $\langle\psi\rangle$ are helpful, even adequate, for inferring structure convection velocity, particle paths, and momentum transport. In certain measurement situations, e.g., with a rake of sensors, $\langle\psi\rangle$ provides the simplicity so that, in flows with two-dimensional structures, it may be adequate to measure the streamwise component of the velocity only.

Of course, on the basis of the definition of the coherent structure, coherent vorticity is the most fundamental quantity. Except for situations of exactly periodic structures, determination of Ω_c contours involves the use of the Taylor hypothesis in the phase-average flow field (see Sec. VIIM). The next critical properties are coherent and incoherent Reynolds stresses $-u_c v_c$ and $-\langle u_r v_r\rangle$, these being the transports of momenta by coherent and incoherent motions. Contours of these allow evaluation of how significant is the momentum transport by coherent structures in comparison with that by incoherent turbulence of the time-mean turbulent momentum transport $-\bar{u}\bar{v}$. Contours of $-u_c v_c$ are especially interesting to indicate relative amounts of cogradient and countergradient coherent momentum transports. The next significant properties are the contours of coherent strain rates and coherent shear and normal productions. Note that, unlike their time-average values, the coherent normal and shear strain rates should be comparable. The contours of incoherent turbulence and vorticity intensities would indicate where in the structure cross section incoherent turbulence is mostly concentrated as well as the direction of their steep gradients. The incoherent vorticity intensities are a much harder measurement and can be excluded in most cases.

Note that the properties Ω_c, $\langle S\rangle$, but not $\tilde{\psi}_c$ or $\langle\psi\rangle$, are invariant under Galilean transformation. Thus, streamlines or contours of $\tilde{u}_c$ or $\tilde{v}_c$ are not helpful in identifying the coherent structure boundaries. (Note that it is a rare, but fortunate, coincidence that contours of $\tilde{u}_c$ closely agree with the structure boundary in the case of the spot.[130–132]) The contours of coherent vorticity being invariant under Galilean transformation, they constitute the primary identifiers of coherent structure boundary. When the structure is surrounded by an irrotational flow, contours of coherent inter-

TABLE I. Relevant properties in coherent structure studies.

	Double decomposition	Triple decomposition
Coherent vorticity Ω_c	$\partial v_c/\partial x - \partial u_c/\partial y$	$\partial\tilde{v}_c/\partial x - \partial\tilde{u}_c/\partial y$
Coherent Reynolds stresses	$-\langle u_c v_c\rangle$	$-\langle\tilde{u}_c\tilde{v}_c\rangle$
Incoherent Reynolds stress (time and phase averages)	$-\overline{u_r v_r}$, $-\langle v_r v_r\rangle$	
Incoherent turbulence intensities	$\langle u_r^2\rangle^{1/2}$, $\langle v_r^2\rangle^{1/2}$, $\langle w_r^2\rangle^{1/2}$	
Coherent strain rate	$\langle S\rangle = \partial u_c/\partial y + \partial v_c/\partial x$	$\langle\tilde{S}\rangle = \partial\tilde{u}_c/\partial y + \partial\tilde{v}_c/\partial x$
Time-average strain rate		$\bar{S} = \partial U/\partial y + \partial V/\partial x$
Coherent structure shear production		$\tilde{P}_c = -\langle\tilde{u}_c\tilde{v}_c\rangle\bar{S}/2$
Coherent shear production	$\langle P\rangle = -\langle u_r v_r\rangle\langle S\rangle/2$	$\langle\tilde{P}\rangle = -\langle u_r v_r\rangle\langle\tilde{S}\rangle/2$
Coherent normal production	$-\langle u_r^2\rangle(\partial u_c/\partial x)$, $-\langle v_r^2\rangle(\partial v_c/\partial y)$	$-\langle u_r^2\rangle(\partial\tilde{u}_c/\partial x)$, $-\langle u_r^2\rangle(\partial\tilde{v}_c/\partial y)$
Coherent structure normal production		$-\langle\tilde{u}_c^2\rangle(\partial U/\partial x)$, $-\langle\tilde{v}_c^2\rangle(\partial V/\partial y)$
Incoherent voriticity intensity	$\langle\omega_x^2\rangle^{1/2}$, $\langle\omega_y^2\rangle^{1/2}$, $\langle\omega_z^2\rangle^{1/2}$	
Instantaneous vector patterns	$\hat{\psi}_c = \langle u_c, v_c\rangle$	$\tilde{\psi}_c = \langle\tilde{u}_c, \tilde{v}_c\rangle$
Instantaneous streamlines	$dx/u_c = dy/v_c$	$dx/\tilde{u}_c = dy/\tilde{v}_c$
Pseudostream function	$\langle\psi\rangle$	
Coherent intermittency	$\langle\gamma_c\rangle$	

mittency are also reliable boundaries of the structure.[133]

The measured spatial contours of these properties denote not only the structure shape, size, and strength, but also indicate where in the cross section of the coherent structure different quantities have their peaks or saddles, where incoherent turbulence or coherent vorticity is the maximum, which way it is being transported or diffused, where turbulence is produced, etc. These contours, therefore, not only explain the mechanics of coherent structures but also help to determine if these structures are dynamically dominant. For a structure to be dominant, its peak vorticity, coherent Reynolds stress, and production are expected to be considerably larger (by an order of magnitude) than their time-mean values.

In a flow with heat and mass transport, the instantaneous temperature θ and species concentration s can be decomposed as $\theta = \theta_c + \theta_r = \bar{\theta} + \tilde{\theta}_c + \theta_r$ and $s = s_c + s_r = \bar{s} + \tilde{s}_c + s_r$. The properties of interest are shown in Table II.

Also important are the different phase-averaged energy flux terms over the spatial extent of the structure. These may include the advection terms like $u_c(\partial/\partial x)\langle u_r^2\rangle$, $v_c(\partial/\partial y)\langle u_r^2\rangle$, $\tilde{u}_c(\partial/\partial x)\langle v_r^2\rangle$, and $\tilde{v}_c(\partial/\partial y)\langle v_r^2\rangle$; the incoherent transport (of coherent kinetic energy) terms like $(\partial/\partial y)(u_c\langle u_r v_r\rangle)$ and $(\partial/\partial y)(\tilde{v}_c\langle u_r v_r\rangle)$; turbulent heat and mass transports $(\partial/\partial x)\langle\theta_r^2 u_r\rangle$, $(\partial/\partial y)\langle\theta_r^2 v_r\rangle$, $(\partial/\partial x)\langle s_r^2 v_r\rangle$, and $(\partial/\partial y)\langle s_r^2 v_r\rangle$; and gradient production terms like $\langle\theta_r u_r\rangle(\partial\theta_c/\partial x)$, $\langle s_r u_r\rangle(\partial s_c/\partial x)$, $\langle\theta_r v_r\rangle(\partial\theta_c/\partial y)$, and $\langle s_r v_r\rangle \times(\partial s_c/\partial y)$, etc. Of special interest are the spatial distributions of phase-average incoherent dissipation terms like

$$\left\langle\left(\frac{\partial u_r}{\partial x}\right)^2\right\rangle,\quad \left\langle\left(\frac{\partial u_r}{\partial y}\right)^2\right\rangle,\quad \left\langle\frac{\partial u_r}{\partial z}\frac{\partial w_r}{\partial x}\right\rangle,$$
$$\left\langle\frac{\partial u_r}{\partial y}\frac{\partial v_r}{\partial x}\right\rangle,\quad \left\langle\left(\frac{\partial v_r}{\partial x}\right)^2\right\rangle,\quad \left\langle\left(\frac{\partial v_r}{\partial y}\right)^2\right\rangle,$$
$$\left\langle\left(\frac{\partial w_r}{\partial x}\right)^2\right\rangle,\quad \left\langle\left(\frac{\partial w_r}{\partial y}\right)^2\right\rangle,\quad \left\langle\left(\frac{\partial\theta_r}{\partial x}\right)^2\right\rangle,\quad \left\langle\left(\frac{\partial s_r}{\partial x}\right)^2\right\rangle, \text{ etc.}$$

Apart from revealing the roles of different zones of the coherent structures in dissipation, these dissipation terms will also show the accuracy of the assumption of local isotropy. However, because small-scale transverse gradients are not easy to measure, most convenient measurements will be the phase average of squares of longitudinal derivatives (i.e., $\langle(\partial/\partial x)^2\rangle$ terms) only. These would, of course, require the use of the Taylor hypothesis.

The above-listed properties address flows with two-dimensional coherent structures. When the structures are three dimensional, the other components of coherent vorticity, strain rate, production, etc. have to be considered. In most flows of interest, the coherent structures appear to be two dimensional[5,29,134] even though this is not necessarily well accepted.[21,135-137]

TABLE II. Properties of interest for heat and mass transfer.

	Double decomposition	Triple decomposition
Transverse coherent heat transfer rate	$\langle v_c\theta_c\rangle$	$\langle\tilde{v}_c\tilde{\theta}_c\rangle$
Longitudinal coherent heat transfer rate	$\langle u_c\theta_c\rangle$	$\langle\tilde{u}_c\tilde{\theta}_c\rangle$
Transverse coherent mass transfer rate	$\langle v_c s_c\rangle$	$\langle\tilde{v}_c\tilde{s}_c\rangle$
Longitudinal coherent mass transfer rate	$\langle u_c s_c\rangle$	$\langle u_c s_c\rangle$
Transverse and longitudinal phase-average incoherent heat transfer rates	$\langle v_r\theta_r\rangle$, $\langle u_r\theta_r\rangle$	
Transverse and longitudinal phase-average incoherent mass transfer rates	$\langle v_r s_r\rangle$, $\langle u_r s_r\rangle$	
Incoherent temperature fluctuation intensity	$\langle\theta_r^2\rangle^{1/2}$	
Incoherent concentration fluctuation intensity	$\langle s_r^2\rangle^{1/2}$	

D. Some topological features of coherent structures

It can be shown that the equation for coherent vorticity Ω_c of a two-dimensional structure can be written as follows:[133]

$$\frac{\hat{D}}{Dt}\Omega_c = -\frac{\partial^2}{\partial x^2}\langle u_r v_r\rangle + \frac{\partial^2}{\partial y^2}\langle u_r v_r\rangle. \tag{4}$$

That is, the maximum rate of change of coherent vorticity Ω_c occurs at the minimax of the $\langle u_r v_r\rangle$ distribution. Consider a coherent structure across a shear. The constant vorticity contours are denoted schematically in Fig. 2. Because the maximum rate of change of vorticity occurs at the vortex center, the incoherent Reynolds stress distribution will have a minimax distribution at the vortex center. On the other hand, the flow will have a saddle at the center of the braid, midway between two structure centers, say at point A, which is also a stagnation point in a frame moving with the structure center. The vorticity is the minimum at A where the strain rate is the maximum. Hence, production is also the maximum at point A but minimum at point B. Because of the motion associated with the vortex, vorticity is continually being advected away from point A and deposited in the structure core. This vortical fluid also carries with it incoherent turbulence produced in the braid and, as a result, the core vorticity peak is reduced via turbulent diffusion. On the other hand, incoherent turbulence intensities will have their maxima within the structure cores. Detailed contours of measured coherent structure properties are consistent with these expected distributions (see Sec. VII).

V. DETECTION AND EDUCTION OF COHERENT STRUCTURES

For understanding the physics of coherent structures or explicitly including these in a viable turbulence theory, it is first necessary to measure the properties of these structures.

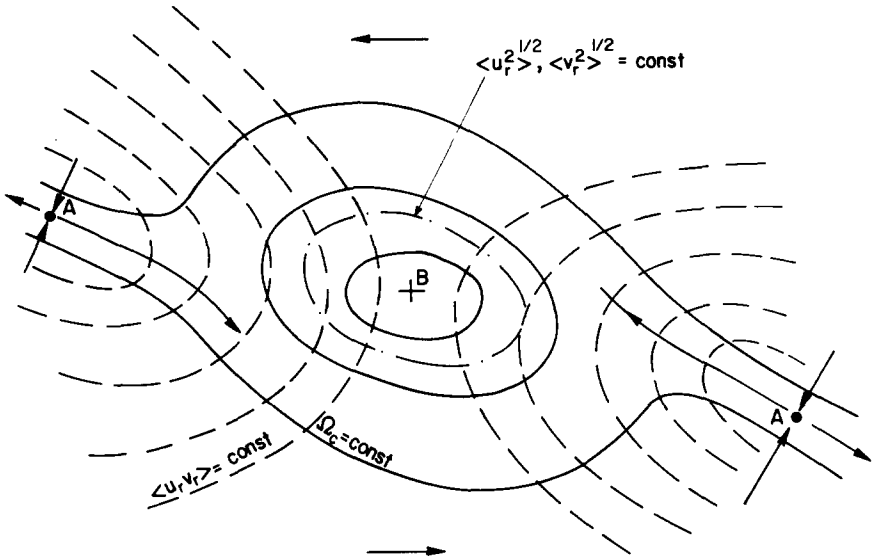

FIG. 2. Schematic of a coherent structure in a shear flow.

The coherent structure resulting from instability of laminar flows is quite periodic and repeatable in the early stages of formation. The periodicity can be enhanced via controlled excitation. In either case, the structure properties can be determined via phase-locked measurements.[29] However, in the fully developed turbulent shear flows there is a large dispersion in the shape, size, orientation, strength, and convection velocity of the coherent structures, and the structures pass by a sensor at random intervals, and they have random trajectories. The dispersion increases with increasing distances from the point of structure formation. These present formidable constraints in the eduction of coherent structures.[138–148] Even in periodically induced structures, the constraints become serious with increasing distances downstream.

In the case of the wall boundary layer, the eduction of coherent motions suffers from additional complexities (see later). The following discussion is more relevant to structures in free turbulent flows and to outer structures in boundary layers.

In order to determine the coherent structure properties, the incoherent part has to be subtracted from any realization. This can be achieved via ensemble averaging, which retains phase information. That is, an average of a large number of successive structures at the same phase (or stage) of evolution will be free from the incoherent contribution. Care has to be taken to assure that only structures of the same mode and same subclass are included; otherwise, the ensemble-averaged structure will be too smeared to represent the physics.

A. Preferred mode

The mode denotes the characteristic geometric configuration of the structure in the physical space; for example, Hill's spherical vortex, hairpin vortex, vortex ring ($m = 0$), helical vortex ($m = \pm 1$), double helix ($m = \pm 2$), etc. The identification of the mode itself is a formidable undertaking as a variety of modes can occur in the same flow. Even for a single mode, there are large dispersions due to tilting, twisting, and other distortions. The mode detection would in general require simultaneous monitoring of signals from a large number of measurement points in a three-dimensional space traversed by the structures. If a mode is both dynamically significant and occurs frequently in a flow, this is called the "preferred mode" of the flow. One can then plan to investigate only the preferred mode and classify this mode in the parameter space defined by characteristic parameters like size, orientation, strength, convection velocity, etc., and then obtain the ensemble average for each subclass. This is a formidable, and clearly unwanted, undertaking.

The effort can be significantly economized if the multidimensional probability density function in the parameter space has a limited few peaks, or, in other words, if the flow has a few dominant preferred modes. In such cases, eduction of the dominant preferred modes may be all that is necessary as these can be assumed to perform most of the transport and to represent the essence of the shear flow. The most fortunate situation of all would be if the flow has a unique preferred mode. (The near field of an axisymmetric jet appears to be blessed as such[4] and has been examined in detail via controlled excitation[149] as well as via conditional sampling for natural structures.[140]) For simplicity, preferred mode will be used to denote the dominant preferred mode.

B. Phase alignment via cross correlation

Even when a turbulent flow has a unique preferred mode, eduction is complicated by the unavoidable jitter. Typically, the structure, at least in its early stage of formation, may have a characteristic "front" or ramp as a signature in the signal that will allow alignment of successive signal realizations for obtaining phase average. In other situations, there is typically a "footprint" of the passage of the structure in a signal obtained from outside the turbulent region.[139–145] In most cases, the structure signature is buried in high-amplitude incoherent turbulence and is devoid of a characteristic feature or front on which successive (signal) realizations can be phase aligned before taking ensemble average. (This is likely to be the case where there is no high-speed free stream as in the far fields of jets or outer layer structures in turbulent pipes and channels.) In such cases,

alignment can be obtained via successive improvement of the ensemble average, provided that signal records with hidden "signatures" of the structure can be captured. This is typically unsuccessful except via some method of pattern recognition. When the structure is induced, the approximate arrival time of the structure at a downstream location can be inferred from the consideration of an average structure convection velocity.[145] The eduction then involves time shifting each realization via optimization of the cross correlation of the realization with the ensemble average.[145,146] This extremely time-consuming (iterative) process can be significantly economized by smoothing the individual realizations before alignment. For smoothing, either filtering or short-time averaging (i.e., zero phase-shift filtering) can be used. However, smoothing should be used only to determine optimum time shifts; the unsmoothed signals, after being appropriately time shifted, should be used to obtain ensemble averages.[145,133]

Even after these elaborate steps, eduction is often unsatisfactory and the educed structure is typically weak (i.e., smeared); this calls for further refinement. One way to accentuate the educed structure is to selectively discard realizations which weaken the educed structure, for example, those realizations which require excessive time shifts for optimum alignment as this suggests unusual distortions of the structure.[145] A further refinement should be possible by discarding realizations which produce weak cross correlation with the ensemble average. In this way, the "weaklings" can be excluded; this method of enhancement is being used in our laboratory.[147,148]

C. Dynamical significance

In coherent structure eduction via selective ensemble averaging, care has to be taken to assure that a majority of the realizations is not discarded. Otherwise, the educed structure will be too select to have any dynamical significance. In all coherent structure investigations, the percentage of occurrence of the educed structure as a function of the total number of structures as well as the percentage of the times these structures occur must be stated. Of course, the key question to be answered in coherent structure investigations is: How important are these structures? That is, one must state their statistical as well as dynamical significance. Note that as the eduction criteria are made more stringent, the accepted structure population will decrease and the structure will appear more and more dominant, reaching an asymptote. The asymptotic structure, provided it is statistically significant, is the goal of the eduction. Depending on the optimum effort or patience of the experimentalist, refinement of eduction is justified up to a point, beyond which any refinement will have a marginal effect on the dynamical significance of structures.

In order to capture the spatial details of the structure, a large number of sensors would be required. Apart from the prohibitive cost, probe interference can become a problem. If the structure occurs periodically, a single probe will suffice to obtain spatial distributions of properties via phase-locked measurements.[29,149] When structure passages are not periodic, a significant economization results if spatial distribution in the streamwise direction is inferred from time traces. Such use of the Taylor hypothesis is restrictive[150–157] (see Sec. VII M). The property distribution in the transverse direction within the plane of measurement is typically obtained by a few sensors arranged in a convenient array. When "alignment" is used to educe structure properties, time shifts for different properties must be the same. In such a case, a simple approach is to determine the required time shift for optimum alignment from the signal containing the peak vorticity (i.e., from the sensor closest to the structure center). Signals from other sensors must be time shifted by the same amount. The best way to align signals from a rake of sensors is to achieve simultaneous optimization of cross correlation of signals from all sensors; that is, to determine the time shift that will produce maximum cross correlation over the sectional plane of the structure.

D. Eduction of natural structures

In the absence of any phase reference, eduction of natural structures is a sophisticated art. A technique developed by us involves recording the vorticity traces from a rake of X wires in a plane. These traces are then smoothed via short-time averaging. From these smoothed traces, time evolution of vorticity contours in the plane of the sensors is known. While locations of vorticity peaks (within a specified bound) identify vortex centers, the structure sizes are determined by requiring that short-time cross correlation of vorticity between two extreme transverse points across each center has a certain minimum value. Those structures with similar peak values of coherent vorticity and contour sizes are then aligned with respect to their centers (identified by peak vorticity) and then ensemble averaged. (That is, structures which are too small or distorted or have low peak coherent vorticity are rejected.) Further improvement in the alignment can be achieved via maximization of cross correlation of the smoothed vorticity maps in the (y, t) plane with the ensemble average. Our experience shows that the elaborate effort of this alignment over the cross section in the (y, t) plane via cross correlation produces negligible improvement over alignment on the coherent vorticity peaks alone.

If a flow has a variety of coherent structures it is not a terribly encouraging situation as eduction of these structures will be a prohibitive undertaking. Therefore, the coherent structure concept is interesting only if a select few kinds of coherent structures are predominant. Because of the unavoidable dispersion in the coherent structure characterstics and the complex, but subjective, criteria required for obtaining convergent ensemble average, it is tempting to capture an individual realization and perform some kind of spatial smoothing. This approach is both subjective and unsatisfactory, because the educed structure is dependent on the smoothing scheme, the length scale of smoothing cannot be constant everywhere over the cross section of the structure, and there is no test for convergence of the educed structure. Consequently, the educed structure (for example, Ref. 48) may not be the true structure as there is no way to tell if it has been excessively or inadequately smoothed; that is, whether the incoherent turbulence has been successfully removed!

On the other hand, such smoothing will remove large spatial gradients of properties, which are retained in the ensemble average. Furthermore, some evidence is necessary to assure that the educed structure is statistically significant and not a freak event.

E. Induced versus natural structures

In an attempt to circumvent the eduction problems introduced by the jitter in characteristic parameters of coherent structures, these structures have been explored in a number of studies via controlled excitation.[29,133,149] While controlled excitation has permitted documentation of the coherent structure properties via phase-locked measurements in more detail than is likely to be possible with natural structures, we must consider the relevance of these excited structures to the natural structures.

One point of view is that the excitation merely triggers or paces the initiation of a structure at the lip. Since its evolution in space and time must be governed by the given basic flow (and the governing equations with the specified initial and boundary conditions), the evolution of an excited structure cannot be different from a natural structure. This is perhaps a reasonable point of view provided that the excitation amplitude is small. Even then, structure evolution may depend on whether it is excited or not, as well as on the method of excitation. If the excitation is sinusoidal,[29,149] presumably at a frequency within the receptivity band of the basic state or at the preferred mode, all structures are started identically and are free from interaction with natural structures. However, the evolution of a structure in a similar crowd is quite different from that of an isolated structure in a random environment. If the excitation is impulsive,[133,145] the induced structure is interspersed between natural structures (with a large dispersion in their characteristics) with which it interacts as it evolves. It is also important to recognize that natural structures can vary distinctly in modes (say, $m = 0$, 1, 2,... in an axisymmetric jet), which may occur at random; on the other hand, the excited structure is typically of a single mode. Thus, higher modes, especially the $m = 1$ mode, may be suppressed or, at least, not forced by axisymmetric excitation. In this sense, evolution of an induced structure can be different from that of a natural structure.[52]

When the excitation amplitude is large, the structure formation and evolution are quite likely to be dependent on the excitation amplitude.[140] (Note that if the excitation period is an integral multiple of the instability period, then excitation can generate strong structures separated by weaker structures. Depending on the amplitude of excitation, this may result in simultaneous amalgamation of all natural structures around each strong structure. That is, if N structures are rolled up during each period of excitation, as many as N structures may wrap around one another in a single stage to form a single structure.[158–160])

VI. BRIEF COMMENTS ON COHERENT MOTIONS IN THE BOUNDARY LAYER

The understanding of coherent structures in turbulent wall layers is considerably poorer than in free shear flows. Even though the inhibition of transverse wandering of the structures by the presence of the wall is a decided advantage for eduction purposes, the wall itself presents problems. The poorer understanding is partly due to the fact that the most significant zone of activity, say $y^+ \lesssim 100$, is too narrow a slice of the boundary layer and too close to the wall to allow detailed measurements or flow visualization. Motion in the boundary layer is expected to be complex; intuitively, unlike the free shear flows, the boundary layer is not characterized by a single length scale and a single time scale. The existence of outer variables (U_∞, δ) and inner variables (U_*, ν) guarantees three regions of flow, the third being a thin region adjacent to the wall where motion is totally viscosity-dominated. (Even this apparently simple sublayer is shrouded with an amazing number of unresolved questions.[161–165]) Because of the inherent complexities, the boundary layer is quite likely to have more than one kind of coherent motion (typical eddies, hairpins, pockets, folds, streaks, fronts, bulges, vortex loops, Λ vortices) and as such, it is not surprising that understanding of the physics is not clearer. In fact, successive investigations continue to raise more questions than they answer.

A. The bursting phenomenon

It is generally agreed that the bursting process plays a dominant role in transports of mass, heat, and momentum and in production in a turbulent boundary layer.[166–171] The characteristic stages and the seemingly universal nature of bursting were established by Kline *et al.*[3] However, the understanding of the physics associated with the bursting event is at best qualitative. In spite of numerous studies of this event, it has not yet been possible to educe contours of any property (say, coherent vorticity, coherent Reynolds stress, incoherent Reynolds stress and turbulence intensities, coherent production, etc.) of the bursting coherent structure, presumably because of the random occurrence in location and time of this structure. Only Nishioka *et al.*[172] recently educed the contours of $\partial \langle u \rangle / \partial y$ during a particular accelerating phase of a bursting event in a turbulent pipe flow; similar contours presumably can be extracted from the ensemble average $\langle u(y) \rangle$ profiles in a flat plate boundary layer educed by Blackwelder and Kaplan.[173] It should be emphasized that $\partial \langle u \rangle / \partial y$ is neither the coherent shear rate nor the coherent vorticity because $\partial \langle v \rangle / \partial x$ is of comparable magnitude in turbulent shear flows.[157]

Thus, a lot remains unknown about bursting and the bursting coherent structure. What is the precise definition of bursting? What is the role and significance of bursting? What causes bursting? Is bursting the consequence of a vortex impinging on the wall or of the interaction with the wall of a high-speed front? How do the different phases of bursting as observed visually relate to the details of signals from sensors in the flow? What is the wall pressure signature of bursting? Is the reported high bursting rate the artifact of false alarms or noise in the signal? Do the sensors themselves trigger bursting? What do low counts of bursting mean? Should bursting be counted at a point, along a line or over an area?

It is now generally agreed that maximum production occurs in a thin region adjacent to the wall and primarily during the ejection phase and somewhat less so during the sweep phase of bursting. Since this wall-dominated production mechanism via the bursting event should occur for the entire flow length, coherent motion in the turbulent boundary layer appears to be ever dominant. The structures involved are considerably smaller than the boundary layer thickness and are, by our definition, coherent substructures. The large-scale coherent structures in the turbulent boundary layer, which are obviously characteristic of the outer layer, are not yet known to play any dominant role.

B. Turbulent spot

The understanding regarding the turbulent spot in a laminar boundary layer[130–132] is considerably more detailed, allowing adequate description of the flow. This is perhaps because the spot signature and boundary are well defined. Different detection schemes have produced essentially identical spot boundaries, even though the celerity ($0.65U_\infty$) measured by Wygnanski *et al.*[131] differed considerably from that ($0.85U_\infty$) measured by Coles and Barker.[130] However, the recent realization prompted by Klebanoff[174,175] and Perry *et al.*[176] that the spot is not a single structure, but an assemblage of hairpin-like vortices[34] suggests that reexamination and modification of the contours of the spot properties are in order; the studies so far have missed the internal details of the spot. It is likely that the turbulent boundary layer involves successive stages of local instability, perhaps mostly of the Kelvin–Helmholtz type rather than the Tollmien–Schlichting type. However, there is as yet no evidence that the spot is a characteristic structure of the turbulent boundary layer. It appears that studies of the spot in a laminar boundary layer, while extremely interesting in their own right, are not of any direct relevance to the turbulent boundary layer. The behavior of a cluster of hairpin eddies in a laminar environment should be quite different from the behavior of the cluster in a sea of random hairpin eddies.

Even though the existence of hairpin vortices in a turbulent boundary layer was mentioned and emphasized previously,[175–179] a convincing demonstration of the hairpin-like vortices in the fully turbulent boundary layer has been made only recently via flow visualization.[27] However, the connection of these hairpin vortices with the large-scale structures in the boundary layer[164,180–183] is not known. The origin of the Brown–Thomas structure[182] and its connection with bursting and the hairpin vortices is also quite elusive. Since Brown and Thomas suggest this structure to be responsible for triggering bursting, the Brown–Thomas structure is supposed to occur frequently. However, a variety of flow visualization studies in a number of laboratories have failed to show the Brown–Thomas structure, let alone its overwhelming presence. Falco's[183] claim that the typical eddy—which is of the size of the Taylor microscale and hence at least an order of magnitude smaller than the boundary layer thickness—is responsible for production of most Reynolds stress in the outer flow, needs careful verification. Falco has not explained why the typical eddy, being a characteristic feature of the outer layer, scales on the inner variables. Falco[164] disagrees with the suggestion of Head and Bandyopadhyay[27] that the typical eddy is the tip of a hairpin vortex because the former occurs in isolation and has a rotation opposite to that of the hairpin vortex.

C. Streaks

The mechanisms for the formation of the counter-rotating vortices and their connection with bursting are quite complex and still not understood. Even though it has been long contended by many that streaks mark the stagnant regions between counter-rotating longitudinal wall vortices, which are responsible for scooping fluid up from the wall and contributing to heat, mass, and momentum transport near the wall and especially in the production of wall shear stress, there is yet no clear understanding of their origin, their role in transporting (spanwise) vorticity from the wall, or even whether they always occur in pairs. Whether these vortices form from interaction of the front and the ejection or from pockets formed by a ring approaching the wall[164] is debatable. Are these vortices the legs of the hairpin vortices? If they are, their circulation will be opposite to those suggested by the two formation mechanisms just mentioned. It is not known if the wall vortices terminate into hairpin eddies extending all the way into the outer region. Since vortices must either close or end in a wall it is not clear how the longitudinal vortices end. Whether the longitudinal vortices are responsible for liftup and thus initiation of bursting, or whether these play a crucial role in the dynamics of the boundary layer motion, remains unresolved. While the spanwise spacing of $\Delta Z^+ \simeq 100$ of longitudinal streaks, first proposed by Kline *et al.*,[3] has been verified by many other investigators (actual numbers vary between 60 and 200), the role of the sublayer in initiation of bursting appears to be in contention. Grass[184] has shown that the ejections and sweeps near the wall are unaffected by surface roughness. This would suggest that the sublayer is irrelevant to the bursting phenomenon—which appears to be different from the observations of Kline *et al.*[3]

D. Bursting frequency

Perhaps because of the ease of its measurement, the average time T_b between bursts has been measured by many investigators.[3,185–191] The association of bursting with the sublayer structures motivated early investigators to scale it with wall variables.[3] However, Rao *et al.*[185] showed that this scales with the outer variables. Even though many investigators have found T_b to be essentially constant across the boundary layer, data show significant scatter. After examining accumulated data, Cantwell[32] concluded "Now it appears to be fairly well established that T_b scales with the outer variables and the generally accepted number is $T_b U_\infty/\delta \simeq 6$." This author feels that bursting, which is visualized to originate near the wall, must scale on the wall variables. In fact, there are some claims supporting this view,[192,193] and it appears that further careful studies are necessary. Whether the bursting frequency scales with the outer or inner variables is intimately connected with the question of coupling of motions in inner and outer layers. A number

of experiments have been carried out addressing this question, and a number of qualitative models have been proposed, but none appears to be convincing.

Even though it was initially believed that the bursting structure grows to form the outer structure, the converse is beginning to emerge as more likely. That is, bursting is perhaps triggered by outer layer structures. It is not clear whether this effect is via the pressure field of the large-scale motions of the outer layer or through the direct effect of a front or a vortex moving wallward. It is quite likely that the entire chain of events works in a closed loop via feedback. This is suggested by the fact that the frequency of passage of outer layer large-scale structures is of the same order as the bursting frequency. However, if this feedback is central, it would seem that bursting in the pipe and channel flow should differ from that in the boundary layer because the outer structures should be different. Also, the effect of the other wall should be felt through the pressure field. So far, no difference has been reported between bursting in an external boundary layer and in a channel or a pipe. Is the inner–outer flow coupling in the pipe and channel flow different from that in a boundary layer? The answer to this question is not known. The mechanism for formation, sustenance, and destruction of bulges is also not known. Nor is it known how the bulges scale and if there is any Reynolds number effect.

There is a great deal of data on the wall pressure. However, these pressure signatures are yet to be explained in terms of the motion in the boundary layer or related closely with the wall shear stress. This is a complex problem because the wall pressure is a "footprint" of motions everywhere within the flow and cannot be uniquely related to the motion adjacent to the wall only. A close look at the wall pressure and boundary layer flow, perhaps via simultaneous measurements, is necessary.

E. Some unanswered questions

Many other related questions remain unanswered. For example: Does the bursting frequency and intensity vary with R_θ? If bursting is only a low-Reynolds-number phenomenon, then it cannot be as dynamically significant as it has so far been supposed to be. What is the effect of suction and blowing on bursting? Can periodic suction or blowing significantly alter the coherent structure in the boundary layer? How does bursting vary with the pressure gradient?[3,194] What is the variation of the size and angle of inclination of the hairpin vortices with R_θ and pressure gradient? Do the hairpin vortices undergo pairing? Are there hairpin vortices at very large R_θ? How are the statistics of large and small scales related?[195,196] What is the dynamical role of the streaks? What is the mechanism of formation of streaks? How do they depend on the Reynolds number? In what way are the pockets or folds related to the counter-rotating vortex rolls near the wall?[197,198] How is a pocket formed? What happens to the longitudinal vortices when sweep occurs? Are the large-scale bulges of the outer region the colonies of hairpin vortices? What is the mechanics of entrainment in a boundary layer? Is the penetration of the irrotational fluid into the boundary layer induced by circulation associated with the outer layer large-scale structure or by a local low pressure near the wall? Which way are the outer layer structures in the pipe or the channel different from those in the boundary layer? Does a turbulent pipe flow consist of axisymmetric or helical structures? What are the relative roles of coherent structures and incoherent turbulence in production and transport? How large is the coherent vorticity in the bulges, streaks?

Therefore, not only are there a variety of coherent substructures in the turbulent boundary layer, their details are also not well understood. It seems that it should be possible to induce bursting at a fixed location at regular intervals and thus educe contours of its properties at different phases in its evolution. It should also be possible to modulate/control natural bursting structure through controlled pulsation of the boundary layer. Since bursting is more energetic and less frequent in the presence of polymer additives,[199] it seems that a boundary layer with a polymer additive would provide a better opportunity for the investigation of the bursting structure.

If the coherent structure plays a key role in the transport phenomena in a boundary layer, then excitation at the bursting frequency should alter the bursting event and thus the overall characteristics of the boundary layer. However, all experiments of periodic modulation of the boundary layer show lack of any influence of the excitation on the time-average measures like $U(y)$, $u'(y)$ except very close to the wall, i.e., $y^+ < 50$,[200–202] even though experiments of Mizushina *et al.*[203] showed some effects. Furthermore, destruction of coherent structures by some obstruction should also produce significant changes in the boundary layer behavior. Even though the interference of the boundary layer with a screen or a honeycomb has resulted in decrease of skin friction downstream,[204–206] it is not certain that the decreased skin friction can compensate for the device drag; that is, that the total drag can be reduced; Nagib (private communication) claims to have achieved such a device. A clear explanation has not yet been possible establishing that the drag reduction is due to coherent structure modification alone. There is some prospect for boundary layer coherent structure control via periodic suction[207] and perhaps even periodic injection. Optimum choices may be found which might produce a net drag reduction. Success of such an approach is yet to be demonstrated.

VII. COHERENT STRUCTURES IN FREE TURBULENT SHEAR FLOWS

Coherent structures have been the objects of extensive investigations in the author's laboratory. In the following, results of a few of these studies will be very briefly reviewed. This paper is not intended to be a comprehensive survey of studies of coherent structures. Nor will any attempt be made to review results from other laboratories except in cases when those directly relate to our results. (For a review on coherent structures, see Ref. 32.)

A. The axisymmetric mixing layer

The axisymmetric mixing layer is a complex flow because of the influence of two length scales: the shear-layer

thickness and the radius of curvature. Provided that the initial (shear-layer) momentum thickness θ_e is considerably smaller than the jet diameter D (i.e., $\theta_e/D \ll 1$), the instability and rollup of the axisymmetric shear layer is similar to that of the plane layer. However, when the thickness becomes appreciable, say at $x/D \sim 1$, the effect of the curvature becomes significant. The initial instability of the shear layer is found to follow that of an inviscid parallel flow theory[208–210] even though the nonparallel nature of the shear layer must be taken into account for accurate prediction of the subsequent evolution.[14,211]

Because of the two length scales, the axisymmetric mixing layer has two kinds of coherent structures: the shear-layer mode scaling on the initial momentum thickness and the jet-column mode scaling on the jet diameter.[158] The latter may form independent of the former or when the flow is excited in the jet-column mode directly; it can also result from pairing (see later) or evolution of the shear-layer mode structures. Additional complication of the axisymmetric layer arises from evolution of azimuthal lobes[29,212–214] of the initial axisymmetric ring structures. The resulting breakdown into azimuthally distributed substructures and their interactions near the end of the potential core have escaped detailed examination so far. It is quite likely that the flow becomes fine grained due to breakdown of the coherent structures soon after the end of the potential core, and that the turbulent jet farther downstream undergoes its own instability determined by the local instantaneous flow state (further discussion later).

The rollup of the initial shear layer into axisymmetric modes does not appear to be unique, as some investigators have observed helical modes.[215–220] However, the presence of any puffing due to the unavoidable background disturbances, no matter what the source, will force the rollup of the shear layer into axisymmetric modes. Thus, this question cannot be easily answered in any practical jet. The initial instability of the mixing layer in various jets in our laboratory has been found to be axisymmetric. Instantaneous velocity signals from a number of hot wires aligned azimuthally in the shear layer near the exit of a large air jet reveals that the instability and rollup of an unexcited shear layer, as well as the large-scale structure following the rollup are instantaneously almost axisymmetric.[221] Contours of educed natural coherent structure properties remained insensitive to the azimuthal location of the trigger probe, thus confirming that the naturally occurring turbulent coherent structures up to $x/D \sim 3$ are virtually axisymmetric.[140] Furthermore, careful flow visualization of a large submerged water jet ($D = 10$ cm) in our laboratory, in a facility where the jet flow is maintained under a constant head from an overhead tank and thus remarkably free from any disturbance, showed the initial rollup to be always axisymmetric even though the vortex rings are occasionally tilted after one or two pairings. This tilting appears to originate from an interaction (between two adjacent axisymmetric vortex rings) which is not uniform azimuthally. It is possible that many investigators have interpreted this tilting as helical mode instability of axisymmetric shear layers. Helical mode instability of a fully developed laminar jet[215] or even the turbulent jet far field is possible. We have not observed the initiation of a helical rollup near the lip of an axisymmetric jet, somewhat like peeling off of the rolled-up vortex successively around the perimeter of the jet lip. Drubka and Nagib[219] have claimed that the initial instability consists of both axisymmetric and helical modes, the two modes switching from one to the other in an intermittent manner. This claim, also made by Moore,[222] is puzzling because a helical vortex terminating on axisymmetric rings at either end does not appear to be kinematically possible. Further careful studies are necessary to interpret the observations of Drubka and Nagib.

The sensitivity of all measures of the axisymmetric mixing layer to the initial condition (say, laminar versus turbulent), found in the axisymmetric mixing layer of a small jet,[115,118,119] prompted a study of this sensitivity in larger jets of diameters up to 27 cm.[120,74] However, all time-average measures of the layer like its thickness, turbulence intensity, Reynolds stress, etc., were found to be strongly dependent on the initial condition. On the other hand, as speculated earlier,[116,117] the plane mixing layer has been found to achieve a universal state independent of the initial condition, at a distance of about $2000\theta_e$ from the origin.[124]

The coherent structures in the axisymmetric mixing layer also reveal dependence on the initial condition. This dependence has been studied via flow visualization,[50] wavenumber-celerity spectra,[74] and educed (excited and unexcited) coherent structures.[29,140]

High-speed ciné films reveal that the mixing layer, which is well organized at a low Reynolds number Re_D, becomes comparatively more disorganized with increasing Re_D. The survival distance of a structure does not appear to be much larger than one average structure size. In contrast with the initially laminar layer, the initially turbulent axisymmetric mixing layer is comparatively more organized and the structures are smaller and comparatively more periodic. Evolution of the large-scale structures in time occurs not through complete pairing,[18] as widely believed, but mostly through a combination of tearing, fractional pairing between segments torn from different large-scale structures, or partial pairing when one structure captures only a (low-speed) part of a downstream structure. These complex interactions explain[74] the heretofore puzzling observation that the structure passage frequency shows a large variation (about threefold) across the thickness of the mixing layer.[50,144] The flow-visualization study does not bear out the two-vortex street model proposed by Lau[144] as an explanation for the freuquency jump. Figures 3(a)–3(c) show some picture sequences from high-speed ciné films for laminar and turbulent initial shear layers. Note that in the initially turbulent case [say frame 11 in Fig. 3(b) and frame 14 in Fig. 3(c)], the shear layer consists of structures which are more compact and more periodic than in the initially laminar case.

Because of the complex nature of the motion in the axisymmetric mixing layer,[31,50,141] the motion is less coherent across the layer than in the plane mixing layer.[30,109,140] Thus, eduction will unavoidably suffer from some smearing. Therefore, in order to characterize the structures, a statistical approach is perhaps of interest. With this in mind, the large-scale structures were studied via hot-wire measure-

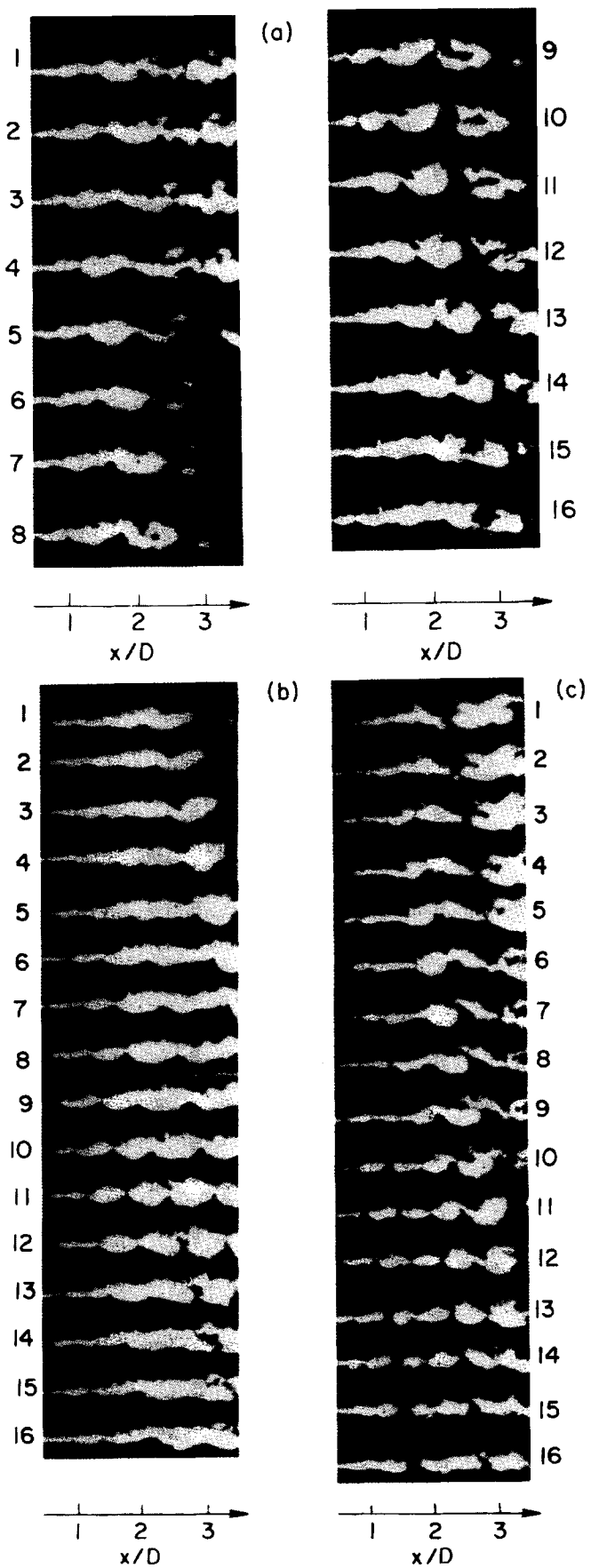

FIG. 3. Visualization picture sequences in an axisymmetric mixing layer of an 18 cm jet at $U_e = 30$ m/sec. Here, δt denotes time lapses between successive frames. (a) Laminar, $\delta t = 0.5$ msec, (b) turbulent, $\delta t = 1.67$ msec, and (c) turbulent, $\delta t = 1.61$ msec.

ments of the wavenumber-celerity spectrum $W(k, U)$ obtained from double-Fourier transformation of space-time correlation data taken along lines of constant velocity.[74] Figures 4(a) and 4(b) show contours of constant percentage values of W as a function of the wavenumber k and the convection velocity U. Note that the dominant structure size (corresponding to the peak of W) is smaller in the initially turbulent case, consistent with the observations made via flow visualization. Care was taken to assure that the trip produced a fully developed turbulent boundary layer, in accordance with the criteria listed in Sec. III. Since the flow conditions were identical in every detail, except for the presence of the trip for the turbulent case, the obvious differences observed in the structures [both flow-visualization pictures in Fig. 3 and $W(k, U)$ data in Fig. 4] cannot be attributed to any pecularity of the facility; these differences are uniquely due to the initial condition. Note that these pictures (Fig. 3) represent visualization of the axisymmetric mixing layer at the highest-Reynolds-number jet flow ($\mathrm{Re}_D = 3.7\times 10^5$) reported so far.

There is a curious observation regarding the instability of the unexcited, laminar axisymmetric shear layer. While the maximum amplification rate is found to occur at the Strouhal member $\mathrm{St}_\theta \cong 0.017$[159] (consistent with Michalke's[208] theory) and the maximum amplification is found to occur at a much lower value ($\mathrm{St}_\theta \sim 0.011$),[87] the natural instability (of an unexcited laminar shear layer) is found to occur at an intermediate value. This value appears to depend on the jet radius and the free-stream turbulence level.[223] These suggest that some kind of feedback from downstream coherent structures is involved in triggering the instability.

B. Vortex pairing in an axisymmetric jet

The coherent structure in the near field of a circular jet can be of the shear-layer mode or jet-column mode and can undergo pairing in two distinct modes.[158,224] The time-average turbulence intensity and Reynolds stress distributions show large increases when pairing is stabilized, that is, when it occurs at the same location at regular intervals. Stable vortex pairing has been found to occur at two specific conditions: shear-layer mode pairing at $\mathrm{St}_\theta \cong 0.012$ and the jet-column mode pairing at $\mathrm{St}_D \cong 0.85$.[158,159] The former involves near-exit thin vortex rings when the exit boundary layer is laminar, independent of St_D. The latter involves thicker vortex rings at $x/D \simeq 1.75$ independent of St_θ or of whether the initial layer is laminar or turbulent. Pairing tends to be more intermittent with increasing Re_D and exit fluctuation level. In an axisymmetric jet, the terminal St_D near the end of potential core, which represents the preferred mode,[149] is in the range 0.3–0.5. Browand and Laufer[19] suggested that this terminal St_D results from successive pairings of shear-layer mode structures (see also Ref. 224). We have shown that such a requirement is not essential.[158,159] The evolution of the coherent structure downstream (say, at $x/D \simeq 1$) is not always dependent on the initial rolled-up structure. If the roll-up frequency f_s happens to be about $2^N f_t$ (where f_t is the terminal structure passage frequency corresponding to $f_t D/U_e \simeq 0.4$ and N is an integral number), and if N is not very large (i.e., $N = 1$ to 3), then f_t results from

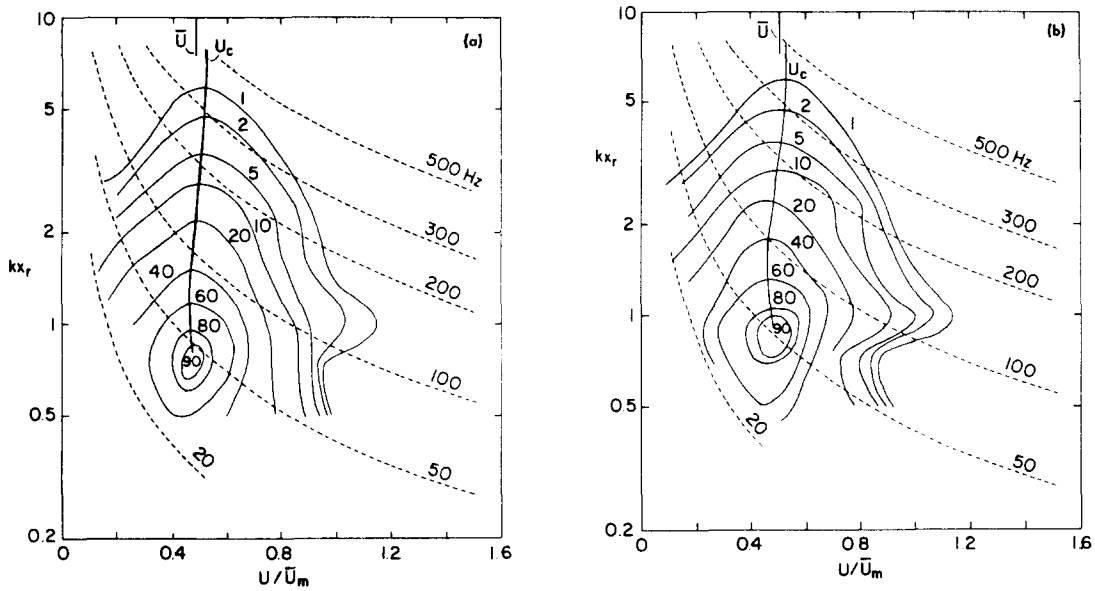

FIG. 4. Wavenumber-celerity spectrum $W(k, U)$ for $U_c = 30$ m/sec, $x_r = 1.41D$ at the half-mean velocity point; U_c is the wavenumber-dependent convection velocity, $\bar{U}$ is the local mean velocity, and $\bar{U}_m$ is the jet centerline velocity. (a) Initially laminar; and (b) initially turbulent.

successive N stages of the shear-layer mode of pairing. The number of successive pairings depends on θ_e/D but has not been found to exceed 3. If $f_s \gg 2^3 f_t$, a number of shear-layer structures may roll up together to form the jet mode structure.[158] Ho and Huang[160] have also shown subsequently that under controlled excitation, a number of vortices can be rolled up together; they termed it collective interaction.

Stable jet-column mode pairing was induced in a 7.6 cm air jet at $\mathrm{Re}_D = 32\,000$ and the contours of coherent structure properties were educed over the spatial extent of the structures via phase-locked measurements (thus without invoking the Taylor hypothesis) with hot wires under the automated control of a laboratory computer. These measurements include different phases during the pairing event as well as locations preceding and following the pairing event. The pairing event is associated with large excursions of the $\widetilde{uv}(t)$ signal. The coherent Reynolds stress is high during pairing (the zone-average coherent Reynolds stress over the cross section of the merging vortex pair is much larger than over a single vortex preceding or following pairing), being the highest at an early stage of pairing; see Sec. VIIN. On the other hand, entrainment, turbulent breakdown, and rapid diffusion of vorticity occurs at a later stage of the pairing event. The merger of two like-signed vortices results in a decrease of the core peak vorticity. The rapid decrease of peak vorticity is caused by the incoherent turbulence produced at the saddles but advected to the structure core. Controlled excitation enhances the initial circumferential coherence of the vortical structures, but is ineffective in delaying turbulent breakdown near the end of the potential core via growth of the azimuthal lobe structures.[29] The coherent Reynolds stress is found to be much larger than the incoherent Reynolds stress only initially, but these two are comparable near the end of the potential core.

Vortex pairing has a number of interesting implications regarding entrainment and noise production (see Secs. VIID and VIIE). Winant and Browand[18] claimed that pairing was responsible for most of the entrainment in a mixing layer. However, from the image processing of the mixing layer ciné films of Brown and Roshko, and Herman and Jimenez[33] found that 80% of the entrainment involved no pairing.

C. Preferred mode of the axisymmetric jet

The Strouhal number St_D of the preferred mode of a jet depends somewhat on the Reynolds number and the Mach number, and falls in the range 0.3–0.5. The preferred-mode structure was enhanced via controlled excitation and the detailed spatial distributions of properties of the structure were determined via phase-locked measurements for both laminar and turbulent initial conditions and for a range of the Reynolds number.[149] These properties of the induced structures are found to be independent of the initial condition but show some mild but systematic dependence on the Reynolds number. No phase-locked coherent structure could be detected beyond $x/D \simeq 6$. The continually evolving shape (including tilting) of the coherent structure explains the transverse variations of the wavelength and convection velocity across the mixing layer. Data cover contours of coherent longitudinal and lateral velocities, incoherent turbulence intensities and Reynolds stress, coherent Reynolds stress, vorticity, strain rate, and production, streamlines, and pseudo-streamfunction in far greater detail than has been possible for other situations because the structures are induced and noninteracting. These contours provide the detailed topological relationships between the contours of these different properties. These contours, not presented here, are consistent with the expectations briefly discussed in Sec. IVD.

D. Coherent structure and jet noise

The widespread belief that coherent structures play a key role in jet noise production[222,224–235] is relevant to address

here briefly. Unfortunately, neither the extent to which the large-scale coherent structures are significant in noise production nor the precise mechanism is known yet. Laufer[234] proposed that vortex pairing was the primary mechanism for noise production. Even though this notion found support from many sources (for example, Ffowcs-Williams and Kempton,[235] Kibens,[224] and Crighton[225]), we felt[149,236] this was unlikely and suggested an alternative mechanism.

Our basis for discarding vortex pairing as the key factor in jet noise production was as follows. In most practical jets, vortex pairing is known to be complete before $x/D \simeq 2$.[19,20,31,141] On the other hand, most noise originates in the range $3 < X/D < 12$,[229,237] the peak moving downstream with increasing Mach numbers. The noise contribution varies with frequency, the maximum contribution being from the preferred mode which peaks at $x = 6D$.[229] Furthermore, excitation at the preferred mode can completely suppress pairing,[149] but is not likely to alter noise production noticeably (an effort is underway in our laboratory to verify this experimentally). Also, all practical jets are initially turbulent; they typically roll up at the preferred mode and thus involve no pairing. Therefore, while vortex pairing can produce noise and noise production can be enhanced by inducing vortex pairing, it is not likely to be the mechanism responsible for most noise production in practical jets.

An alternative mechanism was proposed by the author [first informally a few years back, then more formally at the 1981 IUTAM Symposium on Unsteady Turbulent Shear Flows at Toulouse, France, and the 1981 Stanford Workshop on Jet Flow (organized by Nagib and Reynolds); see also Ref. 236]. It is now well known that the near-field vortex rings in the axisymmetric jet develop azimuthal lobes via the so-called Widnall instability,[212–214] starting from about two diameters (depending on Re_D) from the exit. The proposal is that it is the rapid breakdown of the toroidal rings into azimuthally distributed substructures and the interactions of these substructures which are responsible for most jet noise production. (Details of the noise-producing events are not clear but most likely involve "cut and recombination" of vortex tubes resulting in the formation of substructures.) An unambiguous test of this hypothesis is not likely to be straightforward, because of the extremely complex flow involved in the noise-producing region as well as the difficulty in visualizing the flow details and in controlling the events in this region.

E. Broadband noise amplification via pure-tone excitation

Contrary to Kibens' recent dramatic results[224] showing that excitation of a jet at $Re_D = 5 \times 10^4$ produces broadband far-field noise suppression, Bechert and Pfizenmaier[226] and Moore[222] had independently discovered earlier that pure-tone excitation of a jet (at higher Re_D) can produce broadband far-field noise amplification. This observation has captured a lot of attention because not only is it unexpected and unexplained, but this might be the explanation for the excess or core noise, which is the difference (about 10 dB) between scaled-up model data and jet engine data. Since there are many aerodynamic or thermal sources of internal fluctuations, inherent differences in the broadband noise of two rigs due to such fluctuations (if these cause broadband noise amplification) may render comparison of data from two rigs meaningless.

Kibens[224] claims that pairing produces significant jet noise and argues that in situations where pairing locations are not spatially fixed (as achieved first in our laboratory[158] via controlled excitation), the interaction of jet-column and shear-layer modes will introduce jitter in the shear-layer mode pairings, which should produce broadband noise amplification. A similar explanation for broadband noise amplification is implied by Ffowcs-Williams and Kempton[235] and Crighton.[225]

A piece of technological research in our laboratory with the whistler nozzle[92] has provided some insight into the question of broadband noise amplification. It has been shown that self-sustained excitation with the whistler nozzle—which works for both laminar and turbulent exit boundary layers—produces broadband *turbulence* amplification in the noise-producing region[91] as well as broadband *noise* amplification (about 10 dB) in the far field.[94] For the initially turbulent shear layer of typical laboratory jets, there is no shear-layer mode of pairing.[158] The self-excitation via a whistler nozzle being always within the St_D range 0.35–0.6, the structures formed by the whistler excitation are the jet preferred modes,[149] which occur at the terminal Strouhal number within the jet near field and do not undergo pairing. Thus, jitter in pairing cannot be the explanation for broadband noise amplification. It was shown that controlled axisymmetric excitation cannot prevent the breakdown of the initially formed toroidal structures in a jet.[29] Even when excited, the turbulence spectrum shows no peak for $x/D \gtrsim 6$. Also, noninteracting structures are ineffective in radiating noise at subsonic speeds. The breakdown of the toroidal structures into azimuthally distributed substructures and interactions of these sub-structures appear to be viable mechanisms for noise production; formation of these substructures may have phase coherence with each other but their interactions would appear random in their far-field acoustic signature. The effect of tonal excitation on the interaction of these substructures is not known. We propose that controlled axisymmetric excitation delays the evolution of the azimuthal lobes farther downstream; consequently, less time is allowed for the breakdown of the toroidal structures before the end of the potential core, and the resulting rapid breakdown into the substructures and their interactions produce broadband noise amplification.

F. Evidence of coherent structure feedback

In case of self-sustained oscillations of free shear flows impinging on solid objects, as in the case of jet tone, hole tone, ring tone, plate tone, and shear-layer tone,[83–89] upstream feedback of coherent structures triggers instability and formations of successive structures. However, even in the absence of an impingement surface, it has been speculated for long by us and others (for example, Ref. 238) that large-scale structures produce a feedback upstream. This is perhaps the reason why even an unexcited jet or shear layer

has an essentially periodic rollup when the Reynolds number or exit fluctuation level is not high.[140] However, no one has yet been able to produce a definitive proof of this feedback. It seems that our whistler nozzle excitation studies provide a direct evidence of upstream feedback.

It has been shown that the whistler nozzle is an organ-pipe resonance of the pipe nozzle driven by the shear-layer tone between the lips of the pipe and collar.[92] Thus, any of the $\lambda/2, \lambda, 3\lambda/2, 2\lambda$, etc., organ-pipe modes of the pipe nozzle can be excited. However, it appears that the excitation driven by the shear-layer tone always prefers a mode for which St_D is in the range 0.3–0.6. This being the range of occurrence of the dominant coherent structure (i.e., the preferred mode) in the flow downstream, it would appear that the mode selection happens via upstream feedback from the dominant coherent structure in the jet. Even though the shear-layer tone is the driving mechanism for the whistler nozzle phenomenon,[92] it seems that organ-pipe resonance will be receptive to excitation from outside also. That is, when the shear-layer tone frequency is irrelevant to the organ-pipe modes of the pipe nozzle, a disturbance from the flow, if it matches an organ-pipe mode, can trigger the latter resonance. This disturbance can originate from the quasiperiodic preferred-mode coherent structures in the jet near-field. Since the dominant coherent structures in a jet occur in a range of St_D (i.e., 0.3–0.6),[149] an organ-pipe mode can be typically found within this frequency range. The facts that the preferred-mode structures are neither exactly periodic nor perhaps produce strong feedback are no obstacles to our hypothesis because it has already been shown that whistler nozzle excitation is possible by disturbances which are neither pure-tone nor strong.[92] Thus, there appears to be a convincing demonstration of the upstream feedback of coherent structures. Note that Kibens[239] also appears to have independently observed weak pipe-nozzle resonance without a collar, which tends to support the feedback concept.

G. Turbulence suppression via controlled excitation

While controlled excitation typically organizes and enhances instability, experimentations revealed turbulence suppression (by as much as 80%) near the exit of an axisymmetric jet under controlled excitation.[240] We found our data puzzling because Crow and Champagne's data[4] did not show this suppression; it now appears that it is not likely that this suppression can be avoided. After we observed the suppression phenomenon, we learned that Vlasov and Ginevskiy[241] also had found similar suppression. However, they neither explained nor focused on this apparently curious phenomenon.

Explorations in a number of axisymmetric and plane jets and plane mixing layers in our laboratory helped us to establish the universal nature of this suppression phenomenon and its unique connection with the shear-layer instability and inhibition of pairing of the shear-layer structures.[36] In circular jets, the suppression occurs over the range $0.75 \lesssim x/D \lesssim 8$, while in the plane mixing layer, suppression can be detected as far as at $x/\theta_e \cong 6000$. The suppression effect produced by controlled excitation is summarized in Figs. 5(a) and 5(b) by plotting the ratio of longitudinal peak fluctuation intensity under excitation (u'_{ex}) to the unexcited value (u'_{ux}). Figure 5(a) shows that the suppression is the maximum at the Strouhal number $St_\theta \simeq 0.017$; at each frequency of excitation, the St_θ variation was achieved by changing the jet speed. Figure 5(b) shows that u'_{ex}/u'_{ux}, measured along a $y = \text{const}$ line in a number of facilities, becomes the minimum at $x/\theta_e \sim 400$. Note that other components of turbulence and the Reynolds stress also show similar suppression.[36] It was shown that suppression is a straightforward consequence of earlier transition, induced by the excitation, of the shear-layer vortices which otherwise naturally grow to larger sizes and survive for larger x. Exci-

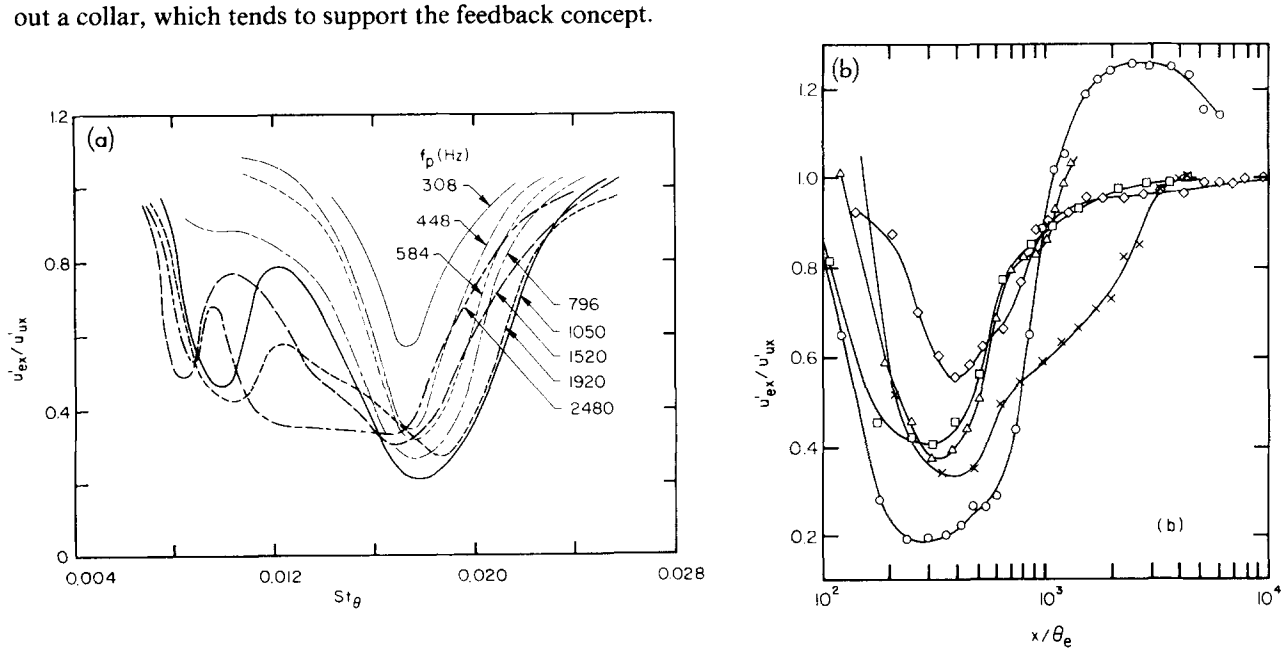

FIG. 5. Turbulence suppression in shear flows. (a) Dependence of u'_{ex}/u'_{ux} on frequency and St_θ in a 2.54 cm jet, measured on the jet centerline at $x/D = 4$. (b) Downstream variation of u'_{ex}/u'_{ux} for $St_\theta \simeq 0.017$, measured along a $y = \text{const}$ line near the lip. ×, 18 cm circular jet; ○, 2.54 cm circular jet; △, 3.18 cm plane jet; □, single-stream plane mixing layer at $U_c = 10$ m/sec; ◇, single-stream plane mixing layer at $U_c = 20$ m/sec.

tation at $St_\theta \cong 0.017$ produces a growth of the instability wave considerably faster than the natural instability (occurring at a lower St_θ) and thus produces earlier saturation, rollup, and breakdown and an associated inhibition of pairing. The result is a suppression everywhere of fluctuation intensities and the Reynolds stress. The higher growth rate, early rollup and breakdown of the structures, as well as inhibition of the last stage of pairing under excitation and the associated reduced shear-layer thickness, have been further documented in detail via flow visualization and via eduction of the coherent structures employing conditional sampling.[36] (The time-average measures of the axisymmetric shear layer including shear-layer thickness, turbulence intensities, Reynolds stress, normal and shear productions for controlled excitation at a frequency at $St_\theta \simeq 0.017$, and at its integral fractional frequencies have been documented via precision measurements.[120] These results show that the response of the shear layer to controlled small-amplitude excitation is considerably different from the results reported by Oster and Wyganski[242] for uncontrolled, large-amplitude excitation.)

It is necessary to emphasize that the suppression discussed here is different from the excitation-induced suppression (tail-pipe effect) in a jet resulting from the superposition of acoustic and hydrodynamic waves.[92,243,244] The possible coupling of these two separate effects is interesting and needs to be investigated.

The effect of controlled excitation on turbulence suppression has been investigated numerically by representing the shear layer by an array of a large number of point vortices, and the sensitivity of the suppression effect to the excitation wavelength and amplitude, as well as incoherent initial turbulence, have been determined. The computations[245] confirm the experimental results.

H. Turbulent "spots" in axisymmetric and plane mixing layers

How does a highly localized three-dimensional disturbance evolve in a mixing layer? In an attempt to answer this interesting question, an electrical spark was produced in the boundary layer slightly upstream of the lip of a large circular jet.[145] Unlike the sinusoidally induced periodic structures, the spot in this case is separated by natural structures with which it interacts as it evolves. The induced structure occupies about 4% of the time between two sparks. Using the spark as the phase reference, and considering an approximate structure convection velocity, 200 realizations of signals were captured with an X wire, the data sampling being controlled by an on-line laboratory computer. Signal alignment was done via iterative optimization of cross correlation of each realization with the ensemble average.

The spark induces a local boundary layer spot on the nozzle wall and simultaneously triggers a coherent structure in the shear layer. The spot decays downstream due to the lack of a sustaining mechanism. The coherent structure grows downstream in a non-self-preserving manner, traveling at about 60% of the core velocity. The eduction of this free shear-layer structure is far more complex than the boundary layer spot. The spark-induced structure undergoes complex interactions which produce its decay after $x \simeq D$. Because the induced structure interacts with other naturally occurring structures, the structure would have to be educed at much closer intervals in order to capture the details of its evolution. This study showed how to educe a structure in a highly turbulent environment and documented the topological details of the properties at three stations. Figure 6 shows the coherent vorticity contours of the educed spot structure at $x/D = 4.5$. Note that in comparison with the time-average vorticity (denoted on the right-hand side of the figure) the peak coherent vorticity is about 50% higher. For other coherent structure properties and further details see Ref. 133.

In an attempt to understand the interaction of two spots, two sparks located at diametrically opposite points were fired simultaneously, and the resulting structure properties were educed at different azimuthal planes. The variation of the properties with the azimuthal angle was found to be marginal.[246] This suggested to us that perhaps even a single spark induces an axisymmetric structure also. With a single spark, the structure properties were then educed at different azimuthal planes and these showed that the highly localized spark induces a structure which is essentially axisymmetric.[221]

It was then considered interesting to explore if the instability induced by the spark was instantaneously axisymmetric. For this, seven single wires were placed equally spaced in the azimuthal direction at the radius where $U/U_c = 0.8$. It was observed that the shear-layer instability, triggered by the spark, is instantaneously almost axisymmetric and that the front of the mixing layer spot is also aligned azimuthally. That is, all instantaneous undulations in the signals at different azimuthal locations are in phase around the periphery of the jet. Sufficiently away in time from the spot signature, natural instability is amplitude modulated and this modulation is also instantaneously axisymmetric.

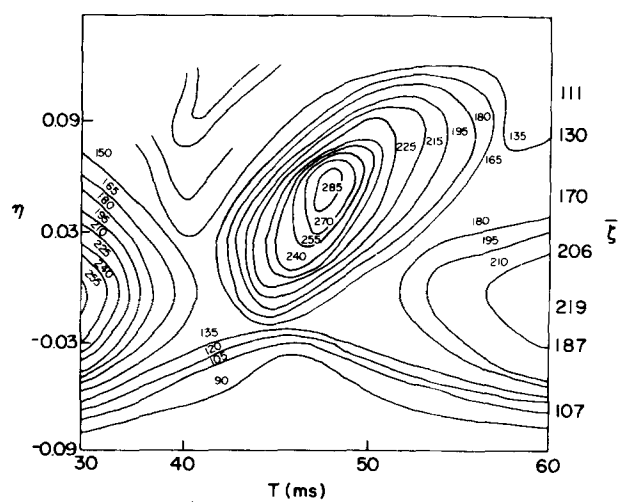

FIG. 6. Coherent vorticity contours of the mixing layer spot at $x/D = 4.5$; $D = 12.7$ cm; $\eta = (y - \frac{1}{2}D)/x$; $U_c = 20$ m/sec; and T is the time elapsed since spark.

A similar study with a spark in a plane mixing layer shows that the structure grows in a self-similar fashion in the downstream direction but the strength falls off in the spanwise direction.[247] A spark was fired in an initially fully turbulent plane mixing layer; however the eduction technique as described above failed to educe any structure.

I. Interaction of coherent structures in the near field of a plane jet

Effects of controlled excitation on the time-average measures in the near field of a plane jet[248] were found to be noticeably different from that in the axisymmetric jet.[4,19,20,159] This suggested that the nature of the coherent structure interactions in the near field might also be different. The investigations of Sato[249,250] and Mattingly and Criminale[251] addressed early stages of instability but not the structures downstream. Earlier flow-visualization pictures[252,253] suggested virtually independent evolutions of the two shear layers of the plane jet and suggested quite different near-field activities in the plane jet as opposed to those in the axisymmetric jet.[4,29,31,144,254,255]

The two shear layers of an initially laminar jet (aspect ratio 96:1, the gap width $D = 0.317$ cm, $\mathrm{Re}_D \cong 2000$) were marked with fluorescent dyes of two different colors and the interactions of the two shear layers were studied via ciné color films of the flow field illuminated with a sheet of laser light in different planes.[147] This study has been carried out for two exit conditions: thin laminar exit boundary layers following the contraction and laminar channel flow at the end of a channel attached to the downstream end of the nozzle. In the case of channel flow, the two shear layers roll up periodically into vortices, alternately. Adjacent (like-signed) vortices pair up independently on each side. Typically, the paired vortex (sometimes after two pairings) pulls part or all of a (single or weaker) vortex on the opposite side across the jet centerline because of the stronger circulation of the former and gets the weaker vortex wrapped around itself. There is an intense mixing associated with this wrapping process. In the case of thin boundary layers following a contraction, the symmetric mode appears to dominate; the instability, rollup, pairing, and breakdown of the two shear layers appear to occur in a symmetric manner. These visual observations are based on low-Re_D jets and need to be extended to higher-Re_D jets. However, the merger of two large-scale structures of opposite vorticity is unknown to this author and appears to be unique for the near field of a plane jet. These visual observations suggest that turbulent transport, entrainment, and aerodynamic noise production in the near field of a plane jet are likely to be of different character from those in the axisymmetric jet.

J. Natural coherent structures in the axisymmetric mixing layer

The large dispersions in the characteristic parameters of the structures encouraged their studies via controlled excitation, which induces identical structure and thus provides the convenience of phase-locked measurements. A number of questions remained outstanding regarding: the relationship between the induced and natural structures, the optimum conditional sampling technique for eduction, the sensitivity of the natural structures to the Reynolds number and the initial condition, etc.

It has been shown[140] that by phase-locking onto the longitudinal velocity $\tilde{u}$ signal extrema, the natural coherent structures can be successfully educed. The optimum location for the trigger probe is the high-speed edge of the mixing layer, say the transverse location where $U/U_c \simeq 0.99$, as the structure footprint is the strongest on the high-speed edge and is further accentuated by the axisymmetric configuration. Since the smearing is larger with increasing time lapses between the trigger and the structure center, the trigger criterion should be chosen such that it occurs closest (in time) to the structure center. Eduction triggered on the positive peaks of the $\tilde{u}$ signal is more successful than when triggered on the negative peaks, because the positive peaks occur closest to the structure center. Even though progressively higher peaks produce better eduction, threshold levels higher than twice the standard deviation σ of the $\tilde{u}$ signal are not worthwhile as only marginal improvements are obtained while prohibitively increasing the experiment time. Use of the transverse velocity $\tilde{v}$, or a joint criterion based on both $\tilde{u}$ and $\tilde{v}$, from the high-speed side produces no improvement in the eduction.

The extrema of any signal from the low-speed edge of the layer do not facilitate eduction. Furthermore, there is no significant phase relationship between the peaks of the $\tilde{u}$ signal on the high-speed and zero-speed edges of the mixing layer. Both of these observations may suggest that the peaks in the $\tilde{u}$ signal at the outer edge of the axisymmetric mixing layer are not uniquely related to the primary structure, contrary to the suggestions by Bruun[141] and Yule.[31] The weaker organization on the outer edge of the axisymmetric layer is a consequence of the geometry since a much stronger organization is observed in the single-stream plane mixing layer. The unavoidable flow reversal[29,50,256-258] is not responsible for this poorer eduction; in fact, the instants of flow reversal are uniquely related to advecting coherent structures, and the rectified signal peaks can also be used to detect structures. Therefore, since peaks on the zero-speed side signal must be footprints of some highly energetic events, the foregoing observations suggest that the axisymmetric mixing layer does not consist of structures always spanning the thickness of the layer, but consists of substructures formed via tearing and partial pairing (observed via flow visualization[50]). The lack of correlation between $\tilde{u}$ peaks on the high-speed and low-speed edges of the axisymmetric mixing layer supports this notion and is also consistent with the observed large variation (about threefold) in the structure passage frequency across the layer.[74,144]

The simple eduction scheme of triggering on the positive peaks ($> 2\sigma$) of the high-speed edge $\tilde{u}$ signal was applied to axisymmetric mixing layers with different Reynolds numbers Re_D and initial conditions. The technique successfully educed structures for the highest Re_D jet available, i.e., $\mathrm{Re}_D = 8 \times 10^5$. While no noticeable Re_D dependence of the natural structures was observed over the range $5 \times 10^4 < \mathrm{Re}_D < 8 \times 10^5$, the educed structure at $x/D = 3$

showed mild but persistent dependence on the initial condition. The initially turbulent case showed a higher organization, consistent with observations via flow-visualization and wavenumber-celerity spectra.[74,75]

In the case of eduction of natural structures, what basis should be used to judge successful eduction? Clearly, the conditional sampling technique that produces the sharpest structure features, in particular, the highest peak vorticity, is the optimum. We validated this basis by applying the technique for excited structures. The optimum conditional sampling technique educed structure property contours which were identical with those educed using the phase-locked technique in periodically induced structures. Furthermore, it was observed that the educed natural structure agreed well with the educed excited structure when the excitation amplitude was small (i.e., $u_f'/U_e \lesssim 0.1\%$).

K. Coherent structure in the plane mixing layer

The time-average measures of the axisymmetric mixing layer have been found to be functions of the initial condition, because of the limited extent of the layer (perhaps also due to upstream feedback). Data have suggested similar dependence of the plane mixing layer[112–114] on the initial condition. We speculated that the persisting influence of the initial condition in these data was due to limited streamwise lengths of the flows investigated. With this in mind, a large plane mixing layer facility was built. It was shown that sufficiently farther downstream from the origin, the single-stream mixing layer does achieve a universal state independent of the initial condition.[124] It was felt interesting to investigate the coherent structure in the self-preserving region of the mixing layer. In order to eliminate any possible effect of the initial instability, the boundary layer was tripped; care was taken to assure that the initial boundary layer satisfied all the criteria of a fully turbulent boundary layer as outlined in Sec. IIIA.

The *initially fully turbulent* mixing layer undergoes an instability and rolls up into well-identified coherent structures which then amalgamate as they advect downstream. These structures are detected for the entire length of measurement, i.e., for $x = 3$ m or $5000\theta_e$. The average structure passage frequency decreases with increasing x so that the Strouhal number $\mathrm{St}_\theta (= f_m\theta/U_e)$ remains a constant ($\cong 0.024$) at all x. Here θ and θ_e are the local and exit momentum thicknesses and U_e is the free-stream velocity (25 m/sec). The coherent structures in the single-stream mixing layer have been educed at different stages of their development via an optimized conditional sampling triggered on the peaks of a local reference $\tilde{u}$ signal obtained from the high-speed edge of the mixing layer.[109] The technique explained in the preceding section for the axisymmetric mixing layer was also found to be the optimum eduction technique for the plane mixing layer. In contrast with the axisymmetric case, the signals are better correlated between the high-speed and zero-speed sides in the plane mixing layer. Since flow reversal, associated with the passage of large-scale structures, must be similar in both configurations, it is clear that the poorer correlation in the axisymmetric case is not due to a flow reversal effect on the hot wire. Even though the zero-speed side footprint is relatively stronger in the plane layer, eduction based on the zero-speed side signal alone is still less successful than that based on the extrema of the high-speed edge signal. A joint criterion based on signal peaks on the high- and zero-speed sides failed to noticeably improve the eduction or even capture a specified phase of structure eduction. Since a joint criterion was successfully used by Browand and Weidman[30] for eduction of a pairing phase at a much lower Reynolds number Re_δ, it appears that while complete pairing is typical at lower Re_δ, other complex modes of interaction like partial and fractional pairings and even tearing are involved at higher Re_δ. This was what Hussain and Clark[50] suggested. Contours of structure properties like coherent vorticity, coherent production, and incoherent Reynolds stress and intensities over the cross section of the structure reveal that the structure formation and evolution are complete before $x \cong 500\theta_e$, beyond which the structure achieves an equilibrium state in all measurable details.

In the formative region, the phase-average incoherent Reynolds stress in the initially fully turbulent mixing layer is found to be much larger than the coherent Reynolds stress; both of these increase during the roll-up process, reaching constant and comparable values at $x \gtrsim 500\theta_e$. The peak coherent vorticity and coherent shear production associated with the center of the equilibrium structure are about 50% higher than the corresponding time-average peak values. It is to be expected that these peak values have been smeared out somewhat due to ensemble averaging of structures detected from a signal at the high-speed edge only. However, it is quite unlikely that the peak coherent vorticity is an order of magnitude higher than the peak time-mean vorticity as claimed by P. E. Dimotakis (private communication). In fact, when the same eduction scheme was applied to educe excited structures in the near field of a jet, where the structure properties were independently known via phase-locked measurements, no smearing was found. These measurements suggest that in the self-preserving state of the mixing layer, incoherent turbulence is comparably important as coherent structures.

L. Coherent structure in self-preserving regions of axisymmetric and plane jets

Large-scale coherent structures in the near fields of axisymmetric jets have been extensively studied by us and others. Comparatively less is known about coherent structures in the plane jet. The nature of the flow in the intermediate region near the end of the potential core of both jets is quite complex and has remained unexplored. Our success in educing the equilibrium structure in the plane mixing layer encouraged us to expect that the self-preserving region of the plane and circular jets are quite likely to be characterized by large-scale coherent structures. With this in mind the self-preserving regions of axisymmetric and plane jets are being investigated via flow visualization and hot-wire measurements.

The existence of organized motions in the self-preserving region of the axisymmetric jet became apparent from

preliminary measurements of space-time correlation data and smoothed simultaneous velocity traces from a rake of hot wires.[259] Figure 7(a) shows instantaneous velocity vectors as a function of the radial distance and time. From these partly smoothed velocity vector patterns, presence of large-scale structures is apparent. However, successive structures or their boundaries cannot be clearly identified because all the incoherent motion has not been subtracted out. This is a clear demonstration that a short-time sample (obtained visually or with a rake of sensors) in a plane can capture an apparently coherent motion but not the details of a preferred mode or even a characteristic structure. Conditional ensemble averaging is unavoidable in discarding incoherent motion and in educing the topological features of coherent structures.

Figure 7(b) shows the educed coherent vorticity contours obtained from an ensemble of 400 realizations which were accepted after satisfying the conditions that the peak vorticity is above a threshold and that the vorticity is phase correlated between the two ends of the rake across a vorticity peak.[148] (Thus, small, distorted, or weak vortices as well as those radially shifted were discarded.) Note that the mode ($m = 0, \pm 1, \pm 2$) of the structure was determined instantaneously and only structures of the same mode were ensemble

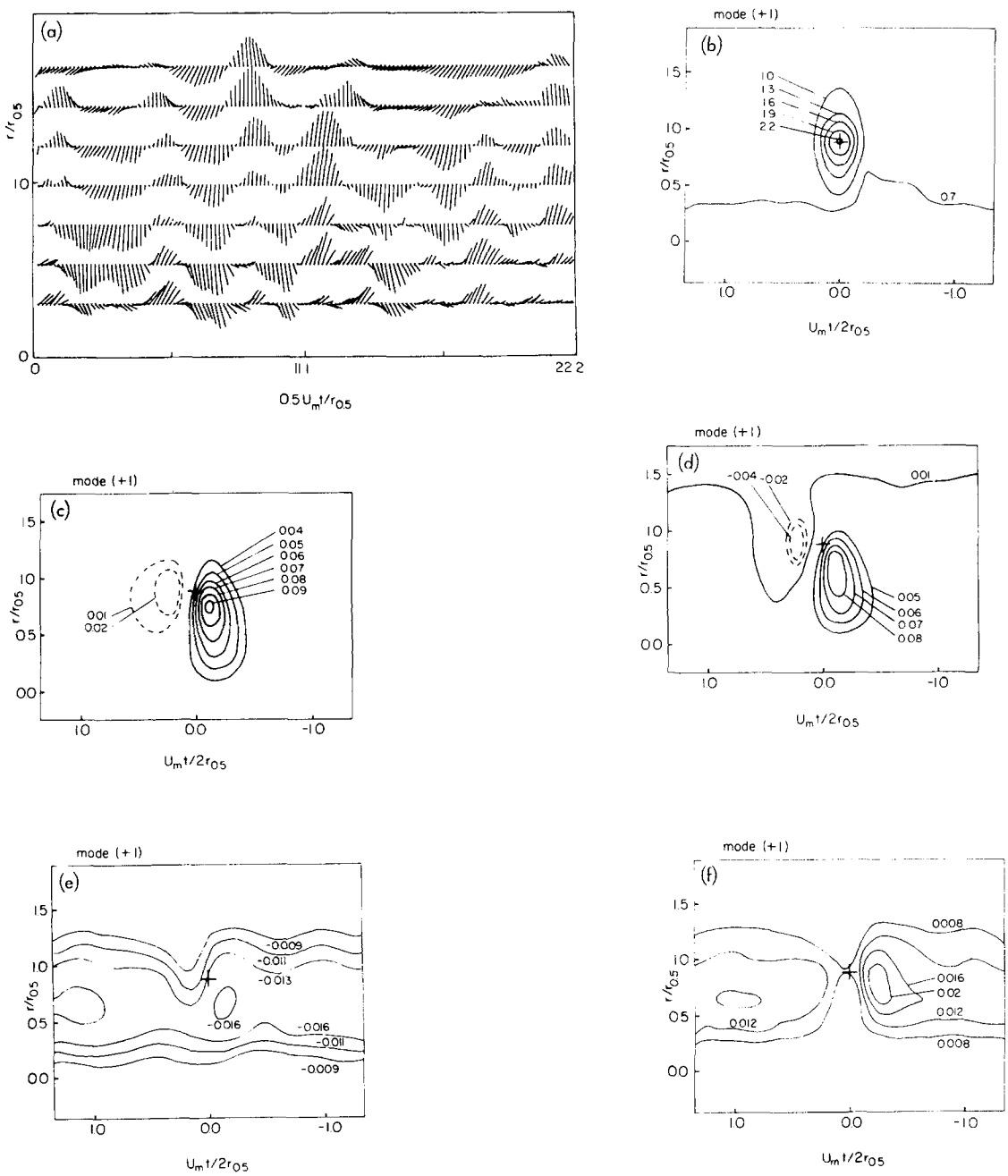

FIG. 7. Organized motion in the self-preserving region of an axisymmetric jet. (a) Instantaneous velocity vectors from seven X wires aligned radially at $x/D = 50$, for $Re_D = 6.5 \times 10^4$. (b) Coherent vorticity nondimensionalized by the peak shear rate $(\partial U/\partial y)_{max}$. (c) Coherent transverse velocity $\tilde{v}_r/U_m$. (d) Coherent Reynolds stress $\langle uv \rangle / U_m^2$. (e) Incoherent Reynolds stress $\langle u_r v_r \rangle / U_m^2$. (f) Coherent production $-\langle u_r v_r \rangle \langle S \rangle / [U_m^2 (\partial U/\partial y)_{max}]$.

averaged after aligning on the structure centers, identified by the peaks of large-scale coherent vorticity distributions. The corresponding contours of transverse coherent velocity, coherent Reynolds stress, incoherent Reynolds stress, and coherent production are shown in Figs. 7(c)–7(f) respectively. Figures 7(b)–7(f) relate to mode 1 structures. Note that all quantities have been appropriately nondimensionalized by the local centerline mean velocity U_m and the maximum shear rate $|\partial U/\partial y|_{\max}$. The convergence of the eduction process is assured by the fact that ensemble averages of 200 and 800 realizations produce no noticeable change in the contours in Figs. 7(b)–7(f) (based on 400 realizations). In Figs. 7(b)–7(f), the + symbol indicates the structure center, inferred from the peak coherent vorticity in Fig. 7(b).

The contours are consistent with a vortical structure centered at the + symbol; compare these contours with those obtained for the preferred mode at $x/D = 3$.[149] Note that by design, structures centered at the half-radius have been captured and phase averaged. The structure front (i.e., the downstream side) is considerably more active than the back (i.e., the upstream end). The radial outward ejection of turbulent fluid at the front, which is much stronger than the radial ingestion of ambient fluid at the back, is a primary mechanism of jet mixing, a conclusion also reached on the basis of flow visualization.[50] The intense shear at the front is also responsible for intense production of incoherent turbulence at the front. Note that the peak values of coherent Reynolds stress, incoherent Reynolds stress, and coherent shear production is only about 20% higher than their time-mean peak total values. These values are about the same at $x/D = 50$ and 100, thus confirming the achievement of equilibrium states of the structures. Of the three modes ($m = 0$, 1, 2) educed, the helical mode ($m = 1$) is the most dominant; the axisymmetric ($m = 0$) and double helix ($m = 2$) modes occur about 40% and 60% as often, respectively. The left-handed and right-handed helical modes occur at the same frequency. The Strouhal numbers of the three modes (based on local jet diameter and centerline velocity) are close to the value of 0.5. Further details of the coherent structures for different azimuthal modes in the self-preserving region of an axisymmetric jet will be presented in the dissertation of Tso.[148]

Visualization of the plane jet via smoke wires reveals that the self-preserving region is characterized by coherent structures which are three dimensional and have both streamwise and spanwise vorticities.[260] Even though the details are yet to be established, the structures appear to be quite different from those suggested by Moallemi and Goldschmidt[261] and Mumford.[96] The coherent structures in the self-preserving region are being quantitatively explored with a rake of X wires.

M. Taylor hypothesis applied to coherent structures

In many aspects of turbulence research, economy and convenience dictate the use of a limited number of sensors which are typically held stationary in the laboratory frame. While these sensors provide time records of flow variables at fixed spatial points, the interest is often in the spatial description of the flow field and the time evolution of a realization of a spatial description. The researcher thus has to endeavor to deduce spatial description from temporal information from a few stationary sensors. The classic example is the deduction of the wavenumber spectrum $E(k)$ from the measured frequency spectrum $E(f)$, in particular, one-dimensional spatial spectra and structure functions from the corresponding time functions. Taylor[262] hypothesized that the time history of a flow signal from a stationary sensor can be regarded as that due to advection of a frozen spatial pattern of turbulence past the sensor with the mean speed U, i.e., $u(x, t) = u(x - Ut, 0)$, and Favre *et al.*[263] were the first to experimentally demonstrate its validity for grid turbulence. Its validity has been reexamined in many subsequent investigations (for example, see Refs. 264 and 265). The factors contributing to errors in the Taylor hypothesis (i.e., $\partial/\partial t = -U_T \partial/\partial x$) have been well explained.[150–152] The error due to the hypothesis is expected to be quite large at the smallest scales.[150–156] It is to be noted that even though the hypothesis appears to be verified statistically via aircraft flight measurements in the atmosphere,[266] a check of the hypothesis on an instantaneous basis has not beeen possible yet.

Two necessary conditions for the validity of the Taylor hypothesis are[150,151]

$$\frac{u'}{U} \ll 1 \quad \text{and} \quad \frac{\partial U}{\partial y} < kU,$$

where k is the wavenumber; that is, the frozen turbulence can be valid when the turbulence level is very small, and for structures which are much smaller than the shear length scale. Both of these are well satisfied in grid turbulence where statistical verification has been made. On the other hand, both of these are invalidated in shear flows, and thus it is widely believed that Taylor hypothesis should not be valid in shear flows. In particular, these conditions suggest that the Taylor hypothesis would be grossly inappropriate in case of coherent structures in turbulent shear flows. This motivated us to attempt a direct test of the Taylor hypothesis on an instantaneous basis.

The unavoidable use of the Taylor hypothesis in the studies of coherent structures[130–133,146] introduces errors which appear in the computation of coherent vorticity Ω_c at two levels: first, in the computation of quantities as functions of time where longitudinal gradients are involved; and second, in converting data in the (t, y) plane to spatial distributions. Both levels are involved in the measurements of $\Omega_c(x, y)$, $\langle S \rangle(x, y)$, $\langle P \rangle(x, y)$, etc. The second-level error occurs in the deduction of the spatial description of properties like $\langle u_c v_c \rangle$ and $\langle u_r^2 \rangle^{1/2}$. The errors introduced by the different choices of U_T in the hypothesis have been quantitatively evaluated by first obtaining the actual spatial distributions through phase-locked measurements without using the hypothesis (Sec. VIIB) and then obtaining the spatial distributions through the Taylor hypothesis. Furthermore, the spatial distributions of the terms neglected by the hypothesis have also been evaluated.

To summarize, contrary to the analytical predictions, the Taylor hypothesis works very well in turbulent shear flows when advection of single structures is involved, pro-

vided that the advection velocity of the structure center only is used for U_T everywhere across the structure. When nonlinear interactions like pairing or tearing are involved, no choice of U_T is satisfactory. For a typical shear flow, use of a constant value of U_T, equal to the average of the velocities across the shear region, everywhere across the shear region is the least objectionable choice. The popular use of the local time-average velocity U introduces unacceptably large distortions. Only the terms associated with incoherent turbulence are insignificant; however, the terms associated with the coherent motion but neglected by the hypothesis are significant; in particular, the pressure term cannot be neglected. For further details, see Ref. 157.

N. Negative production

Much has been made of the fact that in some shear flows (for example, the wall jet or a channel with unequal roughnesses on the two walls), the maxima of the slope of the mean velocity profile and the time-mean Reynolds stress do not coincide, thus producing a region of counter-gradient production, called negative production. Even though this neither violates any basic principle nor should be particularly surprising, this is a clear example of the failure of the gradient transport hypothesis in the time-mean field and as such has been viewed by many as a curious phenomenon.[267–270]

Our experience suggests that negative production is a simple consequence of coherent structures in turbulent shear flows. While other possible configurations may also be involved, negative production has been found to occur for *two* specific coherent structure configurations: namely, when a particular orientation of a single coherent structure or a particular stage of structure interaction like pairing occurs successively at the same location.

As an example of the first configuration, consider the cross section of a vortex tube. For the sake of this discussion, whether the vortex is turbulent or even viscous is of no consequence. If the cross section is circular, it should be clear from orientations of velocity vectors (tangential to the circles) that the coherent Reynolds stress $\tilde{u}_c\tilde{v}_c$ will have four-lobed clover-leaf type distributions: two positive (countergradient) and two negative (co-gradient) distributions as qualitatively shown in Fig. 8. The areas and peak values of the four will be equal.

The coherent structure in a turbulent shear flow is seldom of circular cross section. In its early stage of formation, a structure is typically a spiral of vortical fluid, the irrotational external fluid being trapped or entrained into the spiral. Thus, the instantaneous topology is quite complicated due to folds, connection to braids, and continual deformation under shear. Consider the simplistic case of an elliptic cross section inclined with the flow direction. It is clear that the four regions of $\tilde{u}_c\tilde{v}_c$ in this case will not be equal in area or in the peak values. Depending on the inclination of the major axis of the ellipse with the flow direction, either the cogradient or the countergradient Reynolds stress will dominate. This is a straightforward kinematical consequence and has always been obvious perhaps to anyone who has drawn phase-average streamlines of a coherent structure.[29,31,133,145,149] This point was also emphasized by Browand at an American Physical Society Lecture in 1980. However, it is important to emphasize *two points* which have been overlooked in this connection. In order to understand the coherent Reynolds stress (and production) in the labora-

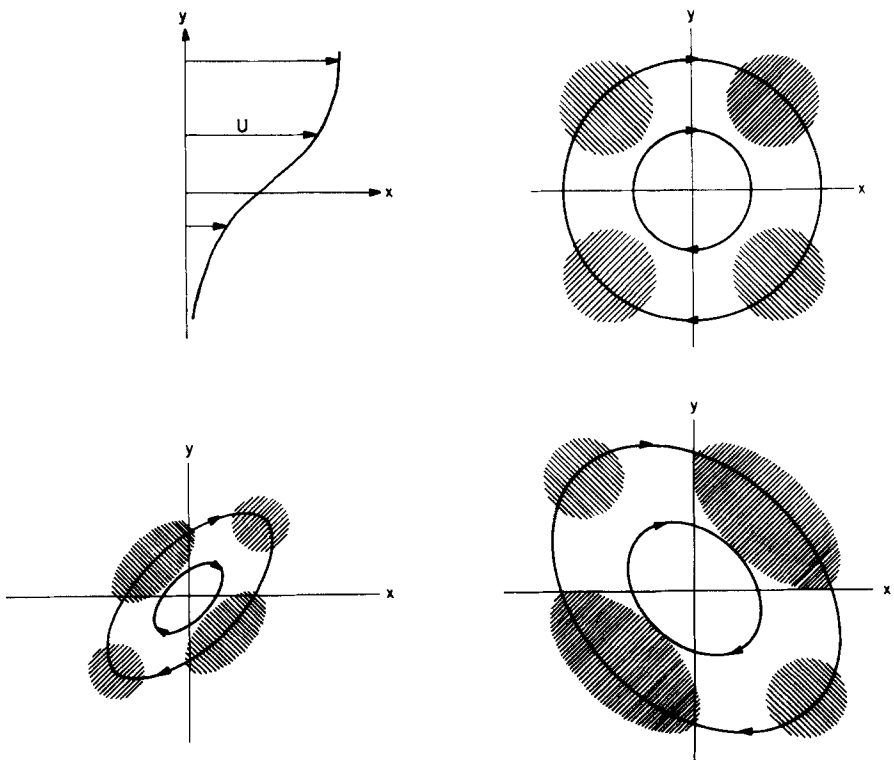

FIG. 8. Coherent Reynolds stress $\tilde{u}_c\tilde{v}_c$ distributions for three orientations of the structure.

tory frame, one must draw contours of $UV + U\tilde{v}_c + \tilde{u}_c V + \tilde{u}_c\tilde{v}_c$. That is, the contours of $UV + U\tilde{v}_c + \tilde{u}_c V$ must be superimposed onto the contours of $\tilde{u}_c\tilde{v}_c$ shown in Fig. 8. There will be orientations when the combined contours of $UV + U\tilde{v}_c + \tilde{u}_c V + \tilde{u}_c\tilde{v}_c$ will have net countergradient contributions. Call such an orientation a negative-production orientation. The second point to be made is that if successive structures acquire this orientation at random locations, the total time average may still be of the cogradient type. In order for negative production to occur (i.e., on a time-average basis), successive structures must repeat this orientation at around the same streamwise location.

The second situation when negative production can occur is vortex pairing. Detailed data[29] show that the flow region consists of different regions of positive and negative total coherent Reynolds stress $\langle uv\rangle = UV + \tilde{u}V + U\tilde{v}_c + \tilde{u}_c\tilde{v}_c$. Figures 9(a)–9(d) show the spatial distributions of coherent Reynolds stress for four successive stages of vortex pairing in the axisymmetric mixing layer. The cores of the two pairing vortices are identified by the + signs.

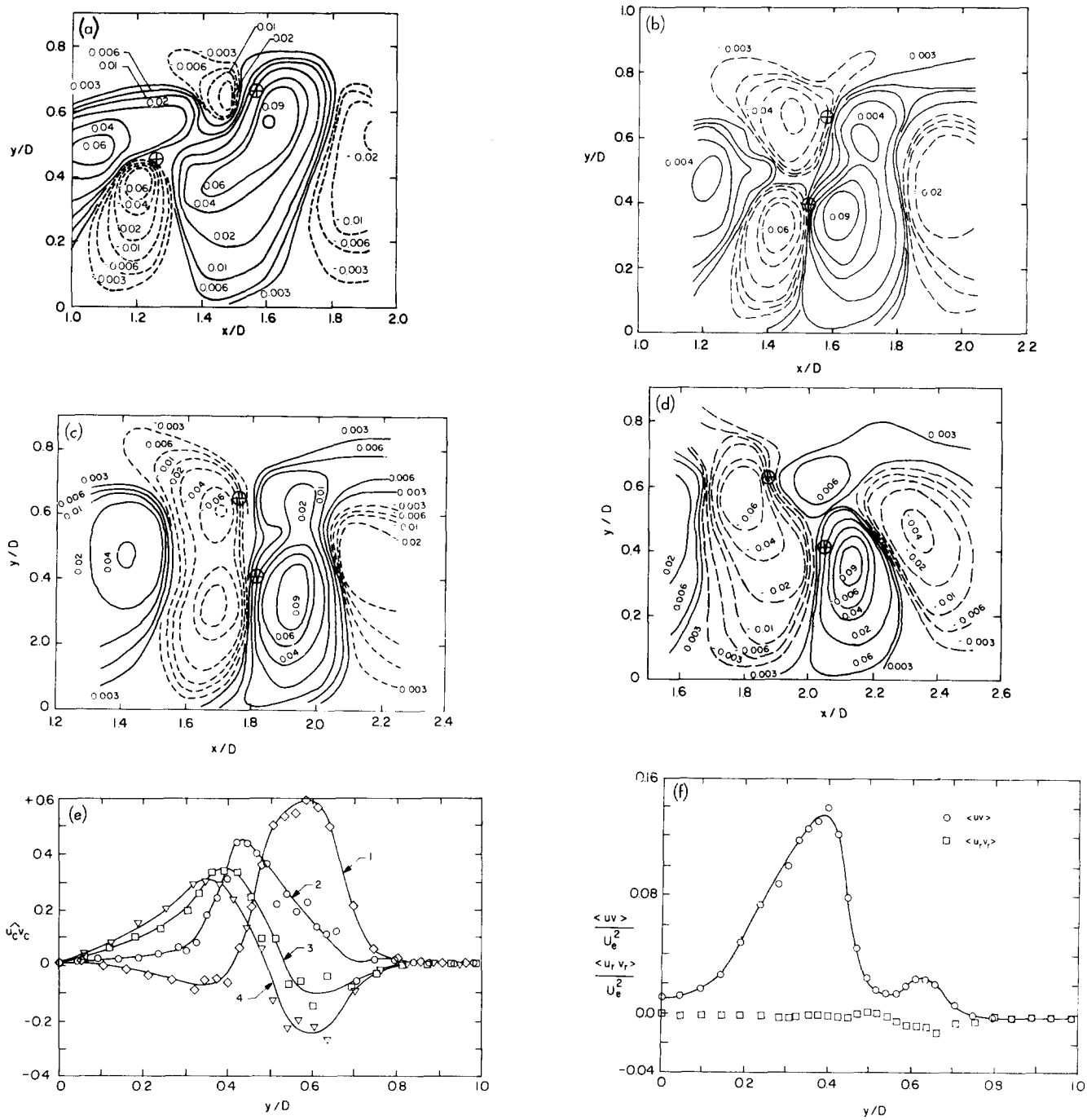

FIG. 9. Reynolds stress distributions during pairing. (a)–(d) Coherent Reynolds stress distribution in four successive stages 1–4 during pairing in an axisymmetric mixing layer. The + indicate vortex centers. (a) stage 1, (b) stage 2; (c) stage 3; and (d) stage 4. (e) Zone-average coherent Reynolds stress $u_c v_c$ over the spatial extent of the pairing vortices for stages 1–4 shows in Figs. 9(a)–(d). (f) Profile through the structure center of coherent and incoherent Reynolds stresses at stage 2 of pairing corresponding to Fig. 9(b).

Note that the regions of positive and negative $\langle uv \rangle$ vary considerably with the stage of pairing. The cograd ient Reynolds stress is a maximum at stage 1, i.e., at a very early stage of pairing. At stage 4, the countergradient $\langle uv \rangle$ is dominant. Thus, the zone-average coherent Reynolds stress may have either sign depending on the stage or phase of pairing [Fig. 9(e)]. The relative importance of the coherent and incoherent Reynolds stresses during the vortex pairing process is compared in Fig. 9(f). It is clear that during pairing of laminar vortices, virtually the entire Reynolds stress is due to the coherent Reynolds stress. However, soon after pairing, transition sets in and the coherent and incoherent Reynolds stresses become comparable. It should be clear that if vortex pairing happens to be stabilized, i.e., if successive pairings occur at the same location, then the time-average value $\overline{uv}$ will also be of the countergradient type and the flow will have a region of negative production. This was demonstrated first in Ref. 20 and subsequently explained in detail in Ref. 29.

Contours of time-average Reynolds stress in an axisymmetric mixing layer are shown in Fig. 10(a) and the corresponding excited shear layer with stable vortex pairing in Fig. 10(b). Not only is there a region of negative production (at $x \sim 2D$), but also the mean-flow field is highly distorted in the presence of stable pairing; compare $U/U_e = \text{const}$ and $\overline{uv}_{\max}$ lines in Figs. 10(a) and 10(b). This is an example of strong influences of structure interaction on the time-average flow field, especially when the interaction for successive structures is fixed in space. The spatial distribution of the incoherent Reynolds stress $\langle u_r v_r \rangle$ at a phase of the pairing event (occurring at $x \simeq 1.5D$) is shown in Fig. 10(c). Note that the $\langle u_r v_r \rangle$ distribution has a minimax distribution at structure centers (identified by the + signs), as suggested by Eq. (4). In the fully developed state of the mixing layer, random locations of successive interactions, as well as comparatively weaker interactions, will fail to manifest such a profound effect on the time-average flow field. In an independent study of localized shear-layer excitation, rather than bulk excitation, negative production associated with pairing has been demonstrated.[120]

O. Is the Reynolds number similarity hypothesis valid?

Reynolds number similarity[54,81] has been and still is perhaps the most fundamental hypothesis in turbulence; yet this presumably sacred principle is questionable. It is interesting to note that Reynolds number similarity, perhaps first coined by Townsend,[54] means just the opposite of what it is supposed to mean.[53]

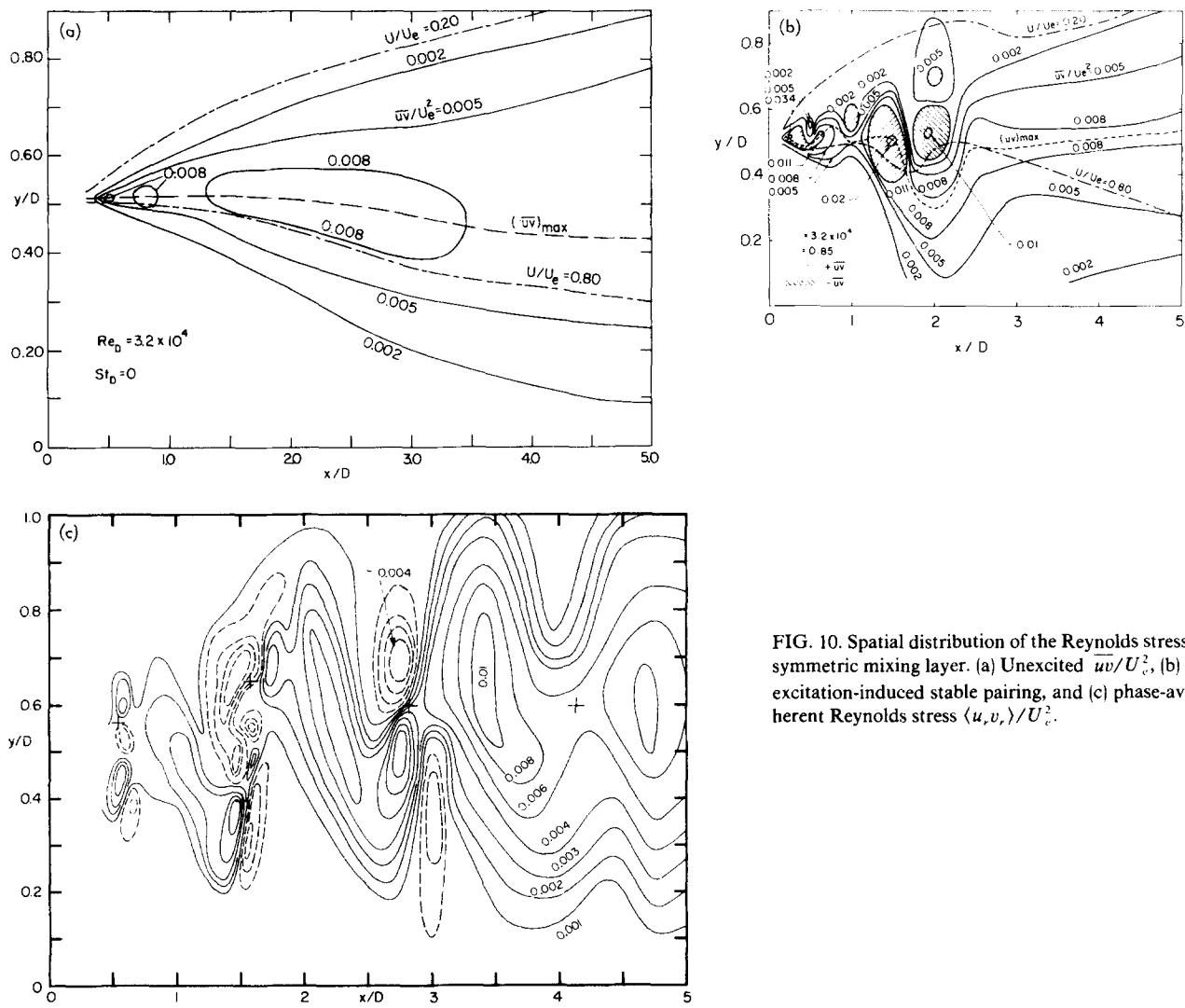

FIG. 10. Spatial distribution of the Reynolds stress in the axisymmetric mixing layer. (a) Unexcited $\overline{uv}/U_e^2$, (b) $\overline{uv}/U_e^2$ for excitation-induced stable pairing, and (c) phase-average incoherent Reynolds stress $\langle u_r v_r \rangle / U_e^2$.

The Reynolds number similarity (or asymptotic invariance) is different from self-preservation (or local invariance). The latter is a statement of achievement of dynamical equilibrium and is not unlike the concept of the limit cycle in nonlinear dynamics. In a shear flow where Reynolds number increases in x, Reynolds number similarity typically implies self-preservation and not vice versa. For example, even at moderate Reynolds numbers, when similarity is not expected, mean profiles of shear layers show self-preservation for $x/\theta_e \gtrsim 400$. However, all time-average measures in the apparently self-preserving region of an axisymmetric shear layer are found to be functions of the initial condition as well as amplitude and frequency of excitation. Coherent structure details also display similar dependence.

Even though there appears to be a universal belief in Reynolds number similarity, there has not been any conclusive evidence of it, nor has there been any study to critically examine it. It may be that the Reynolds number similarity is indeed an asymptotic concept, unachieveable in any finite length of the flow.

How large should the Reynolds number be in order for the similarity to hold? This question remains unanswered. For the sake of convenience in eduction and/or flow visualization, many coherent structure studies have been performed at very low Reynolds numbers (for example, see Refs. 18, 19, 22, 48, 254 and 271). One must guard against a straightforward extrapolation to higher Reynolds numbers, even though many researchers frequently tend to do so. In the case of jets, our experience suggests that the detailed features of jets at Reynolds numbers significantly below 10^5 may not be totally relevant to high Reynolds number jets; this conclusion independently follows from jet noise data.[225]

The underlying concept in the similarity hypothesis is that the flow is dominated by large scales, which remain unaffected with increasing Re, that can only affect the fine scales. The increasing separation of the length scales of large and fine scales with increasing Re suggests decoupling of the two scales at high Re. This scaling argument thus suggests that turbulence is independent of Re when Re is large. However, in a turbulent shear flow, the large and fine scales are not really decoupled. When coherent structures are considered, smaller scales are produced in regions of intense shear within coherent structures and are concentrated in preferential regions of coherent structures;[29,109,133,140,147-149,157] that is, incoherent turbulence is produced and spatially organized by coherent structures in a turbulent shear flow (see Sec. IVA). (It is interesting to note that even without recognizing coherent structures, Kolmogorov specifically included the coupling between large and fine scales in his refined theory.[272-274]) The question of Reynolds number similarity needs a careful investigation.

VIII. CONCLUDING REMARKS

Accumulated results from many investigations in recent years suggest that coherent structures are characteristic features of many, perhaps all, turbulent shear flows. Since these appear to be associated with significant turbulent transport, any viable turbulence theory must take these into account. No such theory has been proposed, nor is any in sight. Theoreticians should feel encouraged to focus some effort in this direction and utilize the comparatively substantial experimental data generated on coherent structures in a number of turbulent shear flows.

Even though coherent structures are the objects of intensive contemporary investigations, there is as yet no agreement on what is precisely meant by a coherent structure. An effort is made here to define a coherent structure on the basis of coherent vorticity and delineate the consequences of such a definition. While it has been suggested that perhaps alternative definitions are possible,[53] the definition presented here appears to us to be the optimum. Two alternative approaches to the decomposition of turbulent signals for educing coherent structures and describing their behavior are presented in the Appendix, where the interpretations of different terms resulting from the two approaches are reviewed. It is clear that either approach is confronted with the closure problem. The closure problem in the double decomposition is analogous to the closure problem resulting from the classical Reynolds averaging except that now closure is required in the time-dependent (phase-average) coherent flow field. Even simplistic approaches like the gradient transport hypotheses in the coherent flow field should provide significant improvements over similar hypotheses in the time-average flow. While there are many examples of failure of the gradient transport hypothesis in the time-average flow field as to be expected, no example has yet been cited for its failure in a phase-average field. The gradient transport hypothesis should work well in the coherent field.

The triple decomposition is intuitively attractive, but suffers from the limitation that the coherent structure is treated as a perturbation superimposed on the time-average flow, which, however, is a result of many coherent structures. That is, a coherent structure is not a mere perturbation of the flow; in some cases, it is the flow. On the other hand, the double decomposition does not recognize the primary source of kinetic energy and thus cannot address the growth or survival of coherent structures. This may be better suited for flows without a free stream or a source flow like in far fields of jets.

The excitement engendered by the coherent structure concept is based on the expectation that these quasideterministic structures should be representable mathematically, and thus turbulent shear flows will be tractable analytically. However, it is not clear if the conventional approach of analysis by substitution of a decomposition of Eularian field variables into the Navier–Stokes equations holds any hope. Perhaps, a quasi-Lagrangian approach would be helpful. For example, if the structure motion is represented in a coordinate system fixed to the structure center, the time evolution of the flow (say, a collection of structures) can be prescribed analytically. Thus, a quasi-Lagrangian description of the motion can be represented as

$$\frac{\hat{D}_c}{Dt}\langle u_i\rangle = -\frac{\partial\langle p\rangle}{\partial x_i} + \frac{1}{\mathrm{Re}}\frac{\partial^2\langle u_i\rangle}{\partial x_j \partial x_j} - U_c\delta_{1j}\frac{\partial\langle u_i\rangle}{\partial x_j} + \frac{\partial}{\partial x_j}(-\langle u_{ri}u_{rj}\rangle),$$

where $\hat{D}_c/Dt$ is the material derivative following a particle in the coherent motion field in a coordinate system advecting downstream with the structure. U_c is the convection velocity of the coherent structure center. Even this approach suffers from a number of constraints. The convection velocity U_c varies from structure to structure, and for a given structure, it varies randomly and considerably in magnitude and direction. The measurement of the convection velocity of a structure center during its trajectory in the three-dimensional space is itself a challenge.

Another problem that arises is the fact that the lifetime of a coherent structure seems to decrease with increasing Re, when a structure appears to undergo fairly rapid evolutionary changes through complex interactions like tearing and fractional and partial pairings. Only in the initial stages of instability (or in unique situations like the Karman vortex street) is the survival time sufficiently long. Thus, a viable theory must accommodate direct interactions (like pairing and tearing) and indirect interactions (like mutually induced motions).

Considering all these, it is not at all clear that a collection of deterministic coherent structures can be assumed to represent a shear flow turbulence. While in the initial stages of formation, the structures are dominant and can, therefore, possibly represent most of the total effect of turbulence, these structures do not account for most of turbulence tranport in fully developed flows. It does not appear very likely that the coherent structure approach is going to solve the turbulence closure problem or even significantly help in acceptable predictions of technological flows. A prospective approach/hope appears to lie with numerical simulation. Both subgrid-modeled computations and models based on discrete point vortices appear to be amazingly successful. Empirical input will continue to be needed for directing and calibrating numerical experiments. The complete solution of the time-dependent Navier–Stokes equation in three dimensions with realistic boundary conditions is still in the distant future.

The presence of coherent structures everywhere in a turbulent shear flow suggests a sequence of formation, evolution, and decay of each structure. The decay may be via interaction with other structures or via turbulent diffusion by the incoherent turbulence. While the formation of a coherent structure is obviously an instability mechanism, there is no clear understanding of this mechanism. We have argued that formation of a coherent structure in the fully turbulent state of the flow cannot be understood by studying the instability of the time-mean profile. Apart from the fact that the instability of a fully turbulent shear flow is inherently nonlinear, the linear instability analysis appears questionable on another count. The instability analysis of even an instantaneous profile, let alone the time-mean profile, will be hardly relevant because the profile changes wildly and with time scales comparable to that of the disturbance. When a structure results from strong interactions (like tearing and complete, partial, or fractional pairings), as is often the case, the structure formation mechanism has no relevance to the instability analysis of a static mean profile (even if it were with a structureless, fine-grained turbulence). One must then at least include the unsteady effect, as the instability of the same profile when unsteady can be quite different[60,61,99,275–278] from that when it is steady.

There have been suggestions that coherent structures in fully developed turbulent flows occur in groups or patches with periodic spacing within each group;[95,96] no explanation has been suggested for this periodicity. It is possible that each instability triggers a few adjacent periodic structures or the destabilizing disturbance occurs for a few periods at a time. No flow visualization, however, has yet revealed the occurrence of such groups of periodic structures.

Many simple questions regarding coherent structures still remain unanswered. Do all turbulent shear flows consist of the same coherent structure module which serves as the building block? The coherent structures in one class of flows tend to differ from another class. For example, the structures in each of the turbulent boundary layer, the plane mixing layer, the plane jet, the axisymmetric jet, and the wake are different from others. Does each flow have a unique coherent structure? Each flow appears to have more than one dominant type of coherent structure; for example, the axisymmetric jet flow has a variety of azimuthal modes ($m = 0, \pm 1, \pm 2$, etc.). Also, the same flow may have a different structure in a different region; for example, near and far fields of a plane jet or a plane wake appear to have different preferred modes. How often do these structures occur? The frequency of occurrence depends on the flow and the region of a given flow. Following the rollup in a free shear flow, coherent structures occur adjacent to each other, perhaps each formation triggering the nascent state of the next. They become less frequent farther downstream, say near the end of the potential core of a jet. In the turbulent boundary layer, or in the self-preserving region of jets, structures can occur less frequently.

Note that the measured frequency of occurrence of a coherent structure is a strong function of the detection scheme. The stricter the detection criterion, the lower will be the percentage of the population captured. This percentage will decrease with increasing distance downstream. The frequency of occurrence of coherent structures is indeed high even in the fully developed states of turbulent shear flows as is evident fron an instantaneous map of coherent vorticity in the (y, t) plane. However, to determine their dynamical significance, coherent structure properties must be determined from ensemble average of structures captured via a fine-tuned detection scheme. The phase alignment required for the ensemble average is best achieved by using the structure centers for phase reference.

While there is little doubt about the occurrence of coherent structures in perhaps all turbulent shear flows, the key question remains: How significant are these structures? If these structures do not play highly important dynamical roles then, perhaps, their occurrence notwithstanding, the computors and theoreticians could be spared the effort of finding ways to incorporate them explicitly. However, if these structures are dynamically highly significant, a theory of shear flow turbulence must be a theory of coherent structures.

If these structures are dynamically significant, then

they must be responsible for most of what turbulent shear flows do, for example, transports of heat, mass, and momentum and aerodynamic noise production. These structures will be dynamically important if one can show that most of the Reynolds stress and turbulence production are associated with coherent structures. Translated to measurable quantities, coherent Reynolds stress and production must exceed significantly the time-average total Reynolds stress and production.

Even though many researchers have made bold speculations that the coherent structures are highly significant and are all that matter in turbulent shear flows, hard data backing up these claims are very rare. To my knowledge, detailed data addressing the dynamical significance of coherent structures have been taken almost exclusively in our laboratory (for example, see Refs. 29, 36, 109, 133, 140, 147–149, 157, 221, and 246). (Some limited data have been reported by Browand[30].) Our measurements include detailed spatial distributions over the structure cross section of coherent vorticity, coherent strain rate, coherent Reynolds stress coherent production, incoherent Reynolds stress, and turbulence intensities, etc. These data for coherent structures occurring naturally as well as induced via controlled excitation show that coherent structures play important dynamical roles in turbulent shear flows; however, these are *not* always as dominant as speculated. While these are dominant only during their formative, posttransition stage or in situations of resonance, these are not dominant in the fully developed states of turbulent shear flows. (Coherent substructures play a dominant role in the wall layer everywhere in a turbulent boundary layer.) Detailed data in a number of flows show that the peak values of coherent Reynolds stress, coherent production, and coherent vorticity are of the order of the peaks of their total time-average values. Contrary to the claims that the coherent peak values must be an order of magnitude higher, these are typically no more than twice the time-average peak values. Smearing cannot be blamed for the measured peak values being low (in contrast with the expectations of some) because the eduction technique has been carefully validated to produce minimal smearing; the ratios of the measured peak values of coherent Reynolds stress, coherent production, and coherent vorticity to the corresponding time-average peak values are found to be the same even when jitter (hence smearing) has been eliminated via controlled excitation[29,109,133,140,149] and the same quantities are independently measured via phase-locked measurements. Independent experiments in a few excited and unexcited free shear flows have produced comparable values of these ratios in the fully developed states. Our eduction scheme based on alignment of structures with respect to the structure centers both in transverse and streamwise directions guarantee a minimal amount of smearing. No matter how stringent the eduction criteria, the peak values of coherent Reynolds stress and coherent production are comparable to the corresponding peak values of time-average totals in the fully developed states of turbulent shear flows.

Once again, coherent structures are integral to perhaps all turbulent shear flows; they are significant, but not necessarily the predominant, features of turbulent shear flows. They can be predominant in especial situations such as transitional and resonant situations or near the wall of a turbulent boundary layer. The incoherent turbulence is comparably important in the fully developed states of turbulent shear flows, where its role cannot be ignored.

ACKNOWLEDGMENTS

This paper is an effort to pull together our ideas and results on different aspects of coherent structures. Some of the ideas summarized here were presented at conferences at Madrid and Bangalore in 1980. The results mentioned in the foregoing are outcomes of collaborative research efforts with Dr. K. B. M. Q. Zaman, Dr. S. J. Kleis, Dr. A. R. Clark, Dr. M. Sokolov, Dr. L. S. G. Kovasznay, Dr. Z. D. Husain, Dr. M. A. Z. Hasan, Dr. J. Tso, Dr. P. Bandyopadhyay, H. S. Husain, and others with whom the author has had extensive interactions, which the author found highly educational. The specific involvements of these colleagues can be identified from the cited references. The author is grateful to Dr. M. Nallasamy, Dr. S. Corrsin, Dr. P. Bradshaw, Dr. A. Michalke, Dr. H. W. Liepmann, Dr. R. Narasimha, Dr. R. Takaki and Dr. J. Tso for reviewing the manuscript and for many helpful comments.

Support for these research efforts have been provided at different times by the National Science Foundation, the Office of Naval Research, the National Aeronautics and Space Administration, and the Air Force Office of Scientific Research.

APPENDIX: GOVERNING EQUATIONS WITH TRIPLE AND DOUBLE DECOMPOSITIONS

A. Triple decomposition

Substitution of (2a) for each variable into the governing equations for incompressible flow and carrying out first the phase average and then the time average produce the corresponding continuity and momentum equations for the three component fields:

$$\frac{\partial U_i}{\partial x_i} = \frac{\partial \tilde{u}_{ci}}{\partial x_i} = \frac{\partial u_{ri}}{\partial x_i} = 0, \tag{A1a}$$

$$\frac{\bar{D}}{Dt} U_i = -\frac{\partial P}{\partial x_i} + \frac{1}{\mathrm{Re}} \frac{\partial^2 U_i}{\partial x_j \partial x_j} + \frac{\partial}{\partial x_j}(-\overline{\tilde{u}_{ci}\tilde{u}_{cj}} - \overline{u_{ri}u_{rj}}), \tag{A1b}$$

$$\frac{\bar{D}}{Dt} \tilde{u}_{ci} = -\frac{\partial \tilde{p}_c}{\partial x_i} + \frac{1}{\mathrm{Re}} \frac{\partial^2 \tilde{u}_{ci}}{\partial x_j \partial x_j} - \frac{\partial}{\partial x_j}(U_i \tilde{u}_{cj}) + \frac{\partial}{\partial x_j}(\overline{\tilde{u}_{ci}\tilde{u}_{cj}} - \tilde{u}_{ci}\tilde{u}_{cj}) + \frac{\partial}{\partial x_j}(\overline{u_{ri}u_{rj}} - \langle u_{ri}u_{rj}\rangle), \tag{A1c}$$

$$\frac{\bar{D}}{Dt} u_{ri} = -\frac{\partial p_r}{\partial x_i} + \frac{1}{\mathrm{Re}} \frac{\partial^2 u_{ri}}{\partial x_j \partial x_j} - \frac{\partial}{\partial x_j}(\tilde{u}_{cj}u_{ri} + U_i u_{rj} + \tilde{u}_{ci}u_{rj}) - \frac{\partial}{\partial x_j}(u_{ri}u_{rj} - \langle u_{ri}u_{rj}\rangle). \tag{A1d}$$

Here,

$$\frac{\bar{D}}{Dt} = \frac{\partial}{\partial t} + U_j \frac{\partial}{\partial x_j} \tag{A1e}$$

is the derivative following a fluid particle in the time-average flow field. Note that *summation* is *not* implied by the subscripts c and r, which identify coherent and incoherent (random) components, respectively. In this derivation, use is made of the notions that (i) the phase average of the time average is just the time average, (ii) the phase and time averages of the incoherent field have zero values, and (iii) the coherent and incoherent motions are uncorrelated, i.e., $\overline{\tilde{f}_c g_r} = \langle \tilde{f}_c g_r \rangle = 0$. The interpretations of each term in Eqs. (A1b)–(A1d) should be fairly obvious. Note that each of the three fields independently satisfy the equation for isochoric motion. There is a hierarchy of momentum transports involved: $-\overline{\tilde{u}_{ci}\tilde{u}_{cj}}$ and $-\overline{u_{ri}u_{rj}}$ are the contributions of the coherent and incoherent motions to the mean momentum field. The modulations in these two terms due to the coherent motion contribute to the coherent field momentum. The interaction of the incoherent field with the time-average and coherent fields, in addition to the self-interaction, instantaneously contributes to the incoherent field momentum. The instantaneous momentum transport due to the incoherent field $-u_{ri}u_{rj} = r_{ij}$ can be viewed as having three components: $\bar{R}_{ij}$, $\tilde{R}_{cij}$, and R_{rij}, i.e.,

$$r_{ij} = \tilde{R}_{ij} + \tilde{R}_{cij} + R_{rij}, \tag{A2a}$$

where

$$\bar{R}_{ij} = -\overline{u_{ri}u_{rj}}, \tag{A2b}$$

$$\tilde{R}_{cij} = -\langle u_{ri}u_{rj}\rangle + \overline{u_{ri}u_{rj}}, \tag{A2c}$$

$$R_{rij} = -u_{ri}u_{rj} + \langle u_{ri}u_{rj}\rangle, \tag{A2d}$$

i.e.,

$$\bar{r}_{ij} = \bar{R}_{ij}; \quad \langle r_{ij}\rangle = \bar{R}_{ij} + \tilde{R}_{cij}. \tag{A2e}$$

The contribution of incoherent turbulence to the mean momentum field is $\bar{R}_{ij}$, to the coherent structure field is $\tilde{R}_{cij}$, and to the incoherent field itself is R_{rij}. It is clear that the three fields are strongly coupled and the unknowns like $\bar{R}_{ij}$, $\tilde{R}_{cij}$, R_{rij}, and $\overline{\tilde{u}_{ci}\tilde{u}_{cj}}$ must be expressed in terms of other variables in order to solve for the three velocity and pressure fields. The corresponding vorticity equations are

$$\begin{aligned}\frac{\bar{D}}{Dt}\Omega_i = {} & \Omega_j \frac{\partial U_i}{\partial x_j} + \frac{1}{\mathrm{Re}}\frac{\partial^2 \Omega_i}{\partial x_k \partial x_k} \\ & + \frac{\partial}{\partial x_j}\left(\overline{\tilde{u}_{ci}\tilde{\omega}_{cj}} - \overline{\tilde{u}_{cj}\tilde{\omega}_{ci}}\right) \\ & + \frac{\partial}{\partial x_j}\left(\overline{u_{ri}\omega_{rj}} - \overline{u_{rj}\omega_{ri}}\right),\end{aligned} \tag{A3a}$$

$$\begin{aligned}\frac{\bar{D}}{Dt}\tilde{\omega}_{ci} = {} & \tilde{\omega}_{cj}\frac{\partial U_i}{\partial x_j} + \Omega_j \frac{\partial \tilde{u}_{ci}}{\partial x_j} + \frac{1}{\mathrm{Re}}\frac{\partial^2 \tilde{\omega}_{ci}}{\partial x_k \partial x_k} \\ & + \frac{\partial}{\partial x_j}\left(\tilde{u}_{ci}\tilde{\omega}_{cj} - \overline{\tilde{u}_{ci}\tilde{\omega}_{cj}}\right) \\ & - \frac{\partial}{\partial x_j}\left(\tilde{u}_{cj}\tilde{\omega}_{ci} - \overline{\tilde{u}_{cj}\tilde{\omega}_{ci}}\right) - \frac{\partial}{\partial x_j}\left(\tilde{u}_{cj}\Omega_i\right) \\ & + \frac{\partial}{\partial x_j}\left(\langle u_{ri}\omega_{rj}\rangle - \overline{u_{ri}\omega_{rj}}\right) \\ & - \frac{\partial}{\partial x_j}\left(\langle u_{rj}\omega_{ri}\rangle - \overline{u_{rj}\omega_{ri}}\right),\end{aligned} \tag{A3b}$$

$$\begin{aligned}\frac{\bar{D}}{Dt}\omega_{ri} = {} & \left(\Omega_j + \tilde{\omega}_{cj}\right)\frac{\partial u_{ri}}{\partial x_j} + \omega_{rj}\frac{\partial}{\partial x_j}\left(U_i + \tilde{u}_{ci}\right) \\ & + \frac{1}{\mathrm{Re}}\frac{\partial^2 \omega_{ri}}{\partial x_k \partial x_k} - u_{rj}\frac{\partial}{\partial x_j}\left(\Omega_i + \tilde{\omega}_{ci}\right) \\ & - \tilde{u}_{cj}\frac{\partial \omega_{ri}}{\partial x_j} + \frac{\partial}{\partial x_j}\left(u_{ri}\omega_{rj} - \langle u_{ri}\omega_{rj}\rangle\right) \\ & - \frac{\partial}{\partial x_j}\left(u_{rj}\omega_{ri} - \langle u_{rj}\omega_{ri}\rangle\right).\end{aligned} \tag{A3c}$$

Note that Eqs. (A1) and (A3), which could be further simplified, are nondimensionalized by appropriate velocity and length scales U_s and L_s so that $\mathrm{Re} = U_s L_s/\nu$ is the appropriate Reynolds number. Pressure is nondimensionalized by ρU_s^2.

The complexities of the Eqs. (A1) and (A3) do not permit a direct appreciation for the interaction between the three fields. However, some further insight can be obtained from a consideration of the energetics. Since the total kinetic energy must be equal to the sum of the average kinetic energies of the three fields,

$$\tfrac{1}{2}\overline{u_i u_i} = \underbrace{\tfrac{1}{2}\overline{U_i U_i}}_{E} + \underbrace{\tfrac{1}{2}\overline{\tilde{u}_{ci}\tilde{u}_{ci}}}_{\mathscr{E}} + \underbrace{\tfrac{1}{2}\overline{u_{ri}u_{ri}}}_{e}, \tag{A4a}$$

$$\begin{aligned}\frac{\bar{D}E}{Dt} = {} & -\frac{\partial P U_i}{\partial x_i} - \underbrace{\left(-\overline{\tilde{u}_{ci}\tilde{u}_{cj}}\right)\frac{\partial U_i}{\partial x_j}}_{\mathrm{I}} - \underbrace{\left(-\overline{u_{ri}u_{rj}}\right)\frac{\partial U_i}{\partial x_j}}_{\mathrm{II}} \\ & - \frac{\partial}{\partial x_j}\left[U_i\left(\overline{\tilde{u}_{ci}\tilde{u}_{cj}} + \overline{u_{ri}u_{rj}}\right)\right] \\ & + \frac{1}{\mathrm{Re}}\frac{\partial}{\partial x_j}\left(U_i \bar{S}_{ij}\right) - \bar{\epsilon},\end{aligned} \tag{A4b}$$

$$\begin{aligned}\frac{\bar{D}\mathscr{E}}{Dt} = {} & -\frac{\partial}{\partial x_j}\left[\overline{\tilde{u}_{cj}\left(\tilde{p}_c + \frac{1}{2}\tilde{u}_{ci}\tilde{u}_{ci}\right)}\right] - \underbrace{\overline{\tilde{u}_{ci}\tilde{u}_{cj}}\frac{\partial U_i}{\partial x_j}}_{-\mathrm{I}} \\ & - \underbrace{\left(-\overline{\langle u_{ri}u_{rj}\rangle\frac{\partial \tilde{u}_{ci}}{\partial x_j}}\right)}_{\mathrm{III}} - \frac{\partial}{\partial x_j}\left(\overline{\tilde{u}_{ci}\langle u_{ri}u_{rj}\rangle}\right) \\ & + \frac{1}{\mathrm{Re}}\frac{\partial}{\partial x_j}\left(\tilde{u}_{ci}\tilde{S}_{cij}\right) - \tilde{\epsilon}_c,\end{aligned} \tag{A4c}$$

$$\begin{aligned}\frac{\bar{D}e}{Dt} = {} & -\frac{\partial}{\partial x_j}\left[\overline{u_{ri}\left(p_r + \frac{1}{2}u_{ri}u_{ri}\right)}\right] - \underbrace{\overline{u_{ri}u_{rj}}\frac{\partial U_i}{\partial x_j}}_{-\mathrm{II}} \\ & - \underbrace{\overline{\langle u_{ri}u_{rj}\rangle\frac{\partial \tilde{u}_{ci}}{\partial x_j}}}_{-\mathrm{III}} - \overline{\tilde{u}_{cj}\frac{\partial}{\partial x_j}\left\langle\frac{1}{2}u_{ri}u_{ri}\right\rangle} \\ & + \frac{1}{\mathrm{Re}}\frac{\partial}{\partial x_j}\left(\overline{u_{ri}S_{ri}}\right) - \epsilon_r,\end{aligned} \tag{A4d}$$

where

$$\bar{S}_{ij} = \frac{\partial U_i}{\partial x_j} + \frac{\partial U_j}{\partial x_i}, \quad \tilde{S}_{cij} = \frac{\partial \tilde{u}_{ci}}{\partial x_j} + \frac{\partial \tilde{u}_{cj}}{\partial x_i},$$

$$S_{rij} = \frac{\partial U_{ri}}{\partial x_j} + \frac{\partial u_{rj}}{\partial x_i}, \tag{A4e}$$

and

$$\bar{\epsilon} = (1/2\mathrm{Re})\bar{S}_{ij}\bar{S}_{ij}, \quad \tilde{\epsilon}_c = (1/2\mathrm{Re})\overline{\tilde{S}_{cij}\tilde{S}_{cij}},$$
$$\epsilon_r = (1/2\mathrm{Re})\ \overline{S_{rij}S_{rij}} \tag{A4f}$$

are the dissipations in the three fields. Once again, *no summation* is implied by subscripts c and r. In each of the equations, the first, fourth, and fifth terms represent the transport (redistribution) of energy within the flow as their integrals over the entire flow region are zeroes. The first represents the flow work and the fifth reversible viscous work. The term identified as I represents the production of coherent kinetic energy by the action of the average coherent Reynolds stress $-\overline{u_{ri}u_{rj}}\ \overline{u_{ri}u_{rj}} - \overline{\tilde{u}_{ci}\tilde{u}_{cj}}$ against the mean strain rate $\bar{S}_{cij}/2$. The same term appears as a source term in the equation for coherent kinetic energy. Similarly, the term identified as II represents the production of incoherent turbulence by the action of the incoherent Reynolds stress $-\overline{u_{ri}u_{rj}}$ against the mean strain rate. The same term appears as a source term in the incoherent kinetic energy equation. The coherent motion also can produce incoherent turbulence by the action of the phase-average incoherent Reynolds stress $-\langle u_{ri}u_{rj}\rangle$ against the coherent strain rate $\tilde{S}_{cij}/2$. Note that this term III appears as a source term in Eq. (A4d).

B. Double decomposition

Substitution of the decomposition (3a) in the governing equation and then taking the phase-average yields

$$\frac{\partial u_{ci}}{\partial x_i} = \frac{\partial u_{ri}}{\partial x_i} = 0, \tag{A5a}$$

$$\frac{\hat{D}}{Dt}u_{ci} = -\frac{\partial p_c}{\partial x_i} + \frac{1}{\mathrm{Re}}\frac{\partial^2 u_{ci}}{\partial x_k \partial x_k} - \frac{\partial}{\partial x_j}\langle u_{ri}u_{rj}\rangle, \tag{A5b}$$

$$\frac{\hat{D}}{Dt}u_{ri} = -\frac{\partial p_r}{\partial x_i} + \frac{1}{\mathrm{Re}}\frac{\partial^2 u_{ri}}{\partial x_k \partial x_k} - u_{rj}\frac{\partial u_{ci}}{\partial x_j} - \frac{\partial}{\partial x_j}(u_{ri}u_{rj} - \langle u_{ri}u_{rj}\rangle), \tag{A5c}$$

$$\frac{\hat{D}}{Dt}\omega_{ci} = \omega_{cj}\frac{\partial u_{ri}}{\partial x_j} + \frac{1}{\mathrm{Re}}\frac{\partial^2 \omega_{ci}}{\partial x_k \partial x_k} + \frac{\partial}{\partial x_j}(\langle u_{ri}\omega_{rj}\rangle - \langle u_{rj}\omega_{ri}\rangle), \tag{A5d}$$

$$\frac{\hat{D}}{Dt}\omega_{ri} = \omega_{cj}\frac{\partial u_{ri}}{\partial x_j} + \omega_{rj}\frac{\partial u_{ci}}{\partial x_j} + \frac{1}{\mathrm{Re}}\frac{\partial^2 \omega_{ri}}{\partial x_k \partial x_k} - u_{rj}\frac{\partial \omega_{ci}}{\partial x_j} - \frac{\partial}{\partial x_j}(\omega_{ri}u_{rj} - \langle \omega_{ri}u_{rj}\rangle) + \frac{\partial}{\partial x_j}(\omega_{rj}u_{ri} - \langle \omega_{rj}u_{ri}\rangle). \tag{A5e}$$

where

$$\frac{\hat{D}}{Dt} = \frac{\partial}{\partial t} + u_{cj}\frac{\partial}{\partial x_j} \tag{A5f}$$

is the material derivative following a fluid particle in the coherent flow field. Once again, *no summation* is implied by subscripts c and r. The corresponding kinetic energy and Reynolds stress equations are

$$\frac{\hat{D}}{Dt}\frac{\langle u_{ci}u_{ci}\rangle}{2} = \underbrace{-\frac{\partial}{\partial x_j}(p_c u_{ci})}_{\mathrm{I}} + \underbrace{\langle u_{ri}u_{rj}\rangle\frac{\partial u_{ci}}{\partial x_j}}_{\mathrm{II}} \underbrace{-\frac{\partial}{\partial x_j}(u_{ci}\langle u_{ri}u_{rj}\rangle)}_{\mathrm{III}} + \underbrace{\frac{1}{\mathrm{Re}}\frac{\partial}{\partial x_j}\left\langle u_{ci}\left(\frac{\partial u_{ci}}{\partial x_j} + \frac{\partial u_{cj}}{\partial x_i}\right)\right\rangle}_{\mathrm{IV}} \underbrace{-\frac{1}{2}\frac{1}{\mathrm{Re}}\left\langle\left(\frac{\partial u_{ci}}{\partial x_j} + \frac{\partial u_{cj}}{\partial x_i}\right)\left(\frac{\partial u_{ci}}{\partial x_j} + \frac{\partial u_{cj}}{\partial x_i}\right)\right\rangle}_{\mathrm{V}}, \tag{A6a}$$

$$\frac{\hat{D}}{Dt}\frac{\langle u_{ri}u_{ri}\rangle}{2} = \underbrace{-\frac{\partial}{\partial x_j}\left\langle u_{rj}\left(p_r + \frac{1}{2}u_{ri}u_{ri}\right)\right\rangle}_{\mathrm{I'}} \underbrace{-\langle u_{ri}u_{rj}\rangle\frac{\partial u_{ci}}{\partial x_j}}_{\mathrm{II'}} + \underbrace{\frac{1}{\mathrm{Re}}\frac{\partial}{\partial x_j}\left\langle u_{ri}\left(\frac{\partial u_{ri}}{\partial x_j} + \frac{\partial u_{rj}}{\partial x_i}\right)\right\rangle}_{\mathrm{III'}} \underbrace{-\frac{1}{2\mathrm{Re}}\left\langle\left(\frac{\partial u_{ri}}{\partial x_i} + \frac{\partial u_{rj}}{\partial x_i}\right)\left(\frac{\partial u_{ri}}{\partial x_j} + \frac{\partial u_{rj}}{\partial x_i}\right)\right\rangle}_{\mathrm{IV'}}, \tag{A6b}$$

$$\frac{\hat{D}}{Dt}\langle u_{ri}u_{rj}\rangle = -\left\langle\left(u_{ri}\frac{\partial p_r}{\partial x_j} + u_{rj}\frac{\partial p_r}{\partial x_i}\right)\right\rangle - \frac{\partial}{\partial x_k}\langle u_{ri}u_{rj}u_{rk}\rangle - \langle u_{rj}u_{rk}\rangle\frac{\partial u_{ci}}{\partial x_k} - \langle u_{ri}u_{rk}\rangle\frac{\partial u_{cj}}{\partial x_k} + \frac{1}{\mathrm{Re}}\frac{\partial^2\langle u_{ri}u_{rj}\rangle}{\partial x_k \partial x_k} - \frac{2}{\mathrm{Re}}\left\langle\frac{\partial u_{ri}}{\partial x_k}\frac{\partial u_{rj}}{\partial x_k}\right\rangle. \tag{A6c}$$

In Eq. (A6a) the terms denote: I, coherent pressure work, II, coherent production of incoherent turbulence, III, coherent energy transport by incoherent turbulence, IV, reversible viscous work by coherent motion, and V, irreversible viscous work by coherent motion (i.e., coherent dissipation). The terms in Eq. (A6b), which results from contraction of Eq. (A6c) denote: I', incoherent turbulent kinetic energy transport by pressure and normal stresses, II', coherent production of incoherent turbulence, III', reversible viscous work by incoherent turbulence, and IV', incoherent turbulence dissipation. For further discussion, see Ref. 129.

[1] H. W. Liepmann, Am. Sci. **67**, 221 (1979).
[2] G. K. Batchelor (private communication, 1982).
[3] S. J. Kline, W. C. Reynolds, F. A. Schraub, and P. W. Runstadler, J. Fluid Mech. **30**, 741 (1967).
[4] S. C. Crow and F. H. Champagne, J. Fluid Mech. **48**, 547 (1971).
[5] G. L. Brown and A. Roshko, J. Fluid Mech. **64**, 775 (1974).

[6]J. A. B. Wills, J. Fluid Mech. **20**, 417 (1964).
[7]G. M. Corcos, J. Fluid Mech. **18**, 353 (1964).
[8]W. W. Willmarth and C. E. Wooldridge, J. Fluid Mech. **11**, 187 (1962).
[9]M. T. Landahl, J. Fluid Mech. **29**, 441 (1967).
[10]A. K. M. F. Hussain and W. C. Reynolds, J. Fluid Mech. **54**, 241 (1972).
[11]W. R. B. Morrison and R. E. Kronauer, J. Fluid Mech. **39**, 117 (1969).
[12]T. R. Heidrick, S. Banerjee, and R. S. Azad, J. Fluid Mech. **81**, 137 (1977).
[13]O. M. Phillips, J. Fluid Mech. **106**, 215 (1981).
[14]P. Plaschko, J. Fluid Mech. **92**, 209 (1979).
[15]M. E. Goldstein, J. Fluid Mech. **91**, 601 (1979).
[16]M. E. Goldstein (private communication, 1982).
[17]M. Gaster, E. Kit, and I. Wygnanski (submitted to J. Fluid Mech., 1982).
[18]C. E. Winant and F. K. Browand, J. Fluid Mech. **63**, 237 (1974).
[19]F. K. Browand and J. Laufer, *Turbulence in Liquids* (University of Missouri, Rolla, 1975), p. 333.
[20]A. K. M. F. Hussain and K. B. M. Q. Zaman, Lect. Notes Phys. **75**, 31 (1978).
[21]C. Chandrsuda, R. D. Mehta, A. D. Weir, and P. Bradshaw, J. Fluid Mech. **85**, 693 (1978).
[22]A. E. Perry and T. T. Lim, J. Fluid Mech. **88**, 451 (1978).
[23]G. R. Offen and S. J. Kline, J. Fluid Mech. **62**, 223 (1974).
[24]E. R. Corino and R. S. Brodkey, J. Fluid Mech. **37**, 1 (1969).
[25]A. K. Praturi and R. S. Brodkey, J. Fluid Mech. **89**, 241 (1978).
[26]R. E. Falco, presented at the 13th AIAA Fluid and Plasma Dynamics Conference, Snowmass, Colorado, July 14–16, 1980, No. 80-1356.
[27]M. R. Head and P. Bandyopadhyay, J. Fluid Mech. **107**, 297 (1981).
[28]M. Gad-el-Hak, R. F. Blackwelder, and J. J. Riley, J. Fluid Mech. **110**, 73 (1981).
[29]A. K. M. F. Hussain and K. B. M. Q. Zaman, J. Fluid Mech. **101**, 493 (1980).
[30]F. K. Browand and P. D. Weidman, J. Fluid Mech. **76**, 127 (1976).
[31]A. J. Yule, J. Fluid Mech. **89**, 413 (1978).
[32]B. Cantwell, Ann. Rev. Fluid Mech. **13**, 457 (1981).
[33]M. A. Herman and J. Jimenez, J. Fluid Mech. **119**, 323 (1982).
[34]I. Wygnanski, Lect. Notes Phys. **136**, 304 (1980).
[35]H. E. Fiedler, B. Dziomba, P. Mensing, and T. Rosgen, Lect. Notes Phys. **136**, 219 (1980).
[36]K. B. M. Q. Zaman and A. K. M. F. Hussain, J. Fluid Mech. **103**, 133 (1981).
[37]W. T. Ashurst, *Turbulent Shear Flows* (Penn. State U. P., University Park, PA, 1977), p. 1143.
[38]E. Acton, J. Fluid Mech. **98**, 1 (1980).
[39]P. Moin and J. Kim, J. Fluid Mech. **118**, 341 (1982).
[40]J. J. Riley and R. Metcalfe, Presented at the 13th AIAA Fluid and Plasma Dynamics Conference, Snowmass, Colorado, July 14–16, 1980, No. 80-0274.
[41]G. M. Corcos, Lect. Notes Phys. **136**, 10 (1980).
[42]B. Coüet, O. Buneman, and A. Leonard, *Turbulent Shear Flows* (Imperial College, London, 1979), p. 1429.
[43]D. D. Knight and B. T. Murray, Lect. Notes Phys. **136**, 62 (1980).
[44]A. Leonard, Lect. Notes Phys. **136**, 119 (1980).
[45]H. Aref and E. D. Siggia, J. Fluid Mech. **100**, 705 (1980).
[46]A. B. Cain, W. C. Reynolds, and J. H. Ferziger, *Turbulent Shear Flows* (University of California, Davis, California, 1981).
[47]J. P. Schon, F. Danel, J. P. Melinand, C. Rey, and G. Charnay, *Symposium on Turbulence* (University of Missouri, Rolla, 1979), p. 99.
[48]P. E. Dimotakis, F. D. Debussy, and M. M. Koochesfahani, Phys. Fluids **24**, 996 (1981).
[49]R. Meynart, Phys. Fluids **26**, 2074 (1983).
[50]A. K. M. F. Hussain and A. R. Clark, J. Fluid Mech. **104**, 263 (1981).
[51]J. L. Lumley, in *Transition and Turbulence*, edited by R. E. Meyer (Academic, New York, 1981), p. 215.
[52]A. Michalke (private communication, 1980).
[53]S. Corrsin (private communication, 1982).
[54]A. A. Townsend, *The Structure of Turbulent Shear Flow* (Cambridge U. P., Cambridge, 1956).
[55]H. L. Grant, J. Fluid Mech. **4**, 149 (1958).
[56]J. F. Keffer, J. Fluid Mech. **22**, 135 (1965).
[57]F. R. Payne and J. L. Lumley, Phys. Fluids Suppl. **10**, S194 (1967).
[58]S. Corrsin, NACA Wartime Reports No. 94, 1943.
[59]A. Roshko, NACA Report No. 1191, 1954.
[60]E. R. Lindgren, Ark. Fys. **12**, 1 (1957).
[61]J. Rotta, Ing. Arch. **24**, 258 (1956).
[62]H. W. Emmons, J. Aero. Sci. **18**, 490 (1951).
[63]S. Dhawan and R. Narasimha, J. Fluid Mech. **3**, 418 (1958).
[64]J. W. Elder, J. Fluid Mech. **9**, 235 (1962).
[65]L. S. G. Kovasznay, H. Komoda, and B. R. Vasudeva, *Proceedings of the Heat Transfer and Fluid Mechanics Institute* (Stanford U. P., Stanford, CA, 1962), p. 1.
[66]G. B. Brown, Phys. Soc. **47**, 703 (1935).
[67]A. B. C. Anderson, J. Acoust. Soc. Am. **26**, 21 (1954).
[68]S. Corrsin, *Proceedings of the First Naval Hydro Symposium* (National Research Council, Washington, 1957), p. 373.
[69]F. R. Hama and J. Nutant, *Proceedings of the Heat Transfer and Fluid Mechanics Institute* (Stanford U.P., Stanford, California, 1963), p. 77.
[70]H. P. Bakewell and J. L. Lumley, Phys. Fluids **10**, 1880 (1967).
[71]A. K. Gupta, J. Laufer, and R. E. Kaplan, J. Fluid Mech. **50**, 493 (1971).
[72]P. Bradshaw, D. H. Ferriss, and R. F. Johnson, J. Fluid Mech. **19**, 591 (1964).
[73]E. Mollo-Christensen, Trans ASME E., J. Appl. Mech. **89**, 1 (1967).
[74]A. R. Clark, Ph.D. thesis, University of Houston, 1979.
[75]A. R. Clark and A. K. M. F. Hussain, in *Turbulent Shear Flows* (Imperial College, London, 1979), p. 2.30.
[76]J. C. Lau, M. J. Fisher, and H. V. Fuchs, J. Sound Vib. **22**, 379 (1972).
[77]A. Michalke and H. V. Fuchs, J. Fluid Mech. **70**, 179 (1975).
[78]R. R. Armstrong, AIAA J. **19**, 677 (1981).
[79]P. Bradshaw (private communication, 1980).
[80]J. L. Lumley, *Stochastic Tools in Turbulence* (Academic, New York, 1970).
[81]H. Tennekes and J. L. Lumley, *A First Course in Turbulence* (MIT Press, Cambridge, 1972).
[82]A. J. Yule, Lect. Notes Phys. **136**, 188 (1980).
[83]R. C. Chanaud and A. Powell, J. Acoust. Soc. Am. **37**, 902 (1965).
[84]K. Karamcheti, A. E. Bauer, W. L. Shields, G. R. Stegen, and J. Woolley, NASA Report No. SP-207, 1969, p. 207.
[85]N. Curle, Proc. R. Soc. London Ser. A **216**, 412 (1953).
[86]A. Powell, J. Acoust. Soc. Am. **33**, 4 (1961).
[87]A. K. M. F. Hussain and K. B. M. Q. Zaman, J. Fluid Mech. **87**, 349 (1978).
[88]D. Rockwell and E. Naudascher, Ann. Rev. Fluid Mech. **11**, 67 (1979).
[89]E. Rockwell and C. Knisley, J. Fluid Mech. **93**, 413 (1979).
[90]W. G. Hill and P. R. Greene, J. Fluids Eng. **99**, 520 (1977).
[91]M. A. Z. Hasan and A. K. M. F. Hussain, J. Fluid Mech. **115**, 59 (1982).
[92]A. K. M. F. Hussain and M. A. Z. Hasan, J. Fluid Mech. **134**, 431 (1983).
[93]C. M. Ho and N. S. Nossier, J. Fluid Mech. **105**, 119 (1981).
[94]M. A. Z. Hasan, O. Islam, and A. K. M. F. Hussain, AIAA J. (to appear).
[95]A. A. Townsend, J. Fluid Mech. **95**, 515 (1979).
[96]J. C. Mumford, J. Fluid Mech. **118**, 241 (1982).
[97]I. Wygnanski and F. H. Champagne, J. Fluid Mech. **59**, 281 (1973).
[98]I. Wyngnanski, M. Sokolov, and D. Friedman, J. Fluid Mech. **69**, 283 (1975).
[99]J. C. Stettler and A. K. M. F. Hussain, Report FM-19, University of Houston, 1983.
[100]D. E. Coles, J. Fluid Mech. **21**, 385 (1965).
[101]C. W. Van Atta, J. Fluid Mech. **25**, 495 (1966).
[102]D. E. Coles and C. W. Van Atta, AIAA J. **4**, 1696 (1966).
[103]E. L. Koschmieder, J. Fluid Mech. **93**, 515 (1979).
[104]J. C. R. Hunt (private communication, 1982).
[105]P. G. Drazin and W. Reid, *Hydrodynamic Stability* (Cambridge U. P., Cambridge, 1981).
[106]W. C. Reynolds, J. Fluid Mech. **54**, 481 (1972).
[107]P. M. Bevilaqua and P. S. Lykoudis, J. Fluid Mech. **89**, 589 (1978).
[108]S. Taneda, J. Phys. Soc. Jpn. **14**, 843 (1959).
[109]A. K. M. F. Hussain and K. B. M. Q. Zaman, University of Houston, Report FM-14., 1982.
[110]P. Bradshaw, J. Fluid Mech. **26** 225 (1966).
[111]A. K. M. F. Hussain and M. F. Zedan, Phys. Fluids **21**, 1100 (1978).
[112]R. G. Batt, AIAA J. **13**, 245 (1975).
[113]H. W. Liepmann and J. Laufer, NACA Report No. TN-1257, 1947.
[114]I. Wygnanski and H. E. Fiedler, J. Fluid Mech. **41**, 327 (1970).
[115]A. K. M. F. Hussain and M. F. Zedan, Phys. Fluids **21**, 1475 (1978).
[116]J. F. Foss, *Turbulent Shear Flows* (Pennsylvania State U. P., University Park, 1977), p. 11.33.
[117]S. F. Birch, *Turbulent Shear Flows* (Pennsylvania State U. P., University Park, 1977), p. 16.10.
[118]Z. D. Hussain and A. K. M. F. Hussain, AIAA J. **17**, 48 (1979).
[119]A. K. M. F. Hussain and Z. D. Husain, AIAA J. **18**, 1462 (1980).
[120]Z. D. Husain, Ph.D. thesis, University of Houston, 1982.
[121]D. E. Coles, Rand Corporation Report No. R-403PR, 1962.
[122]L. P. Purtell, P. S. Klebanoff, and F. T. Buckley, Phys. Fluids **24**, 802

(1981).
[123]A. K. M. F. Hussain and A. R. Clark, Phys. Fluids **20**, 1416 (1977).
[124]S. J. Kleis and A. K. M. F. Hussain, Bull. Am. Phys. Soc. **24**, 1132 (1979).
[125]Y. Kita, A. K. M. F. Hussain, and S. J. Kleis, Bull. Am. Phys. Soc. **24**, 1144 (1980).
[126]A. K. M. F. Hussain, Ph.D. thesis, Stanford University, 1970.
[127]W. C. Reynolds and A. K. M. F. Hussain, J. Fluid Mech. **54**, 263 (1972).
[128]B. Cantwell and D. E. Coles (private communication, 1978).
[129]A. K. M. F. Hussain, in *Cardiovascular Flow Dynamics and Measurements*, edited by N. H. C. Hwang and N. Norman (U. Park P., Baltimore, 1977), p. 541.
[130]D. E. Coles and S. J. Barker, in *Turbulent Mixing in Nonreactive and Reactive Flows*, edited by S. N. B. Murthy (Plenum, New York, 1975), p. 285.
[131]I. Wygnanski, M. Sokolov, and D. Friedman, J. Fluid Mech. **78**, 785 (1976).
[132]B. J. Cantwell, D. E. Coles, and P. E. Dimotakis, J. Fluid Mech. **87**, 641 (1978).
[133]A. K. M. F. Hussain, S. J. Kleis, and M. Sokolov, J. Fluid Mech. **98**, 97 (1980).
[134]F. K. Browand and T. R. Troutt, J. Fluid Mech. **97**, 771 (1980).
[135]R. G. Batt, J. Fluid Mech. **82**, 53 (1978).
[136]N. K. Pui and I. S. Gartshore, J. Fluid Mech. **91**, 111 (1978).
[137]D. H. Wood and P. Bradshaw, J. Fluid Mech. (to appear).
[138]R. F. Blackwelder, Phys. Fluids Suppl. **20**, S232 (1977).
[139]A. J. Yule, in *Turbulent Shear Flows* (Imperial College, London, 1979), p. 7.1.
[140]K. B. M. Q. Zaman and A. K. M. F. Hussain, University of Houston Report No. FM-13, 1982.
[141]H. H. Bruun, J. Fluid Mech. **64**, 775 (1977).
[142]H. H. Bruun, Proc. R. Soc. London Ser. A **367**, 193 (1979).
[143]S. Rajagopalan and R. A. Antonia, J. Fluid Mech. **105**, 261 (1981).
[144]J. C. Lau, Proc. R. Soc. London Ser. A **268**, 547 (1979).
[145]M. Sokolov, A. K. M. F. Hussain, S. J. Kleis, and Z. D. Husain, J. Fluid Mech. **98**, 65 (1980).
[146]M. Zilberman, I. Wygnanski, and R. E. Kaplan, Phys. Fluids Suppl. **20**, S258 (1977).
[147]H. S. Husain, Ph.D. thesis, University of Houston (in progress).
[148]J. Tso, Ph.D. thesis, Johns Hopkins University (research done at University of Houston).
[149]A. K. M. F. Hussain and K. B. M. Q. Zaman, J. Fluid Mech. **110**, 39 (1981).
[150]C. C. Lin, Q. Appl. Math. **18**, 295 (1953).
[151]J. L. Lumley, Phys. Fluids **8**, 1056 (1965).
[152]M. J. Fisher and P. O. A. L. Davies, J. Fluid Mech. **18**, 97 (1964).
[153]G. Heskestad, J. Appl. Mech. **87**, 735 (1965).
[154]F. H. Champagne, J. Fluid Mech. **86**, 67 (1978).
[155]J. C. Wyngaard and S. F. Clifford, J. Atmos. Sci. **34**, 922 (1977).
[156]R. A. Antonia, A. J. Chambers, and N. Phan-Thien, J. Fluid Mech. **100**, 193 (1980).
[157]K. B. M. Q. Zaman and A. K. M. F. Hussain, J. Fluid Mech. **112**, 379 (1981).
[158]K. B. M. Q. Zaman and A. K. M. F. Hussain, *Turbulent Shear Flows* (Pennsylvania State U. P., University Park, 1977), p. 11.23.
[159]K. B. M. Q. Zaman and A. K. M. F. Hussain, J. Fluid Mech. **101**, 449
[160]C. M. Ho and N. Huang, J. Fluid. Mech. **119**, 443 (1982).
[161]W. W. Willmarth, Adv. Appl. Mech. **15**, 159 (1975).
[162]A. Dinkelacker, M. Hessel, G. A. E. Meier, and G. Schewe, Phys. Fluids Suppl. **20**, S216 (1977).
[163]W. W. Willmarth and T. J. Bogar, Physics Fluids Suppl. **20**, S9 (1977).
[164]R. Falco, *Symposium on Turbulence* (U. of Missouri, Rolla, 1979), p. 1.
[165]A. E. Perry and M. S. Chong, J. Fluid Mech. **119**, 173 (1982).
[166]W. W. Willmarth and S. S. Lu, J. Fluid Mech. **55**, 481 (1971).
[167]S. S. Lu and W. W. Willmarth, J. Fluid Mech. **60**, 481 (1973).
[168]R. A. Antonia, Phys. Fluids **15**, 1869 (1972).
[169]A. K. Gupta and R. E. Kaplan, Phys. Fluids **15**, 981 (1972).
[170]J. M. Wallace, H. Eckelmann, and R. S. Brodkey, J. Fluid Mech. **54**, 39 (1972).
[171]R. S. Brodkey, J. M. Wallace, and H. Eckelmann, J. Fluid Mech. **63**, 209 (1974).
[172]M. Nishioka, M. Asai, and S. Iida, in *Transition and Turbulence*, edited by R. E. Meyer (Academic, New York, 1981), p. 113.
[173]R. F. Blackwelder and R. E. Kaplan, J. Fluid Mech. **76**, 89 (1976).
[174]P. S. Klebanoff (private communication, 1980).
[175]F. N. Frenkiel and P. S. Klebanoff, Phys. Fluids **16**, 725 (1973).
[176]A. E. Perry, T. T. Lim, and E. W. Teh, J. Fluid Mech. **104**, 387 (1981).
[177]T. Theodorsen, in Proceedings of the 2nd Midwestern Mechanical Conference (Ohio State U., Columbus, 1952), p. 1.
[178]P. S. Klebanoff, K. D. Tidstrom, and L. M. Sargent, J. Fluid Mech. **12**, 1 (1962).
[179]T. J. Black, NASA Report No. CR-888, 1968.
[180]G. R. Offen and S. J. Kline, J. Fluid Mech. **70**, 209 (1975).
[181]L. S. G. Kovasznay, V. Kibens, and R. F. Blackwelder, J. Fluid Mech. **41**, 283 (1970).
[182]G. L. Brown and A. S. W. Thomas, Phys. Fluids Suppl. **20**, S243 (1977).
[183]R. Falco, Phys. Fluids Suppl. **20**, S214 (1977).
[184]A. J. Grass, J. Fluid Mech. **50**, 223 (1971).
[185]K. N. Rao, R. Narasimha, and M. A. Badri Narayanan, J. Fluid Mech. **38**, 339 (1971).
[186]H. T. Kim, S. J. Kline, and W. C. Reynolds, J. Fluid Mech. **50**, 133 (1971).
[187]J. Laufer and M. A. Badri Narayanan, Phys. Fluids **14**, 182 (1971).
[188]M. A. Badri Narayanan and J. Marvin, in *Lehigh Workshop on Coherent Structure in Turbulent Boundary Layers*, edited by C. R. Smith and D. E. Abbott (Lehigh U., Bethlehem, PA, 1978), p. 380.
[189]J. Sabot and G. Comte-Bellot, J. Fluid Mech. **74**, 767 (1976).
[190]C. R. Smith, see Ref. 188, p. 48.
[191]V. Zakkay, V. Barra, and C. R. Wang, see Ref. 188, p. 387.
[192]R. F. Blackwelder and J. H. Haritonidis, Bull. Am. Phys. Soc. Ser. II **25**, 1094 (1980).
[193]L. K. Sharma and W. W. Willmarth, Bull. Am. Phys. Soc. Ser. II **25**, 1075 (1980).
[194]R. Narasimha and K. R. Sreenivasan, Adv. Appl. Mech. **19**, 221 (1979).
[195]M. A. Badri Narayanan, S. Rajagopalan, and R. Narasimha, J. Fluid Mech. **80**, 237 (1977).
[196]S. Rajagopalan and R. A. Antonia, Phys. Fluids **23**, 1101 (1980).
[197]K. K. Sirkar and T. J. Hanratty, J. Fluid Mech. **44**, 589 (1970).
[198]R. F. Blackwelder and H. Eckelmann, J. Fluid Mech. **94**, 577 (1979).
[199]D. K. Oldaker and W. G. Tiederman, Phys. Fluids Suppl. **20**, S133 (1977).
[200]L. W. Carr, in *Unsteady Turbulent Shear Flows*, edited by R. Michel, J. Cousteix, and R. Houdeville (Springer-Verlag, Berlin, 1981), p. 3.
[201]P. G. Parikh, W. C. Reynolds, R. Jayaraman, and L. W. Carr, See Ref. 200, p. 35.
[202]R. L. Simpson, B. G. Shivaprasad, and Y.-T. Chew, see Ref. 200, p. 109.
[203]T. Mizushina, T. Maruyama, and H. Hirasawa, J. Chem. Eng. Jpn. **8**, 3 (1975).
[204]K. Yajnik and M. Acharya, Lect. Notes Phys. **75**, 249 (1977).
[205]J. N. Hefner, L. M. Weinstein, and D. M. Bushnell, in *Viscous Flow Drag Reduction*, edited by G. R. Hough (AIAA, Dallas, TX, 1980), p. 110.
[206]T. C. Corke, Y. Guezennec, and H. M. Nagib, see Ref. 205, p. 128.
[207]R. Narasimha (private communication, 1982).
[208]A. Michalke, J. Fluid Mech. **23**, 521 (1965).
[209]P. Freymuth, J. Fluid Mech. **25**, 683 (1966).
[210]R. W. Miksad, J. Fluid Mech. **56**, 695 (1972).
[211]D. G. Crighton and M. Gaster, J. Fluid Mech. **77**, 397 (1976).
[212]S. Widnall, Ann. Rev. Fluid Mech. **7**, 141 (1976).
[213]P. G. Saffman, J. Fluid Mech. **84**, 625 (1978).
[214]P. O. A. L. Davies and D. R. J. Baxter, Lect. Notes Phys. **75**, 125 (1978).
[215]G. K. Batchelor and A. E. Gill, J. Fluid Mech. **14**, 529 (1962).
[216]G. E. Mattingly and C. C. Chang, J. Fluid Mech. **65**, 541 (1974).
[217]A. Michalke and H. V. Fuchs, J. Fluid Mech. **70**, 179 (1975).
[218]R. A. Petersen, J. Fluid Mech. **89**, 469 (1978).
[219]R. E. Drubka and H. M. Nagib, Illinois Institute of Technology Fluid and Heat Transfer Report No. R81-2, 1981.
[220]Y. Y. Chan, Phys. Fluids **17**, 46 (1974).
[221]S. J. Kleis, A. K. M. F. Hussain, and M. Sokolov, J. Fluid Mech. **111**, 87 (1981).
[222]C. J. Moore, J. Fluid Mech. **80**, 321 (1977).
[223]Z. D. Husain and A. K. M. F. Hussain, AIAA J. (to appear).
[224]V. Kibens, AIAA J. **18** 434 (1980).
[225]D. G. Crighton, J. Fluid Mech. **106**, 261 (1981).
[226]D. Bechert and E. Pfizenmaier, J. Sound Vib. **143**, 581 (1975).
[227]R. R. Armstrong, A. Michalke, and H. V. Fuchs, AIAA J. **15**, 1011 (1977).
[228]C. Dahan, G. Elias, J. Maulard, and M. Perulli, J. Sound Vib. **59**, 313 (1978).
[229]D. Juvé, M. Sunyach, and G. Comte-Bellot, J. Sound Vib. **71**, 319 (1980).
[230]C. K. W. Tam and P. J. Morris, J. Fluid Mech. **98**, 349 (1980).
[231]J. T. C. Liu, J. Fluid Mech. **62**, 437 (1974).

[232]R. Mankbadi and J. T. C. Liu, Phil. Trans. R. Soc. A **298**, 541 (1980).
[233]K. K. Ahuja, J. Lepicovsky, C. K. W. Tam, P. J. Morris, and R. H. Burrin, NASA Report No. CR-3538, 1982.
[234]J. Laufer, Invited Lecture, American Physical Society/Division of Fluid Dynamics Annual Meeting, Yale University, New Haven, CT, 1973.
[235]J. E. Ffwocs-Williams and A. J. Kempton, J. Fluid Mech. **84**, 673 (1978).
[236]A. K. M. F. Hussain and K. B. M. Q. Zaman, see Ref. 200, p. 390.
[237]W. T. Chu and R. E. Kaplan, J. Acoust. Soc. Am. **59**, 1268 (1976).
[238]P. E. Dimotakis and G. L. Brown, J. Fluid Mech. **78**, 535 (1976).
[239]V. Kibens, McDonnel-Douglas Reserach Laboratories Report MDRL 81-12, 1980.
[240]A. K. M. F. Hussain and K. B. M. Q. Zaman, in *Proceedings of the 3rd Interagency Symposium on University Research in Transportation Noise* (U. of Utah, Salt Lake City, 1975), p. 314.
[241]Y. V. Vlasov and A. S. Ginevskiy, NASA Report No. TTF-15, 1974, p. 721.
[242]D. Oster and I. Wygnanski, J. Fluid Mech. **123**, 91 (1982).
[243]E. Pfizenmaier, Doktor-Ingenieur thesis, Technische Universitaet Berlin, 1973.
[244]D. Rockwell and A. Schaechenmann, J. Fluid Mech. **117**, 425 (1982).
[245]M. Nallasamy and A. K. M. F. Hussain, Bull. Am. Phys. Soc. **27** 1178 (1982).
[246]M. Sokolov, S. J. Kleis, and A. K. M. F. Hussain, AIAA J. **19**, 1000 (1981).
[247]S. J. Kleis and A. K. M. F. Hussain, Bull. Am. Phys. Soc. Ser. II **25**, 1070 (1980).
[248]A. K. M. F. Hussain and C. A. Thompson, J. Fluid Mech. **100**, 397 (1980).
[249]H. Sato, J. Fluid Mech. **7**, 53 (1960).
[250]H. Sato and F. Sakao, J. Fluid Mech. **20**, 337 (1964).
[251]G. E. Mattingly and W. O. Criminale, Phys. Fluids **14**, 2258 (1971).
[252]G. S. Beavers and T. A. Wilson, J. Fluid Mech. **44**, 97 (1970).
[253]D. O. Rockwell and W. O. Niccolls, J. Basic Eng. **94**, 720 (1972).
[254]W. C. Reynolds and E. E. Bouchard, in *Unsteady Turbulent Shear Flows* (Springer-Verlag, Berlin, 1981), p. 402.
[255]H. A. Becker and T. A. Massaro, J. Fluid Mech. **31**, 435 (1968).
[256]N. K. Tutu and R. Chevray, J. Fluid Mech. **71**, 785 (1975).
[257]R. Chevray and N. K. Tutu, Rev. Sci. Instrum. **43**, 1417 (1972).
[258]R. A. Antonia, A. J. Chambers, and A. K. M. F. Hussain, Phys. Fluids **23**, 871 (1980).
[259]J. Tso, L. S. G. Kovasznay, and A. K. M. F. Hussain, J. Fluids Eng. **103**, 503 (1981).
[260]D. J. Shlien and A. K. M. F. Hussain, J. Flow Vis. Soc. Jpn. **2**, 189 (1982).
[261]M. K. Moallemi and V. W. Goldschmidt, Mechanical Engineering Report No. 8, Purdue University, 1981.
[262]G. I. Taylor, Proc. R. Soc. London Ser. A **164**, 476 (1938).
[263]A. Favre, J. Gaviglio, and R. Dumas, *Proceedings of the 8th International Congress on Applied Mechanics*, Istanbul, 1952, p. 304.
[264]F. N. Frenkiel and P. S. Klebanoff, in *Dynamics of Fluids and Plasmas*, edited by S. I. Pai, 1966, p. 257.
[265]G. Comte-Bellot and S. Corrsin, J. Fluid Mech. **48**, 273 (1971).
[266]F. J. Gifford, Mon. Weath. Rev. **83**, 293 (1955).
[267]C. Beguier, F. Giralt, L. Fulachier, and J. F. Keffer, Lect. Notes Phys. **76**, 22 (1978).
[268]K. Hanjalic and B. E. Launder, J. Fluid Mech. **51**, 301 (1972).
[269]J. O. Hinze, *Turbulence* (McGraw-Hill, New York, 1976).
[270]I. Wygnanski, D. Oster, and H. Fiedler, *Turbulent Shear Flows* (Imperial College, London, 1979), p. 812.
[271]A. E. Perry, T. T. Lim, and M. S. Chong, J. Fluid Mech. **101**, 243 (1980).
[272]A. N. Kolmogorov, J. Fluid Mech. **13**, 82 (1962).
[273]A. M. Obukhov, J. Fluid Mech. **13**, 77 (1962).
[274]A. S. Monin and A. M. Yaglom, *Statistical Fluid Mechanics* (MIT, Cambridge, 1975), Vol. 2.
[275]S. H. Davis, Ann. Rev. Fluid Mech. **8**, 57 (1976).
[276]C. S. Yih, J. Fluid Mech. **31**, 732 (1968).
[277]C. E. Grosch and H. Salwen, J. Fluid Mech. **34** 177 (1968).
[278]C. H. von Kerczek, J. Fluid Mech. **116**, 91 (1982).